I. A NUCLEAR MAGNETIC RESONANCE STUDY OF AMIDINIUM IONS IN SOLUTION

II. THE KINETICS OF THE THERMAL DECOMPOSITION OF AZOBISISOBUTYRAMIDINES AND THEIR SALTS IN SOLUTION

Thesis by

Robert Canute Neuman, Jr.

In Partial Fulfillment of the Requirements

For the Degree of

Doctor of Philosophy

California Institute of Technology

Pasadena, California

1963

To Kathleen

Acknowledgements

To properly acknowledge everyone who has directly or indirectly helped me to reach this goal would require a book as large as this thesis. By necessity only a very few can be mentioned.

The inspiration, counsel, and guidance of my research director, Professor G. S. Hammond, has made this thesis possible.

Among my colleagues I wish to especially thank Dr. Karl Kopecky, Dr. Richard Pincock, and Mr. Jack Saltiel for time which they have expended in helping me with both practical and theoretical chemical problems. I wish to acknowledge all those on the faculties of the University of California, Los Angeles, and the California Institute of Technology who have had a part in my undergraduate and graduate training. The National Institutes of Health (1960-1962) and the National Science Foundation (Summer, 1960) are acknowledged for their financial support.

To my parents goes my deepest gratitude. Their training, understanding, and concern have enabled me to realize that no goal is too distant to strive for.

ABSTRACT

Part I

N. m. r. spectra of unsubstituted and symmetrically substituted aliphatic amidinium salts in dimethyl sulfoxide or water demonstrate the presence of hindered internal rotation about the C_{CN}-N bonds in the amidinium groups. The kinetics of nitrogen-proton exchange in dilute aqueous acid and sulfuric acid-water mixtures, containing amidinium salts, have been studied by the n. m. r. method and compared with proton exchange reactions of ammonium ions in similar media. The nature of the nitrogen-proton magnetic resonance signals of amidinium salts is discussed in terms of current theory concerning the effect of the ^{14}N nucleus on magnetic resonance characteristics of bonded hydrogen atoms.

Part II

Rates of the thermal decomposition of two aliphatic azo-bis-amidines, and their first and second conjugate acids, have been determined. The rates of decomposition of the first and second conjugate acids for each azo-amidine are quite similar, but much greater than those of the corresponding neutral azo-amidines. The efficiencies of radical production of the neutral azo-amidines are

only slightly less than those of the second conjugate acids, indicating that the "cage effect" may be only slightly influenced by electrostatic repulsive interactions between geminate radicals. The synthesis of a new aliphatic azo-nitrile is described.

TABLE OF CONTENTS

I. A NUCLEAR MAGNETIC RESONANCE STUDY OF AMIDINIUM IONS IN SOLUTION

Introduction

The amidinium group can be represented by the resonance structures shown in Figure 1,

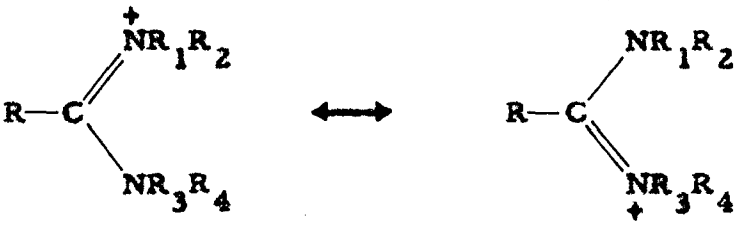

Fig. 1

in which normally at least one of the groups (R_1, R_2, R_3, or R_4) is hydrogen. In this latter case, the group is the first conjugate acid of an amidine shown in Figure 2.

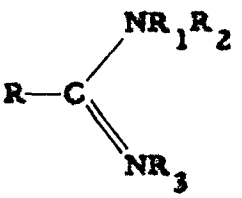

Fig. 2

The remaining groups R, and R_1-R_3 can be protons, alkyl, or aryl groups. When R_1, R_2, R_3, and R_4 are hydrogen, the compound is said to contain an unsubstituted amidinium group.

A wide variety of subatituted and unsubstituted amidines and

amidinium salts have been prepared and a review of the chemistry of these compounds has been presented by Shriner and Neumann (1).

Alkyl and certain aryl amidines are much more basic than the correspondingly substituted amines. This has been explained by the resonance stabilization afforded the first conjugate acid of the amidines (1).

Whereas amidinium salts are considered to be a single resonance stabilized species, the amidine free bases may conceivably exist in the two tautomeric forms (1), Figure 3.

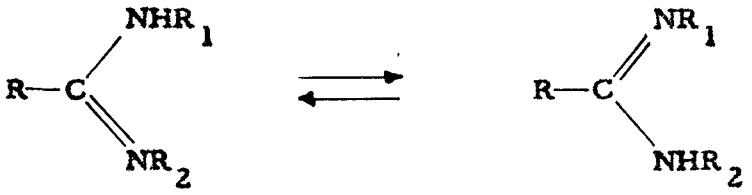

Fig. 3

No successful isolation of these separate forms has been performed (1, 2). Recently, Prevorsek (3) has demonstrated the existence of the separate tautomeric forms by infrared spectroscopic studies. Interconversion is apparently sufficiently rapid to prevent their physical separation.

Natural products containing simple amidinium or amidine groups have not been reported; however, the closely related guanidino group is present in the amino acids argenine and canavanine, and the amidine moiety is incorporated in naturally occurring heterocyclic ring systems.

Relatively simple unsubstituted amidines have been shown to exhibit biologic activity as trypanocidal agents (4) and also as anesthetics (5).

Our interest in a nuclear magnetic resonance study of amidinium groups arose from other studies on water soluble polymerization initiators containing these functional groups. This latter investigation is reported in Part II of this dissertation.

A transient product of the thermal decomposition of azo-bis-isobutyramidinium chloride in water is tetramethylsuccinimidinium chloride (6,7). Formally, this compound may be a mixture of two tautomers involving only proton transfer between nitrogen atoms. To account for ultraviolet spectroscopic data obtained from water solutions of the imidinium chloride, it was postulated that a slow tautomerism was occurring (6). The n.m.r. spectrum of an aqueous solution of acetamidinium chloride was examined and revealed a broad singlet 3.5 ppm. downfield from the water proton resonance (8). This result, indicating slow proton transfer between acetamidinium chloride and water, was considered to be a further confirmation of this hypothesis (8). A reinvestigation of the n.m.r. spectrum of acetamidinium chloride in water, and the n.m.r. spectra of tetramethylsuccinimidinium nitrate and azo-bis-isobutyramidinium chloride in water, have led to the conclusion that slow tautomerism cannot be justifiably used to explain the ultraviolet spectroscopic data (9).

These specific n.m.r. experiments led to a general study of compounds containing amidinium groups. The results obtained have proven to be interesting and valuable in several ways. The spatial geometry of simple amidinium groups in solution has been elucidated, and results applicable to the theory for hindered internal rotation in amides and protonated amides have been obtained. Nitrogen-proton exchange reactions have been studied and are shown to fit mechanisms which are distinct from the major proton exchange processes of ammonium salts. Finally, the nature of the magnetic resonance signals of protons attached to nitrogen in the amidinium salts adds to the meager experimental data which have been accumulated for protons attached to nuclei other than carbon.

The three major fields which are covered in this nuclear magnetic resonance study are conformational analysis, proton exchange reactions, and magnetic resonance characteristics of nitrogen-protons. A review of similar studies on closely related systems is appropriate. Numerous n.m.r. studies on rotation about C-N partial double bonds have been reported. A review of the work prior to 1959 has been compiled by Pople, Schneider, and Bernstein (10). Recently, a reinvestigation of N,N-dimethylamides has been reported by Rogers and Woodbrey (11). Accurate activation parameters for rotation about the C_{CO}-N bonds have been calculated and a discussion concerning the limitations of the n.m.r. method in determining activation parameters

for these systems is presented. Sunners et al. (12) have studied rotation about the C_{CO}-N bond in an unsubstituted amide, formamide-^{15}N. Their results demonstrate that isotopic substitution of ^{15}N for the naturally occurring ^{14}N is extremely useful for studying processes which require n.m.r. examination of protons attached to nitrogen.

The importance of solvent effects on the n.m.r. spectra of amides in solution (13-15), and their influence on the barriers to rotation about C_{CO}-N partial double bonds have been examined (16). Protolysis and proton exchange reactions of amides and their influence on restricted internal rotation in these systems have also been examined (17-20).

Extremely thorough investigations of proton exchange reactions for ammonium salts in aqueous solution have appeared in the literature (21-26). The results of these latter studies, in addition, contain important information concerning the nature of solvation and the properties of solutions.

The nature of nitrogen-proton resonance signals has been reviewed (27-29). Roberts (30) and Tiers (31) have discussed the quadrupole broadening effect of the ^{14}N nucleus on bonded protons with specific application to understanding nitrogen-proton resonance signals for various amides.

The results obtained in the above studies will be discussed where appropriate in the following section.

Results and Discussion

The amidinium salts I-IV (Fig. 4) have been studied in a series of solvents at room temperature and also as a function of temperature by the proton magnetic resonance technique (32). A preliminary report of these results has appeared in the literature (33).

The results and discussion of this study will be divided into three broad categories. The first part will contain the results and discussion of conformational studies on the amidinium groups. The second part will deal with nitrogen-proton exchange reactions which the amidinium groups may undergo. The third part will include specific observations which concern the theory of nitrogen-proton magnetic resonance signals. These sections are not completely independent of one another and therefore strict adherence of content to section title will not always be possible.

At this point I wish to thank Professor J. D. Roberts for the use of the n.m.r. spectrometers. Also, I wish to especially thank Mr. Donald R. Davis for instructions on the use of this equipment, and Mr. George M. Whitesides for assistance and helpful discussions throughout this study.

Fig. 4

AMIDINIUM IONS STUDIED

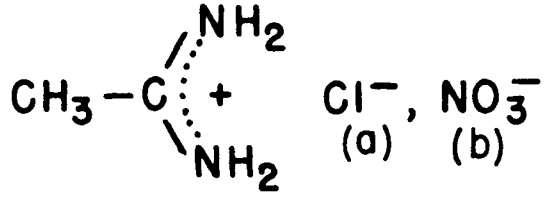

Acetamidinium (I)

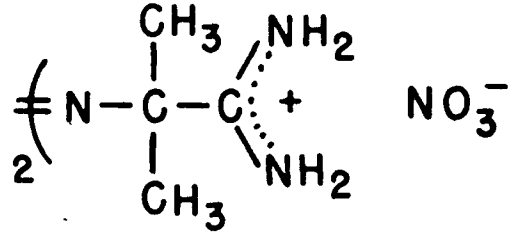

Azo-bis-isobutyramidinium (III)

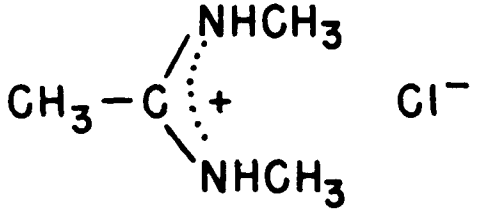

N,N'-dimethylacetamidinium (II)

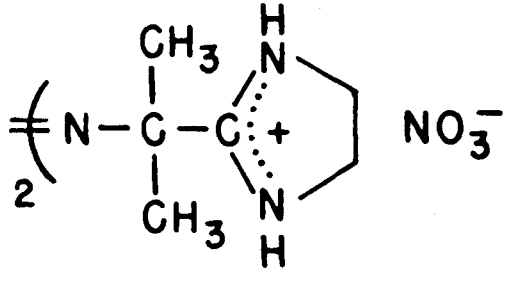

Azo-bis-N,N'-dimethyleneiso-butyramidinium (IV)

Conformations of Amidinium Groups

The choice of solvents used in the conformational studies has been limited by two factors. In order to investigate the conformations of unsubstituted amidinium groups by n.m.r. it is necessary that a solvent be chosen that contains no protons easily exchangeable with the nitrogen protons of these compounds, and also one that is not sufficiently basic to remove protons from these salts. These requirements severely limit the usable solvents since the amidinium salts are insoluble in most solvents that would be suitable. The solvent chosen for these studies was anhydrous dimethylsulfoxide (DMSO), used previously in studies of the thermal decomposition of azo-amidinium salts (34). This solvent possesses extremely high solvation powers (35) and has been used in numerous cases to dissolve difficultly soluble organic as well as inorganic salts. DMSO is also void of easily exchangeable protons (36) and is not sufficiently basic to remove protons from the very weakly acidic amidinium ions (37). One annoying disadvantage of DMSO is that it obscures the methyl and methylene region of the n.m.r. spectrum. When DMSO is used as an n.m.r. solvent, the ^{13}C satellites, spinning sidebands, and major solvent signal make observation of protons in the region 100-200 cps (60 Mcps) below tetramethylsilane difficult. Fortunately, the nitrogen-protons were of major interest and these came sufficiently far downfield from the

DMSO resonances that no solvent interference was encountered. In anhydrous DMSO, at room temperature, the protons on amidinium group nitrogens were observed to give n.m.r. signals in the region 500-600 cps downfield from tetramethylsilane as an external reference. Hereafter, all chemical shifts and spin-spin coupling constants will be given in cps, downfield from tetramethylsilane (0 cps) as an external reference, at a spectrometer frequency of 60 Mcps. The magnitude of H_o, the external magnetic field, increases from left to right on all spectra shown.

The chemical shifts of these nitrogen-protons, although quite different from those of amines (38,39), correspond closely to those of the nitrogen-protons in amides (38,39) and ammonium salts (24). No other protons in the amidinium salts studied would be expected to give resonance signals at such low field. The solvent was shown not to give resonance signals in this area of the spectrum.

Preparation and characterization of the various amidinium salts is discussed in the experimental section.

All amidinium salts investigated, with the exception of IV, gave two nitrogen-proton resonance signals in DMSO at room temperature. The positions of the nitrogen-proton signals for the various compounds in DMSO are given in Table I.

In the spectra of the amidinium salts showing the two nitrogen-proton resonances, the signals are of equal area as determined by electronic or mechanical integration.

Table I

N.m.r. Spectral Data for Amidinium Nitrogen-Protons in DMSO at 30°

Compound	$\nu_{TMS} - \nu_{N-H}$ (cps)	Half-width ($\Delta \nu_{\frac{1}{2}}$) of N-H Signal (cps)
Ia	530	10
	560	11
Ib	530	10
	560	11
II	554	13
	609	16
III	534	9
	547	9
IV	608	15

A comparison of the spectral results for Ia and Ib (Table I) shows that the nature of the anion has no apparent effect on the nitrogen-proton signals. The nitrogen-protons giving rise to the two separate signals in III most probably exist within the same amidinium group as can be seen by the similarity of I (containing only one amidinium group per molecule) and III (containing two amidinium groups per molecule). Symmetrical substitution of methyl groups for two of the four nitrogen protons in I to give II does not remove the

doublet pattern, but symmetrical substitution of two of the four nitrogen protons in III by an ethylene bridge (at each end of the molecule) to give IV changes the nitrogen-proton spectral pattern from two resonance signals to a singlet.

The n. m. r. spectra of the amidinium salts have been recorded only at a spectrometer frequency of 60 Mcps. Thus, the question can be raised as to whether the two nitrogen-proton signals arise from discrete magnetically non-equivalent protons, or are a result of spin-spin coupling of these protons with other nuclei in the molecule (40). An examination of the structure of the amidinium salts I, II, and III leads to the conclusion that spin-spin coupling of protons cannot account for the doublet pattern (41). There are no single protons bound to carbon that can give rise to this pattern. Further, the $C-CH_3$ proton signals in the spectra of the amidinium salts are all relatively sharp singlets. The $N-CH_3$ protons in II show spin-spin coupling with their adjacent nitrogen-protons in appropriate solvents (vide infra), but the coupling constant is 5 cps while the two nitrogen-proton signals are 55 cps apart. The quartet pattern ($J = 5$ cps) expected for each nitrogen-proton signal in II is unresolved. Coupling between nitrogen-protons in II would require interaction across four chemical bonds. Further, this coupling would only be observed when the two protons were magnetically non-equivalent and hence two doublet nitrogen-proton resonances would be expected. In compounds I and III the same

argument can be used against spin-spin coupling between adjacent nitrogen-protons (2-bond coupling) and protons on the two nitrogens (4-bond coupling). Sunners et al. (12) have observed 2-bond coupling between adjacent protons in formamide-^{15}N; however, $J \approx 2$-3 cps, and coupling of this magnitude is obviously unresolved in the nitrogen-proton signals of the amidinium salts (Table I).

Coupling of the nitrogen-protons with the ^{14}N nucleus, although observed in other systems, would produce a triplet pattern (27-29). The effect of the quadrupole moment of ^{14}N on the nitrogen-proton signal shape (Table I) and the lack of proton coupling with the nitrogen nucleus will be discussed in the latter part of this section.

The presence of two magnetically non-equivalent nitrogen-protons in the salts I, II, and III, can be rationalized on the basis of restricted rotation about the C_{CN}-N bonds in the amidinium groups. The strong basicity of amidines has been explained by the favorable delocalization of positive charge which is possible in the amidinium ion (1). This ion can be represented by the mesomeric structure shown in Figure 5.

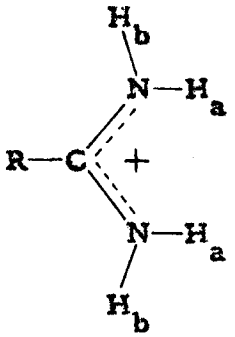

Fig. 5

The partial double bond character imparted to the C_{CN}-N bonds by this charge delocalization thus sufficiently decreases the rate of internal rotation about these bonds so that the two types of protons, H_a ("inside") and H_b ("outside") give distinct resonance signals. This interpretation is analogous to that postulated for hindered rotation in amides (10) and protonated amides (17-20) based on contributions of the resonance forms shown in Figures 6a and 6b, respectively.

(a) (b)

Fig. 6

The single nitrogen-proton resonance for IV can also be explained by the above interpretation since the two protons are restricted to the single "outside" proton positions (Fig. 7).

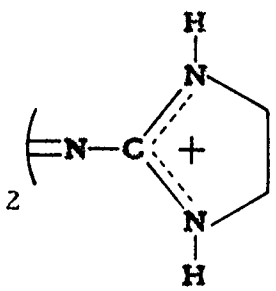

Fig. 7

N,N'-dimethylacetamidinium chloride (II) offers a system which can possess not only magnetically non-equivalent nitrogen protons, but also non-equivalent N-CH_3 groups. This allows conformational studies to be performed in solvents other than DMSO since the much less acidic protons on the methyl groups rather than those on nitrogen may be studied.

The n.m.r. spectrum of II in water at room temperature is shown in Figure 8. Three major signals at 139.5, 177.5, and 187.0 cps are observed. The water resonance is further downfield and is not shown on this spectrum. The signal areas are in the ratio 1:1:1 by electronic integration. The resonances at 177.5 and 187.0 cps are assigned to the N-CH_3 groups, and that at 139.5 cps is assigned to the C-CH_3 group. This is in good agreement with the deshielding effect generally observed for methyl groups attached to nitrogen (42). The nitrogen-protons were not observed in this spectrum due to rapid exchange with the solvent water (43, 24).

In 14% sulfuric acid-water, the spectrum of II appears as is shown in Figure 9. The signal at 142 cps is assigned to the C-CH_3 group, and the two doublets ($J \approx 5$ cps) centered at 179.0 and 188.5 cps are assigned to the N-CH_3 groups. These latter methyl protons are now coupled to their adjacent nitrogen-protons since the rate of nitrogen proton exchange in this system is sufficiently slow (43, 23).

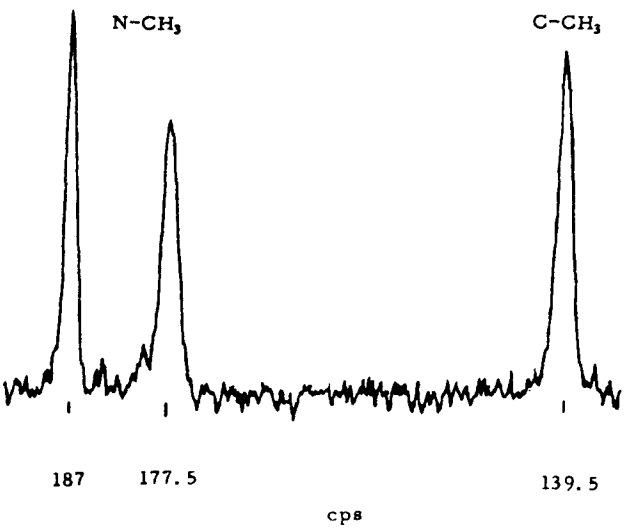

Fig. 8. N.m.r. spectrum of N,N'-dimethylacetamidinium chloride in water. 30°. 60 Mcps.

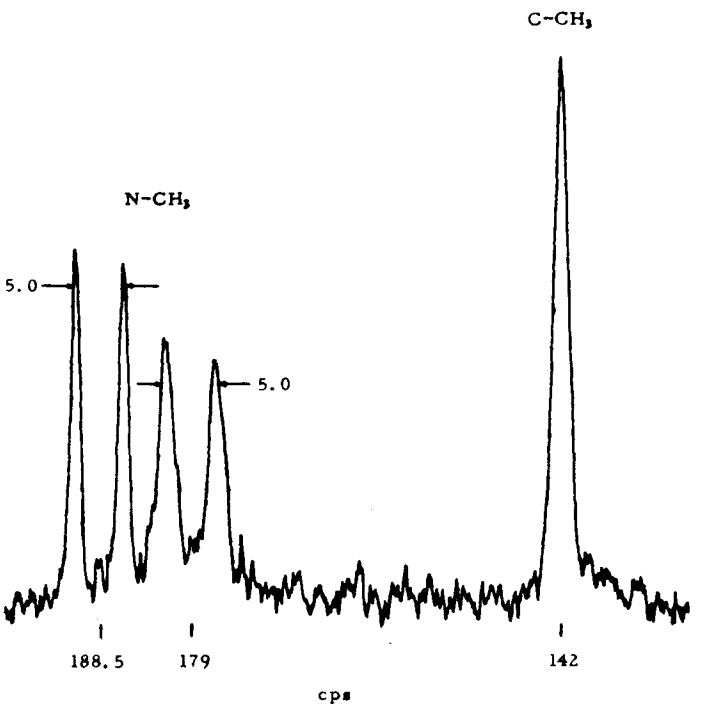

Fig. 9. N.m.r. spectrum of N,N'-dimethylacetamidinium chloride in 14% sulfuric acid. 30°. 60 Mcps.

That this coupling is with the nitrogen-protons has been demonstrated by showing that the N-CH_3 doublets centered at about 184 and 194 cps in 60% sulfuric acid (Fig. 17) are singlets in 60% sulfuric acid-d_2 (Fig. 10). Under these conditions the nitrogen-protons have exchanged completely with the solvent to give II containing only deuterium bound to nitrogen. The value J = 5 cps (Fig. 9) is in good agreement with corresponding coupling constants of 4 and 4.8 cps found for N-methylacetamide and N-methylformamide (19).

Finally, the spectrum of II in DMSO is shown in Figure 11. The assignments are as follows: C-CH_3, 137.5 cps; N-CH_3, two overlapping doublets (J = 5 cps) centered at 171.5 and 176.5 cps; and N-H, 554 and 609 cps.

The presence of the two non-equivalent N-CH_3 groups in II further confirms the previous postulate that rotation is restricted about C_{CN}-N bonds in the amidinium groups. Further, the n.m.r. spectra of II in the various solvents can be accounted for by the single conformation shown in Figure 12. This will explain the two nitrogen-

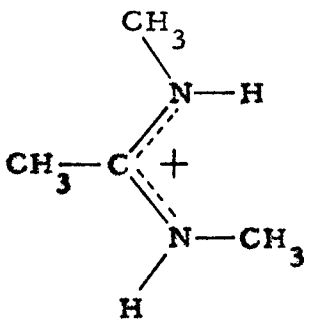

Fig. 12

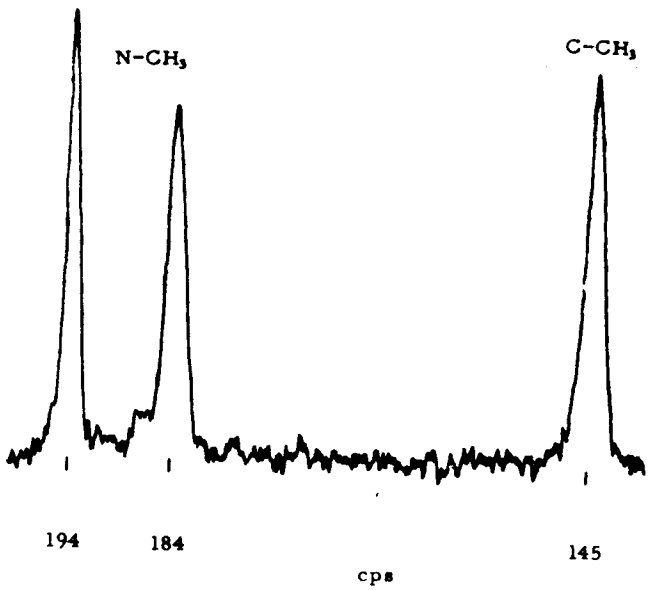

Fig. 10. N.m.r. spectrum of N,N'-dimethylacetamidinium chloride in 60% sulfuric acid-d_2. 30°. 60 Mcps.

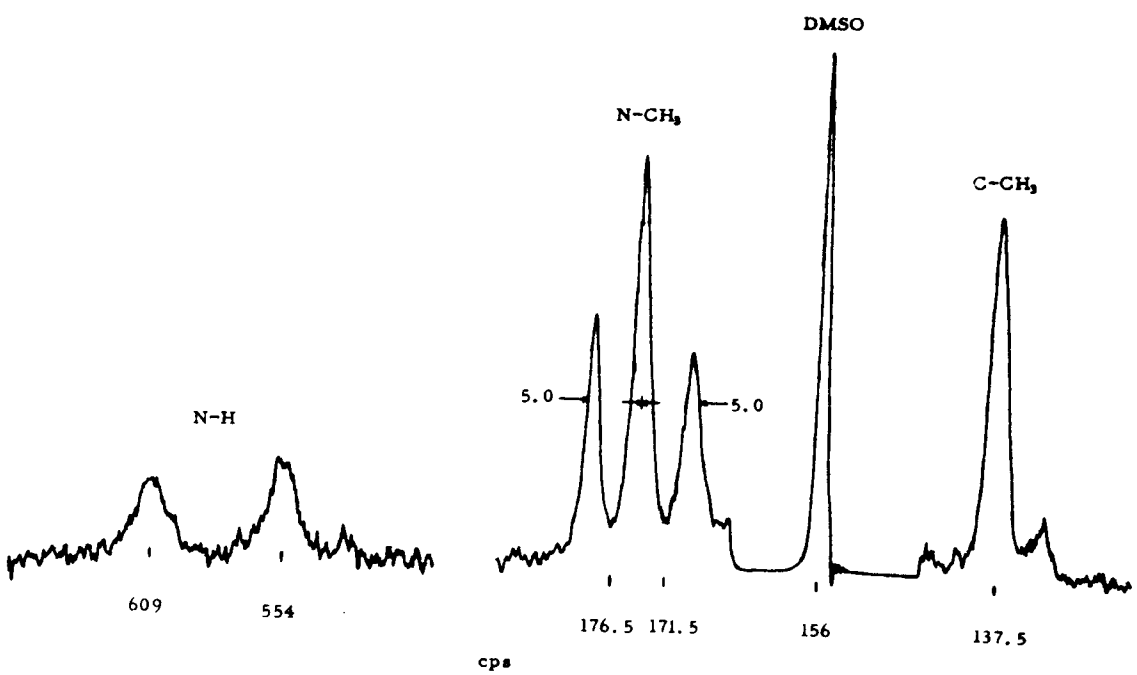

Fig. 11. N.m.r. spectrum of N,N'-dimethylacetamidinium chloride in DMSO. 30°. 60 Mcps.

proton resonances in the ratio 1:1 (Fig. 11, Table I), and the two $N\text{-}CH_3$ resonances in the ratio 1:1 (Figs. 8-11).

The spectra can also be accounted for on the basis of equal populations of the two conformations shown in Figure 13. However,

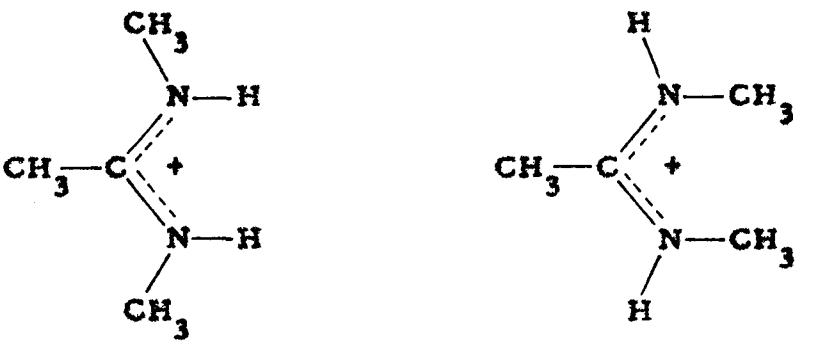

(a) (b)

Fig. 13

the interaction between the "inside" $N\text{-}CH_3$ groups shown in Figure 13b is unfavorable if the planarity of the amidinium system is retained to give maximum resonance stabilization. Scale models show that the conformation represented in Figure 13a is much more sterically favorable than that in Figure 13b. Thus the requirement for equal populations of these two conformations is difficult to rationalize.

A statistical mixture of the three possible conformations (Figs. 12 and 13) would satisfy the spectral requirements only if the chemical shifts of the "inside" $N\text{-}CH_3$ groups in Figure 12 and Figure 13b were identical. This seems rather difficult to imagine because of

the difference of the environments of the methyl groups in the two conformations. The conformation shown in Figure 13a is also considered to be less sterically favorable than that in Figure 12. The three methyl groups approach the unfavorable steric situation of the three methyl groups in 1,2,3-trimethylbenzene (44).

The single "outside"-"inside" conformation (Fig. 12) for N,N'-dimethylacetamidinium chloride thus appears to best fit all of the spectral results obtained.

The effect of variation in temperature on the nitrogen-proton resonance signals for acetamidinium chloride (Ia) in anhydrous DMSO is shown in Figure 14 (Table V). The two clearly distinguishable proton signals progressively decrease in height, broaden, and coalesce into a broad singlet over the temperature range 37.4° to 115.3°. The observed signal separation ($\delta\nu_{\infty}$) at 30° is 29 cps and the line widths at half-height ($\Delta\nu_{\frac{1}{2}}$) are respectively 11 and 10 cps for the low field and higher field signals.

Activation parameters for this process have been calculated using the method of Gutowsky and Holm (45). The observed signal separation at 30° ($\tau \rightarrow \infty$) has been taken as the true signal separation ($\delta\nu$) since $\delta\nu/\delta\nu_{\infty} = 1.002$. This latter value was calculated (45) using $T_2 = 0.03$ sec., obtained from the relationship $2/T_2 = 2\pi\Delta\nu_{\frac{1}{2}}$, where $\Delta\nu_{\frac{1}{2}}$ was the average of values obtained for the two nitrogen-proton signals at 30°.

Fig. 14. Temperature dependence of N-H proton signals of acetamidinium chloride in DMSO. 60 Mcps.

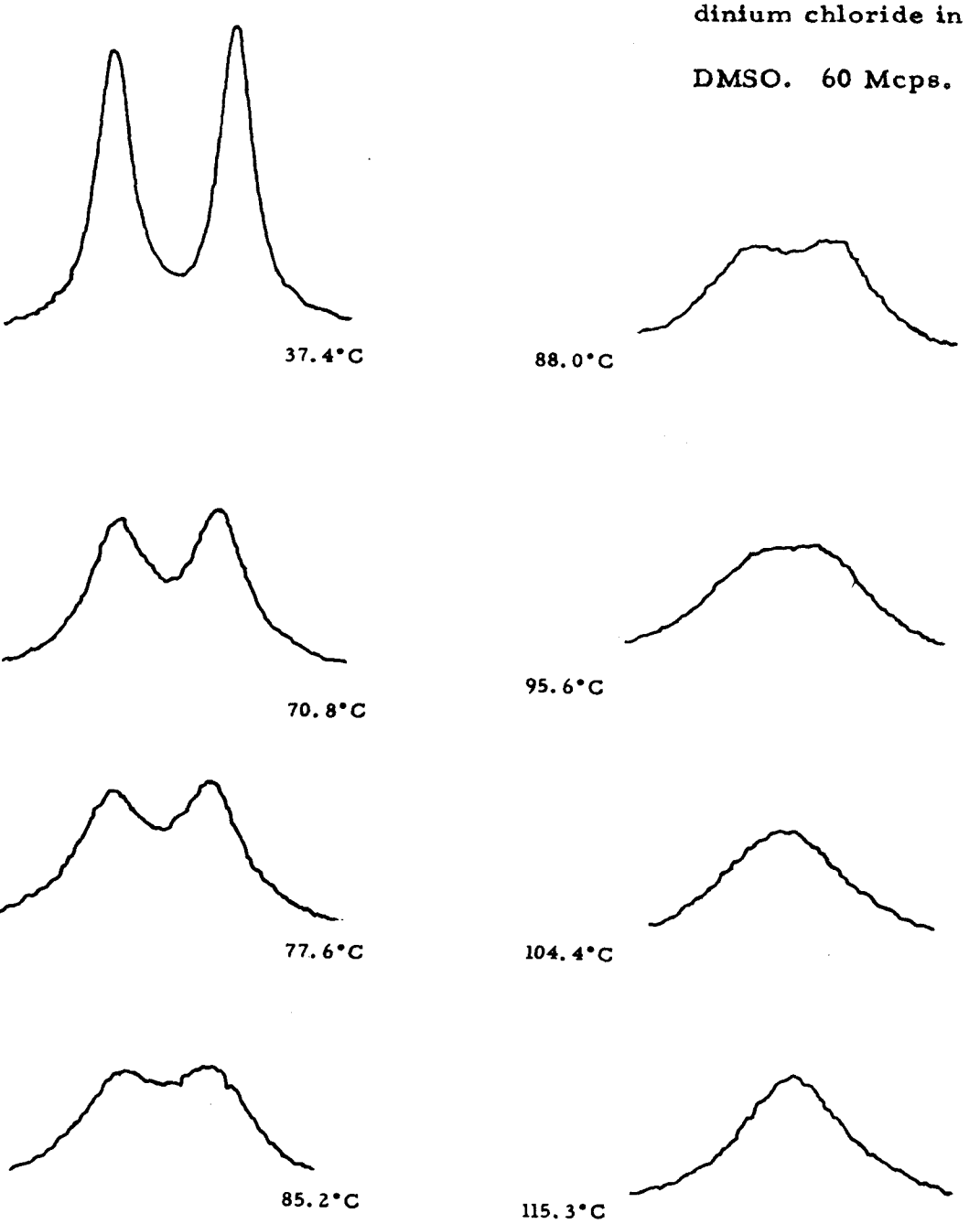

Although $\delta\nu \simeq \delta\nu_{\infty}$ (30°), the quantity $2\pi T_2\delta\nu$ is sufficiently small (5.6) so that as the two signals begin to coalesce with increasing temperature the observed peak separation $\delta\nu_e$ at a temperature must be corrected for overlap of the two collapsing signals (45).

Activation parameters calculated after making these corrections are $E_a = 9 \pm 2$ kcal/mole and the frequency factor k_o is $10^5 - 10^7$.

The method used for this calculation requires that the value of T_2 for the signals be independent of temperature or the exchange process. It is obvious from an inspection of Figure 14 that this is not the case in this study. Whereas $T_2 = 0.03$ sec. for the signals at 37°, the value of T_2 calculated from the signal width ($\Delta\nu_{\frac{1}{2}} = 30$ cps) at 115° is about 0.01 sec. Further increase of temperature did not noticeably sharpen this signal. Since T_2 is markedly temperature dependent in this system, accurate kinetic analysis is impossible unless the mathematical form of this dependence could be obtained. Qualitatively, the decrease of T_2 with temperature will cause the apparent value of E_a to be less than the true value. This is shown by the value of $E_a = 25 \pm 8$ kcal/mole calculated assuming $T_2 = 0.01$ sec. Thus the true value of E_a is undoubtedly greater than the calculated 9 ± 2 kcal/mole.

The process responsible for the coalescence of the two separate nitrogen-proton signals is considered to be rotation about the C_{CN}-N partial double bonds in acetamidinium chloride. A comparison of

amidinium groups with amide groups leads to the conclusion that barriers to rotation in the latter should be less than those in the former. Restricted rotation in amides is rationalised by contributions of resonance structures of the type shown in Figure 6a involving charge separation (10). The C_{CO}-N bond number (46) in amides is no doubt less than 1.5 since the ionic resonance structure (Fig. 6a) is of higher energy than the normal structure. The amidinium group, being symmetric and possessing a formal positive charge, would be expected to have equal double bond character associated with each C_{CN}-N bond (bond number 1.5). Thus the greater double bond character associated with the C_{CN}-N bonds in amidinium groups allows the prediction of a larger barrier to rotation than in amides.

Typical barriers to rotation in amides are the following: formamide-^{15}N, 18 $\pm$ 3 kcal/mole (12); dimethylformamide, 18.3 $\pm$ 0.7 kcal/mole; dimethylacetamide, 10.6 $\pm$ 0.4 kcal/mole; and dimethylpropionamide, 9.2 $\pm$ 0.7 kcal/mole (11). The value of E_a obtained for acetamidinium chloride is the correct order of magnitude for typical rotations about C_{CO}-N bonds, but less than that expected on the basis of the arguments presented above. However, since this value is considered to be too small due to variation of T_2 with temperature, no conclusions can be reached.

Experimental justification for the above argument relating activation energies for rotation to the degree of double bond character

has been obtained by Fraenkel (19). He has shown that the barrier to rotation about the C_{CO}-N bond in dimethylformamide in 100% sulfuric acid is 3 kcal/mole higher than that obtained in pure DMF. The oxygen-protonated form represented in Figure 6b is considered to be responsible for restricted rotation in amides under these conditions. Since the amide now possesses a formal positive charge, it is anticipated that the double bond character of the C_{CO}-N bond should increase. This agrees with the experimental results.

It was thought at one time that the doublet nitrogen-proton resonances in the n.m.r. spectra of I, and III (Table I) could be explained by an unsymmetrical ion-pairing of the anion with its corresponding amidinium group. If the anion were much closer to one of the two nitrogens in the amidinium moiety it would be expected that the two sets of nitrogen-protons would be in different magnetic environments and hence their resonance signals would show different chemical shifts. This was considered possible since it has been pointed out that DMSO has a relatively poor ability to solvate anions (35).

Several subsequent observations required the rejection of this hypothesis. The n.m.r. spectra of Ia and Ib (Table I) are essentially identical although the anions are chloride and nitrate, respectively. The n.m.r. spectrum of IV in DMSO (Table I) shows only a single nitrogen-proton resonance even though the possibility for an

unsymmetrical ion-pair is also present in this system. Finally, N,N'-dimethylacetamidinium chloride (II) shows the two non-equivalent $N-CH_3$ resonances in water (Fig. 8) where solvation of the chloride ion and amidinium ion would be expected to prevent ion-pair formation.

On an intuitive basis, an unsymmetrical ion-pair would localize the positive charge in the amidinium group leading to a considerable loss in resonance stabilization.

N-H and $N-CH_3$ N.m.r. Spectral Assignments

Although the existence of magnetically non-equivalent "inside" and "outside" nitrogen-protons in I, II, and III, and $N-CH_3$ groups in II, has been established, absolute assignments of the resonance signals to the conformationally different protons and methyl groups has not yet been discussed. A comparison of the spectral results for II and IV (Table I) allows a tentative proton assignment to be made. The nitrogen atoms in the amidinium groups of II and IV are similar, each being bound to a central trigonal carbon atom, a tetrahedral methyl group in II, and a tetrahedral methylene group in IV. The similarity between the chemical shifts of the "outside" nitrogen-protons in IV at 608 cps, and the nitrogen-proton signal in II at 609 cps suggests that this latter resonance corresponds to the "outside" proton in II; the "inside" proton thus corresponding to the signal at 554 cps.

An analogous assignment is made by Sunners (12). The nitrogen protons in formamide-^{15}N give two signals which are separated by

12-13 cps depending on the solvent. The higher field proton is assigned to the "inside" position (cis to the carbonyl oxygen) by a comparison of the magnitudes of the splittings produced in these two proton signals by the formyl proton. The higher field nitrogen-proton coupling constant with the formyl proton is ~13 cps while the coupling with the lower field nitrogen proton is ~2 cps. Replacement of the formyl proton by deuterium destroys coupling with the low field proton while $J_{D,H}$ = 2 cps for the higher field proton. This assignment is based on the assumption that trans coupling is stronger than cis coupling in analogy with unsaturated carbon systems (47). This assignment in formamide-^{15}N agrees with the predicted screening of these protons by the carbonyl group (47). Unsubstituted amides and amidinium groups are structurally similar. Thus the same relative screening of the inside and outside protons might be expected.

It should be noted that the lower field nitrogen-proton resonance for acetamidinium chloride (I) is slightly broader than the higher field resonance (Table I). This could be interpreted to mean that unresolved spin-spin coupling of the C-methyl group protons with the nitrogen-proton corresponding to this signal is greater than with the proton corresponding to the higher field signal. If trans-1,3-coupling were greater than cis-1,3-coupling, this analysis would require a reversal of the previously postulated proton assignments. However, the relative magnitudes of trans and cis -1,3-couplings have not been clearly

established (48). Further, by far the greatest contribution to signal shape of these nitrogen protons is quadrupole broadening by ^{14}N (28). Since $\Delta\nu_{\frac{1}{2}} \simeq$ 10-11 cps for these signals, while 1,3-coupling constants are on the order of 0.4-1.7 cps, the slightly greater value $\Delta\nu_{\frac{1}{2}}$ for the low field signal may well be the result of unequal quadrupole broadening of the two nitrogen protons. This is not unreasonable since the N-H bond lengths in formamide (vapor phase) have been found to differ by 0.012 Å. Costain and Dowling (49) have assigned bond lengths of 1.002 and 1.014 Å ($\pm$ 0.005 Å) to the nitrogen-proton bonds trans ("outside") and cis ("inside") with respect to the carbonyl group. Although these parameters were determined for molecules in the vapor phase, there is no obvious reason to suspect that they should become equal in solution. Sunners (12) uses these results to explain his observation of unequal ^{15}N spin coupling with the two nitrogen protons in formamide-^{15}N. If a similar difference in bond lengths existed in amidinium ions, unequal quarupole coupling with ^{14}N might also be expected.

On the basis of chemical evidence presented below, and the nitrogen proton spectral assignments just discussed, an assignment of the two N-methyl group resonances exhibited by N,N'-dimethylacetamidinium chloride (II) (Figs. 8-11) to the "inside" and "outside" positions is possible. The higher field N-methyl group signal has been assigned to the "inside" group, and the lower field signal to the "outside" N-methyl group.

This assignment is further confirmed by an analysis of the shapes of the signals corresponding to the C-CH_3 and N-CH_3 protons. Values of $\Delta\nu_{\frac{1}{2}}$ for the signals given by a water solution of II (Fig. 8) are C-CH_3, 1.6 cps; N-CH_3 (high field), 1.7 cps; and N-CH_3 (low field), 1.0 cps. The same relative magnitudes of $\Delta\nu_{\frac{1}{2}}$ for the C-CH_3, and N-CH_3 signals are observed in all of the spectra of II independent of solvent. It is expected that ^{14}N quadrupole broadening of the N-CH_3 signals should be present, but reduced considerably in comparison to systems in which the protons are bonded directly to the ^{14}N nucleus. The difference in $\Delta\nu_{\frac{1}{2}}$ for the two N-CH_3 signals might be attributed to unequal quadrupole interaction with nitrogen. However, a comparison of $\Delta\nu_{\frac{1}{2}}$ for these protons with that for the C-CH_3 proton signal implies that quadrupole broadening is not the major contributor to the N-CH_3 signal width. Interactions between ^{14}N and the C-CH_3 protons should be less than those between ^{14}N and the directly attached methyl groups. However, the line width of the C-CH_3 proton signal is practically the same as that of the high field N-CH_3 proton signal. These relative line widths can be explained by unequal spin-spin coupling between the C-CH_3 protons and the protons in the two conformationally different N-CH_3 groups. The N-CH_3 group giving rise to the higher field signal is coupled more strongly to the C-CH_3 protons than that corresponding to the low field signal.

The same relative line widths for the high and low field N-CH_3 signals in the spectra of dimethylamides have been observed. Kowalewski (50, 13) has observed a splitting of 0.4-0.5 cps in the high field N-CH_3 signal of dimethylacetamide, while the lower field resonance is only a singlet. A 1,4-splitting of 0.4 cps has also been observed in the N-CH_3 signal of N-methylacetamide (50, 13). Other structural studies on N-methylacetamide indicate that it can be formulated by the single conformation with the N-CH_3 group trans to the C-CH_3 group ("inside") (51). This allows the assignment of the higher field N-CH_3 signal for dimethylacetamide to the "inside" N-CH_3 group. Trans-coupling between methyl groups in dimethylacetamide thus appears to be stronger than cis-coupling. These results agree with the observations that $J_{trans} > J_{cis}$ (1,4-coupling between methyl protons) by Fraser (52) and Richards and Beach (53) in ethylenic systems. By an analogous argument for N,N'-dimethylacetamidinium chloride, the higher field N-CH_3 signal is assigned to the "inside" methyl group conformation; the lower field signal thus corresponding to the "outside" conformation.

Nitrogen-Proton Exchange Reactions for Amidinium Ions

Dilute aqueous acid. The n.m.r. spectra of aqueous acid solutions, 3.2 M in acetamidinium chloride (Ia), show that the nitrogen-proton and water-proton resonance signals are markedly dependent on the acidity of the solution. As the pH of the solutions is

decreased from 5.6 to 3.0 the water-proton resonance changes from a broad to a sharp singlet. The nitrogen-proton resonance, absent at pH 5.6, becomes distinguishable as a very broad singlet as the acidity is increased. The $C\text{-}CH_3$ resonance is a sharp singlet at all pH values. These results indicate that one or several pH dependent, nitrogen-proton, solvent-proton exchange processes occur in dilute acid solutions of Ia.

Grunwald (21, 22) and Meiboom (24-26) have reported very thorough studies on proton exchange reactions of ammonium and methylammonium ions in dilute aqueous acid solutions. The exchange processes which must be considered in these systems are the following:

$$AH^+ + H_2O \xrightarrow{k_4} A + H_3O^+ \qquad (1)$$

$$AH^+ + {}^-OH \xrightarrow{k_5} A + H_2O \qquad (2)$$

$$AH^+ + A \xrightarrow{k_6} A + AH^+ \qquad (3)$$

$$AH^+ + H_2O + A \xrightarrow{k_7} A + H_2O + AH^+ \qquad (4)$$

The numbering of specific rate constants for these reactions is that used by the above authors. The ammonium ions are designated by AH^+, and A refers to the corresponding amine. Reactions 1, 2, and 4 may all involve more than one intermediary water molecule (21).

The resultant rate law for proton exchange is (21, 24):

$$\text{Rate}/(AH^+) = k_4 + k_5K_W/(H^+) + (k_6+k_7)K_A(AH^+)/(H^+) \qquad (5)$$

K_A is the acid dissociation constant for the AH^+ ion, and K_W is the dissociation constant for water.

The rate of proton exchange may be expressed in terms of the mean-lifetime (τ) of an AH^+ molecule before it exchanges one of its protons. The resultant rate expression is thus

$$\text{Rate}/(AH^+) = 1/\tau \qquad (6)$$

It may be seen from an inspection of equations 5 and 6 that the dependence of $1/\tau$ on (AH^+) and (H^+) will allow an elucidation of the proton exchange processes that occur. In the case of the ammonium ion (21), values of $1/\tau$ were obtained from the half-width of the nitrogen-proton resonance. For methylammonium chloride (22, 24), values of $1/\tau$ were calculated from the shape of the $N\text{-}CH_3$ quartet. This latter method is valid since the $N\text{-}CH_3$ quartet pattern of methylammonium ion is due to coupling with the nitrogen-protons. The shape of the pattern is thus determined by the mean-lifetime of the protons on the nitrogen atom.

It was thought that a study similar to those discussed above would be applicable to exchange processes of acetamidinium chloride (Ia). There is no methyl group attached directly to nitrogen in Ia and thus there are no splittings of the type analyzed for methylammonium ion. At the time that this work was initiated, the author was

not aware of the method of determining values of τ from the nitrogen-proton resonance signal. However, in retrospect, results from this method of analysis would perhaps have been meaningless due to the magnetic non-equivalence of the protons on nitrogen in Ia.

An alternative approach was used by Meiboom in the study of methylammonium chloride (24). If one considers only the proton exchange reactions which involve water (equations 1, 2, and 4), a quantity τ' may be defined as the mean-lifetime of an AH^+ molecule before exchange of a proton with water. A rate law is thus obtained (eq. 7) relating $1/\tau'$ to the specific rate constants for proton exchange

$$1/\tau' = k_4 + k_5K_W/(H^+) + k_7K_A(AH^+)/(H^+) \qquad (7)$$

involving water molecules. Although τ' is not directly measurable for the amidinium ion system, or the methylammonium ion system, it may be obtained from transverse relaxation times (T_2) of the water-proton magnetic resonance signals (24).

The quantities $1/T_2$ for the water-proton resonance signals in 1.75 M and 3.06 M solutions of acetamidinium chloride (Ia) in aqueous hydrochloric acid at various acidities are given in Table VI. The values of $1/T_2'$ obtained for a pure water sample run before each sample of Ia are given in Table VII. These values were determined as described in the experimental section. The n.m.r. probe temperature was approximately 33° during these measurements.

The transverse relaxation time of the water-protons under conditions of relatively slow exchange is related to τ_{H_2O}, the mean-lifetime of protons bonded in water before transfer to nitrogen, by the relationship (24, 54)

$$1/\tau_{H_2O} = 1/T_2' - 1/T_2 \qquad (9)$$

T_2' is the transverse relaxation time for water-protons under non-exchanging conditions and is obtained from measurements of T_2 on the pure water sample.

For rigorous application of equation 9, the quantities $1/T_2$ and $1/T_2'$ should be functions of the rate of the exchange process involving water molecules in a uniform magnetic field H_o(55). However, the experimentally measured values of transverse relaxation times are usually less than the theoretically predicted values because of inhomogeneity of the external magnetic field (56). The contribution of field inhomogeneity to the measured transverse relaxation times can be approximated by the expression (57)

$$1/T_2 = 1/T_{2_{ex.}} + 1/T_{2\ field} \qquad (10)$$

in equation 10. $1/T_{2_{ex.}}$ is determined by the exchange process and $1/T_{2\ field}$ is the added broadening due to an inhomogeneous magnetic field. If external field inhomogeneity is constant for all samples, differences of measured values of $1/T_2'$ and $1/T_2$ (eq. 9) bring about a cancellation of the field contribution. The validity of this approximation has been demonstrated by Meiboom et al. (24) with the

observation that values of τ_{H_2O} calculated in the above manner (eq. 9) were essentially identical under conditions such that T_2' was about 0.3 sec. or 1.0 sec. In this study T_2' was about 0.5 sec.

The mean-lifetime of an amidinium group before a proton is transferred to water, τ', is given by equation 11 (24).

$$\tau' = (AH^+)\,\tau_{H_2O}/2(H_2O) \qquad (11)$$

Values of τ_{H_2O} and τ' calculated for each sample of Ia are reported in Table II. A discussion of errors is given in the experimental section.

For each amidinium ion concentration, a plot of log τ_{H_2O} versus pH is acceptably correlated by a straight line of slope 1.0. The mean-lifetime of protons bonded to water before transfer to nitrogen is thus directly proportional to (H^+). The dependence of $1/\tau'$ on acidity is given in Figure 15. The data for both amidinium ion concentrations can be reasonably correlated by the same straight line of slope 8×10^{-4} mole $\ell.^{-1}$ sec.$^{-1}$ in a plot of $1/\tau'$ versus $1/(H^+)$. This shows that $1/\tau'$ is apparently independent of (AH^+) over almost a two-fold variation in the concentration of Ia. This fact is further demonstrated in Figure 16, in which a plot of $1/\tau'$ versus $(AH^+)/(H^+)$ gives two divergent straight lines whose slopes give the ratio 1.8. This corresponds closely to 1.75, the ratio of the two concentrations of amidinium salts.

TABLE II

Mean-Lifetimes of Protons on Acetamidinium Ions and Water in Aqueous Solutions of Acetamidinium Chloride (33°)

(AH^+)(M)	pH	$(H^+)\times10^5$(M)	Density(g./cc)	(H_2O)(M)	$1/\tau_{H_2O}$(sec^{-1})	$1/\tau'$(sec^{-1})
1.750±.002	5.130±.005	0.74±.01	1.0245±.0002	47.68±.02	2.18±.08	119±4
"	4.950±.005	1.12±.01	"	"	1.16±.08	63±4
"	4.810±.005	1.55±.02	"	"	0.93±.08	51±4
3.059±.005	5.080±.005	0.83±.01	1.0449±.0002	41.94±.04	3.86±.08	106±2
"	4.540±.005	2.88±.04	"	"	1.15±.08	32±2
"	4.290±.005	5.13±.06	"	"	0.59±.08	16±2

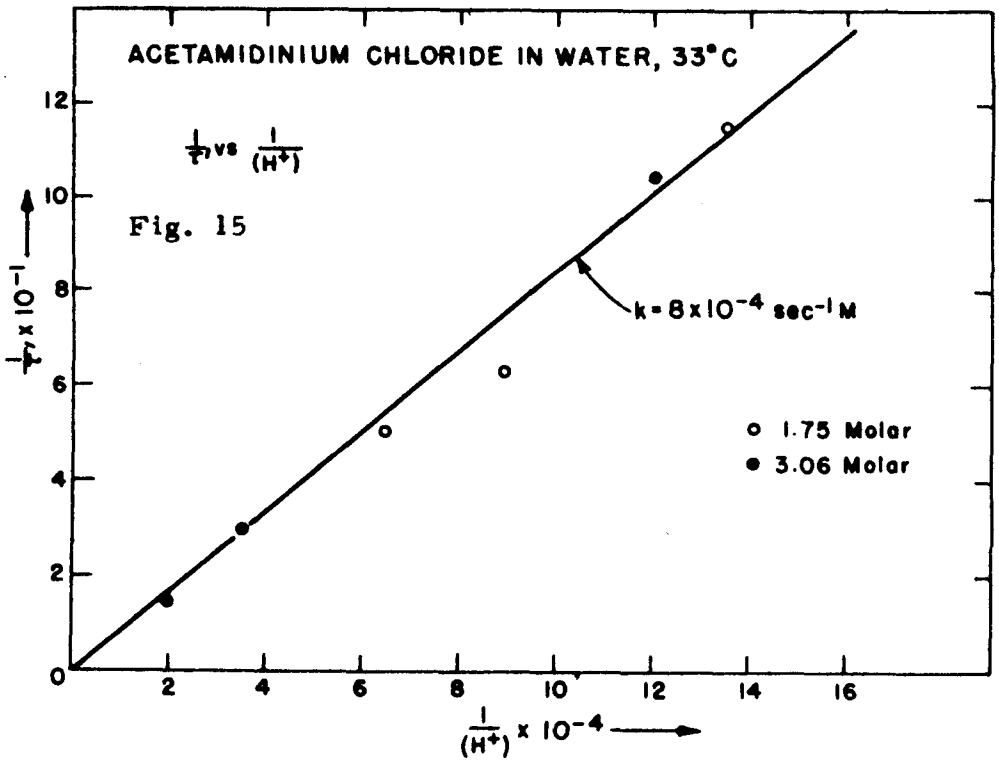
ACETAMIDINIUM CHLORIDE IN WATER, 33°C
$\frac{1}{\tau'}$ vs $\frac{1}{(H^+)}$
Fig. 15
$k = 8 \times 10^{-4}$ sec^{-1} M
○ 1.75 Molar
● 3.06 Molar
$\frac{1}{\tau'} \times 10^{-1}$
$\frac{1}{(H^+)} \times 10^{-4}$

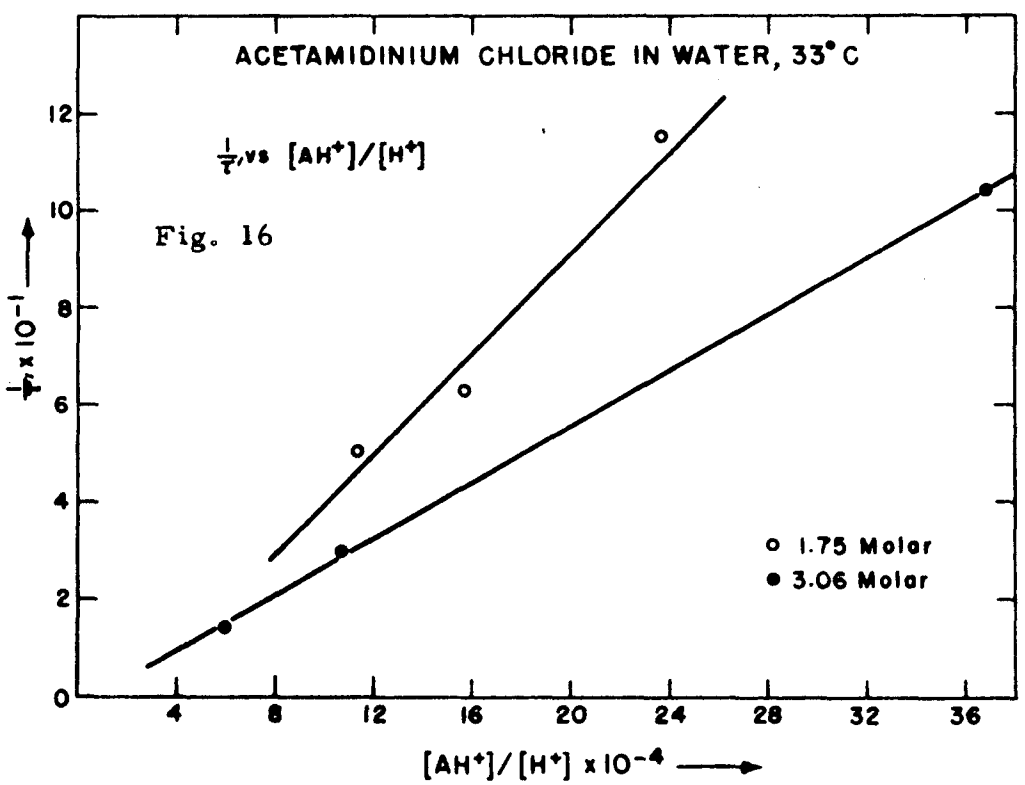
ACETAMIDINIUM CHLORIDE IN WATER, 33°C
$\frac{1}{\tau'}$ vs $[AH^+]/[H^+]$
Fig. 16
○ 1.75 Molar
● 3.06 Molar
$\frac{1}{\tau'} \times 10^{-1}$
$[AH^+]/[H^+] \times 10^{-4}$

From equation 7, the intercept in Figure 15 should give the rate constant k_4. The intercept in this plot is zero within experimental error. An estimation of the largest possible positive intercept allows an upper limit of 6 sec.$^{-1}$ to be placed on k_4. The independence of $1/\tau'$ on (AH^+) and its inverse first order dependence on (H^+) show that $k_7K_A << k_5K_W = 8 \times 10^{-4}$. Assuming a value of $k_4 = 6$ sec.$^{-1}$, an upper limit of $\sim 10^{-5}$ sec.$^{-1}$ can be estimated for k_7K_A. The major process for proton exchange in dilute aqueous acid solutions of Ia is therefore that designated by reaction 2 involving exchange through hydroxide ion.

The rate constants for proton exchange processes in aqueous acid solutions of ammonium ions (22) at 25° along with those for acetamidinium chloride at 33° are shown for comparison in Table III.

All of the rate constants shown in Table III are somewhat dependent on medium effects (22). The values reported for the ammonium ions have been extrapolated to infinite dilution (zero ionic strength). The greatest effect of medium is found for values of k_4 and K_A. The value of k_4 for ammonium chloride (21) decreases from 22.7 to 9.9 sec.$^{-1}$ upon going from 0.25 to 3 M solutions. The value of K_A for ammonium chloride (21) decreases from 5.26×10^{-10} to 2.3×10^{-10} M over the same concentration range. Thus values of $k_7K_A^*$ and k_4^* are not directly comparable to amidinium ion data, but comparisons of the order of magnitude of these constants are valid.

TABLE III

Summary of Rate Constants for Proton Exchange. Ammonium Ions (25°) and Acetamidinium Ions (33°)

Cmpd.	$K_A^{\circ} \times 10^{10}$ (M)	k_4° (sec^{-1})	$k_5 \times 10^{-10}$ ($sec^{-1}M^{-1}$)	$k_5K_W \times 10^{4}$ ($sec^{-1}M$)	$k_6 \times 10^{-8}$ ($sec^{-1}M^{-1}$)	$k_7 \times 10^{-8}$ ($sec^{-1}M^{-1}$)	$k_7K_A^{\circ} \times 10^{-2}$ (sec^{-1})	Ref.
NH_4^+	5.68	24.4	3.0(20°)	1.9	11.5	0.9	5.1	(22)
$CH_3NH_3^+$	0.242	0.90	3.7(25°) 3.2(19°)	3.8 2.0	4.0	5.3	1.3	(22, 24)
$(CH_3)_2NH_2^+$	0.168	0.52	-	-	0.5	7.3	1.2	(22)
$(CH_3)_3NH^+$	1.57	4.0	-	-	0.0	4.0	6.3	(22)
$CH_3C(NH_2)_2^+$	(0.001)	< 6	3.6	8.0	-	(1)	(0.001)	(This Dissertation)

From an inspection of Table III it is obvious that the most important proton exchange processes for the ammonium ions are those represented by equations 3 and 4. While, for acetamidinium ion, process 2 is the greatest contributor. The reason for this switch in mechanism can be understood on the basis of the relative acidities of ammonium and acetamidinium ions. Unfortunately, a value of K_A for acetamidinium ion is not available. However, it will certainly be less than that for the ammonium ions since in synthetic practice, acetamidinium chloride is isolated in excellent yield from solutions containing large amounts of ammonia. Potentiometric titration curves obtained by titrating aqueous solutions of azo-bis-isobutyramidinium chloride with strong base show no detectable inflection point (58) and are practically superimposable on titration curves obtained by the addition of strong base to water. There is, however, buffering action in the high pH region of the curve. These results indicate that K_A for amidinium ions is probably about 10^{-13} M. (59). An estimate of $k_7 \sim 10^8$ sec.$^{-1}$ M^{-1} is thus obtained assuming that $k_7 K_A \sim 10^{-5}$ sec.$^{-1}$ (Table III).

On the basis of this crude approximation to k_7, it may be seen that the lack of contribution of reaction 7 to proton exchange in acetamidinium chloride solutions is probably due to an extremely low concentration of amidine free base (A) and not necessarily a small value of the specific rate constant k_7.

The mechanism postulated by Grunwald (22) for reaction 4 involves as a rate-determining step proton transfer from a water molecule in the solvation shell of an ammonium ion to a neighboring amine molecule. If a similar mechanism accounts for the analogous process in the case of acetamidinium chloride, a rate constant k_7 of the same order of magnitude is not unreasonable.

The rate constant k_5 for ammonium ion (Table III) has been measured by Eigen and Schoen (60). The values of k_5 (Table III) for methylammonium ion have been calculated by Grunwald and Meiboom (24) assuming a diffusion-controlled reaction. Extrapolating a value for K_W at 33° from data given by Meiboom (24), a value of $k_5 = 3.6 \times 10^{10}$ sec^{-1} M^{-1} (33°) is obtained from the measured value of k_5K_W (Table III) for the reaction of acetamidinium chloride with hydroxide ion. The correlation between these three values of k_5 lends strong support to the mechanistic identification of the proton exchange process for acetamidinium chloride. The slightly larger value of k_5 obtained for Ia than would be expected from a comparison of the sizes of ammonium, methylammonium, and acetamidinium ions, may be explained by the higher temperature at which this reaction was studied.

It has not been possible to examine reaction 3, direct proton transfer between amidinium ions and amidines, since this process does not involve water. An examination of values of k_6 for the ammonium ion systems (Table III) shows that they are of the same order

of magnitude as values of k_7. Since the quantity k_6K_A determines the contribution of this process to the overall exchange rate, it may be reasonably concluded that this process is no more important than reaction 4 in the amidinium ion system.

Strong Acid. The spectrum of N,N'-dimethylacetamidinium chloride (II) in water has been previously discussed (Fig. 8). The spectrum contains two equal area resonance signals at 177.5 cps and 187 cps identified as the methyl group protons belonging to the two conformationally different N-CH_3 groups. In 14% sulfuric acid (Fig. 9) the two N-methyl proton signals of II are each split into doublets (J = 5 cps) by adjacent nitrogen protons. Identification of the protons responsible for this splitting was accomplished by showing that the N-methyl proton signals are only singlets in 60% sulfuric acid -d_2 (Fig. 10), while in 60% sulfuric acid two doublet N-CH_3 signals are present (Fig. 17). In D_2SO_4 the acidic nitrogen protons have undoubtedly been replaced by deuterons, which couple much less strongly with the adjacent methyl protons.

That splitting of N-methyl group protons by their adjacent nitrogen-protons is observed in 14% H_2SO_4 but not in water, indicates that the rate of nitrogen-proton exchange is inversely proportional to the acidity of the medium over this range of acid concentration. These results are in accord with the proton exchange rate dependence on acidity found for Ia in dilute hydrochloric acid solutions (vide supra).

Fig. 17. $N\text{-}CH_3$ proton signals of N,N'-dimethylacetamidinium chloride in sulfuric acid. 30°. 60 Mcps.

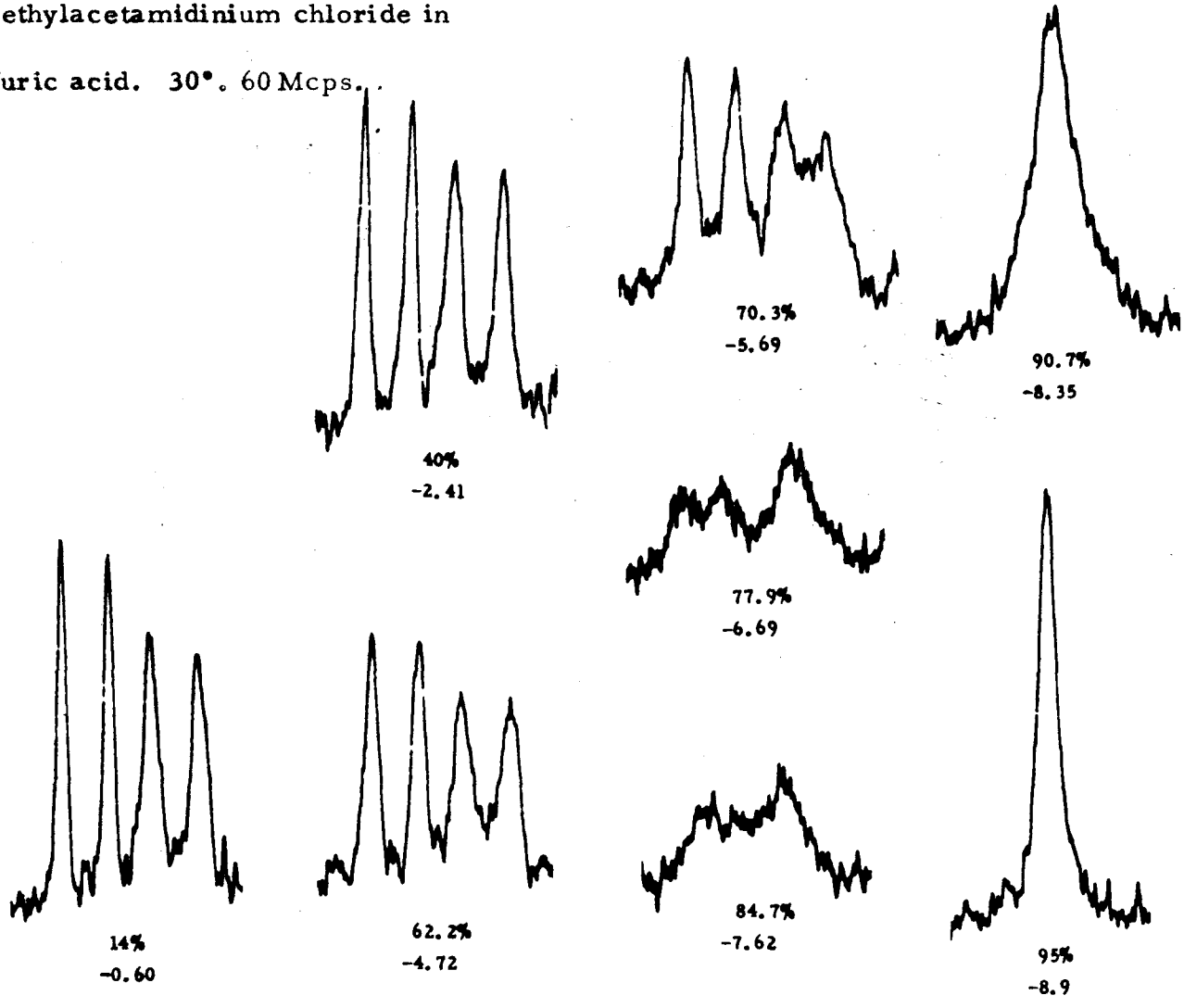

The effect of variation in composition of sulfuric acid-water mixtures on the N-methyl proton spectrum of II is shown in Figure 17. The concentration of II in these solutions is approximately 0.4 M. Only the spectra of the N-CH_3 region is shown. The C-CH_3 resonance signal is a sharp singlet over the entire range of acidity. The nitrogen-protons are not observable in the sulfuric acid-water mixtures between 15 and 62% H_2SO_4. This is due to interference from the H_2SO_4-H_2O solvent signal. In 14% H_2SO_4, the nitrogen protons give two signals at ~425 and ~455 cps. The solvent resonance is a sharp singlet at ~340 cps. As the concentration of sulfuric acid is increased above 15%, the major solvent peak moves downfield obscuring the nitrogen signals and finally at 62.2% H_2SO_4 the two nitrogen-proton signals are again observed at ~433 cps and ~463 cps, while the solvent signal is a sharp singlet at ~550 cps.

The N-methyl proton signals remain essentially unchanged from 14% to 40% sulfuric acid. In 62.2% H_2SO_4, the N-CH_3 doublet patterns are still clearly visible although the signals have begun to broaden and decrease in amplitude. When the percent sulfuric acid is increased to 77.9%, the higher field doublet has almost completely coalesced to a broad singlet while the lower field doublet pattern is still visible although broadened. In 84.7% H_2SO_4, the high field proton signal is a broad singlet and the low field signal is also almost a singlet, although a hint of a doublet structure can be observed. Upon

further increase of sulfuric acid concentration, the two separate broad N-CH_3 resonances coalesce into a singlet resonance.

In 77.9% H_2SO_4-H_2O, the lower field nitrogen-proton signal begins to broaden while the higher field N-H signal remains unchanged. The H_2SO_4-H_2O solvent signal also begins to broaden. In 84.7% H_2SO_4, only the higher field N-H signal at ~410 cps is visible and the major solvent signal is quite broad. As the concentration of acid is increased, the solvent signal broadens further and no N-H resonance signal can be observed at 90.7% H_2SO_4.

The numerical data for the change in the N-methyl proton spectra with an increase in sulfuric acid concentration is given in the Experimental section (Table VIII). The data are presented graphically in Figure 18.

These results indicate the following: 1) The coalescence of the two N-CH_3 doublet signals to two singlets indicates an increase in the rate of nitrogen-proton exchange with increasing acidity; 2) The coalescence of the two separate N-CH_3 singlets into a single sharp singlet implies that the methyl groups lose their distinct "inside"-"outside" conformational identities through a process involving acid; 3) The difference in the acidities for the coalescence of the high field and low field N-methyl doublets implies a difference in rates of nitrogen-proton exchange at the two conformationally different nitrogen atoms in II. A thorough discussion of 3) will be deferred until the process implied by 1) and 2) is discussed.

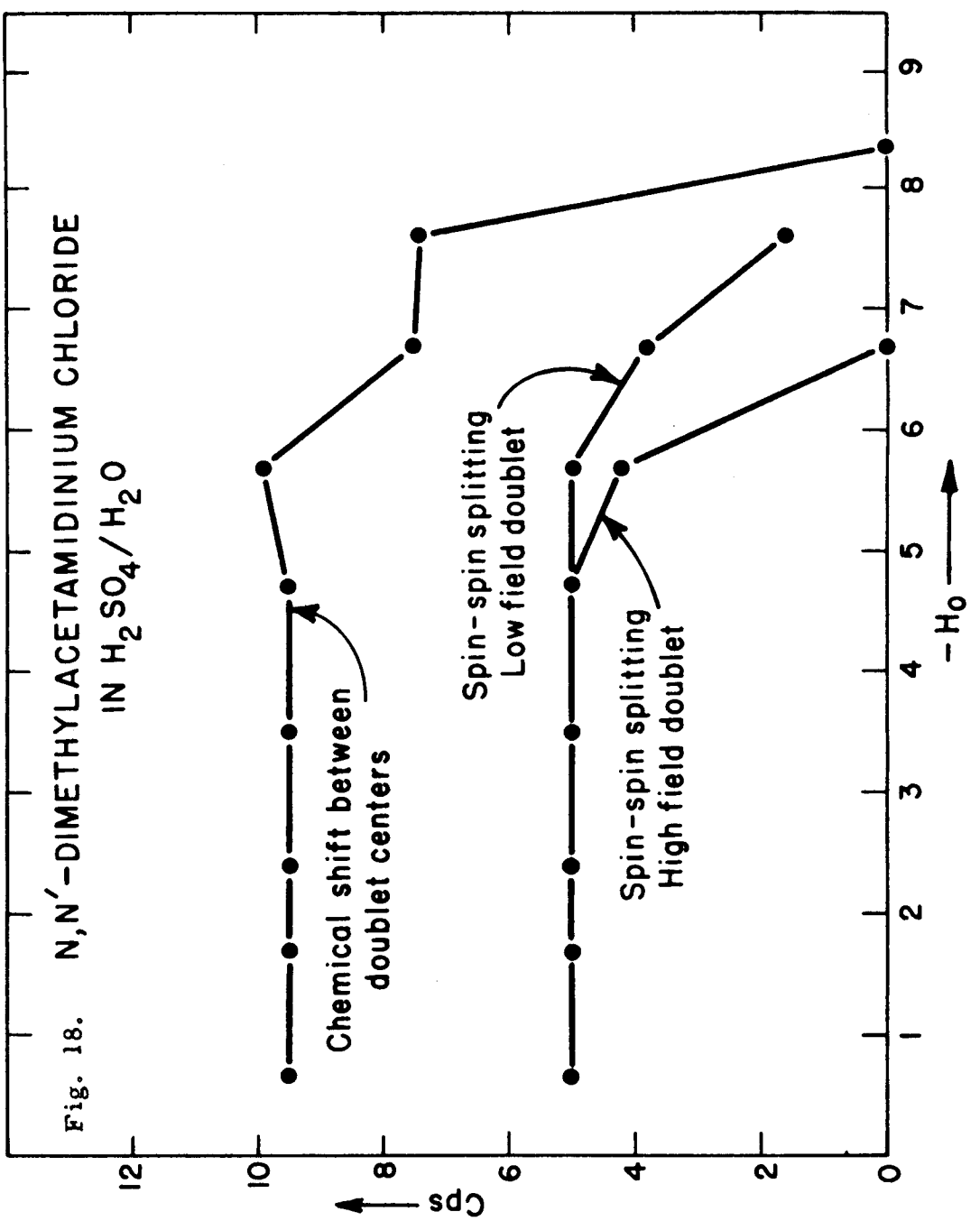
N,N′-DIMETHYLACETAMIDINIUM CHLORIDE
IN H_2SO_4/H_2O
Chemical shift between doublet centers
Spin-spin splitting Low field doublet
Spin-spin splitting High field doublet
cps
$-H_0$
0
2
4
6
8
10
12
1
2
3
4
5
6
7
8
9

Fig. 18.

The coalescence of the two separate N-CH_3 signals of II has been examined in 83-88% D_2SO_4-D_2O mixtures (Fig. 19, Table IX). In the deuterated solvent, the splitting of the N-CH_3 group protons is theoretically reduced by a factor of 7 (J_{D,CH_3} = 0.7 cps) due to replacement of nitrogen protons with deuterons. This allows the process effecting the equivalence of the two N-CH_3 groups to be more clearly studied since spin-spin coupling patterns in these signals are removed. As can be seen in Figure 19, the signals are broad and the maxima poorly defined, preventing an accurate kinetic treatment. Nevertheless, values of $1/\tau$ as a function of acidity have been calculated from these partially coalesced signals by the method of Gutowsky and Holm (45). The value $\Delta\nu_{\frac{1}{2}}$ = 1.7 cps and $\delta\nu_{\infty}$ = 9.8 cps for the N-CH_3 signals of II in 60% sulfuric acid-d_2 (Table IX) were used to calculate a value of $2 \cdot T_2\delta\nu$ = 11, which was used to correct the apparent signal coalescence rate. Values of $1/\tau$ at specified acid concentrations are shown in Table IX . A plot of log $1/\tau$ versus $-D_o$ (61) (Fig. 20) shows considerable scatter and can be correlated by lines of slope 0.8 to 1.3. The best line through the data, determined visually, gives a slope of 1.1.

The samples studied contained approximately 0.05 g. of N,N'-dimethylacetamidinium chloride (II) in 1 ml. of solution. Since the concentration of II in each sample is not accurately known, and because the data do show considerable scatter, it is not possible to estimate the dependence of τ on the concentration of II. However,

Fig. 19. $N\text{-}CH_3$ proton signals for N,N'-dimethylacetamidinium chloride in sulfuric acid-d_2. 30°. 60 Mcps.

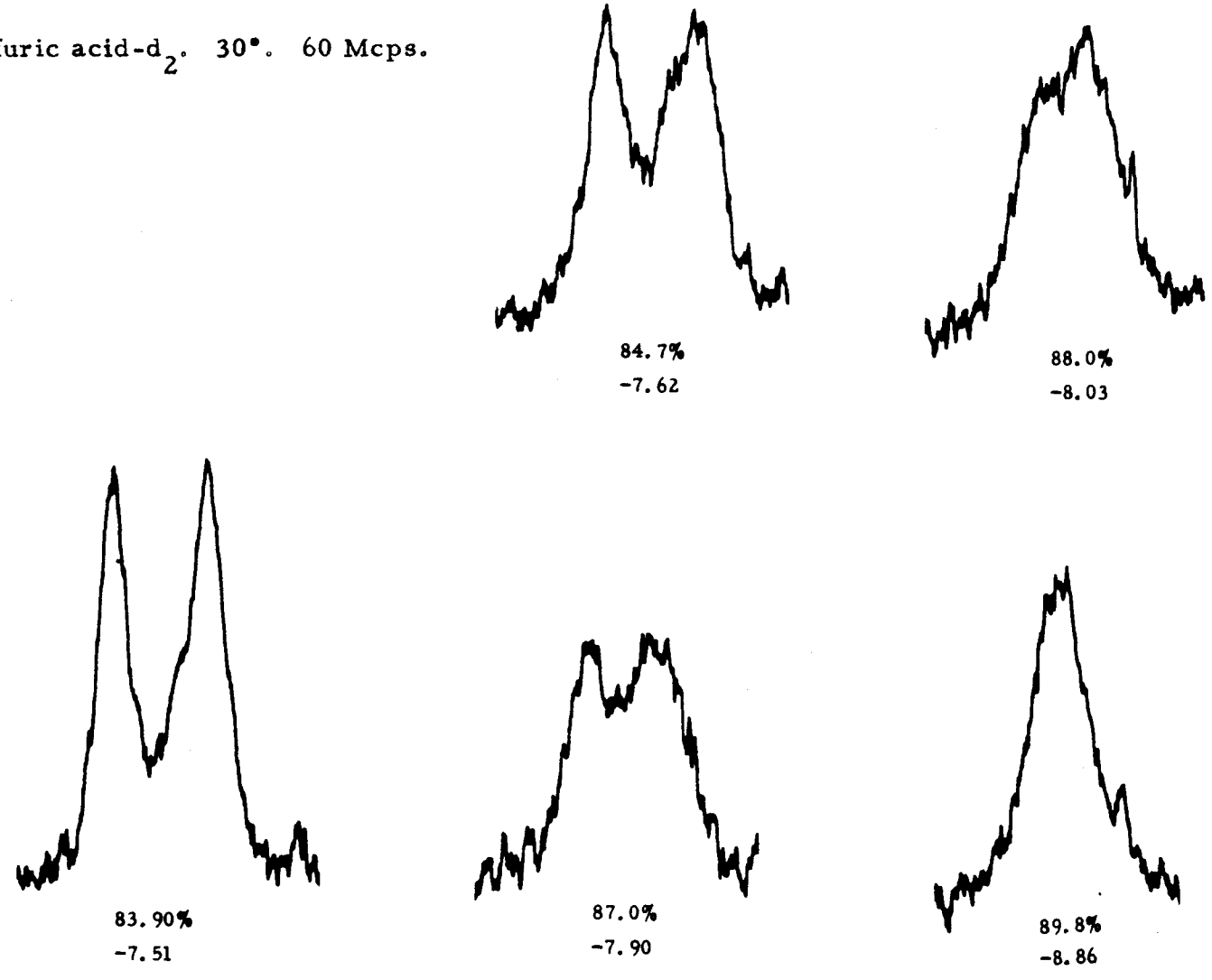

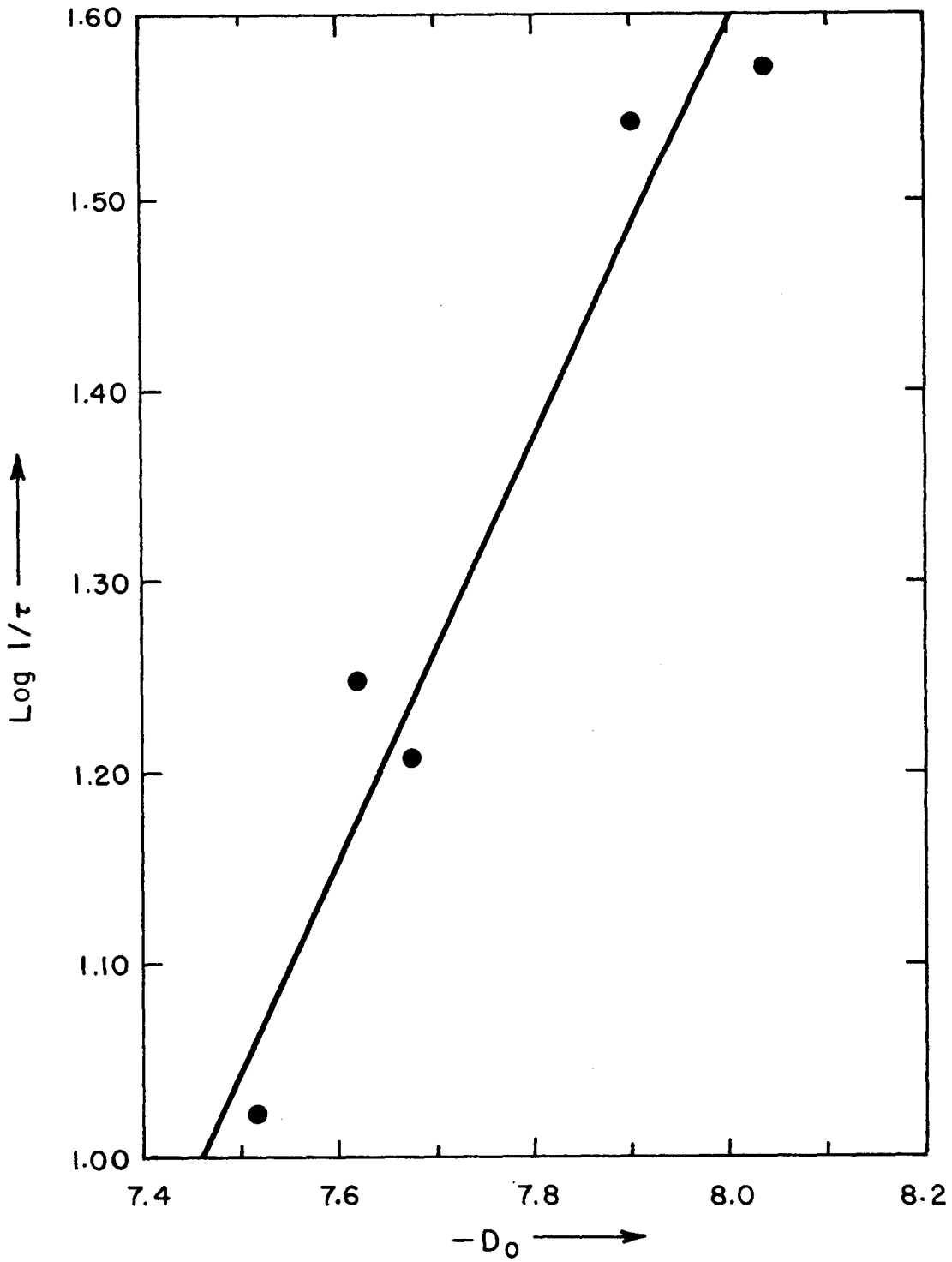

Fig. 20. Log $1/\tau$ versus $-D_o$. N,N'-dimethylacetamidinium chloride in sulfuric acid-d_2. 30°.

since each solution contained approximately the same amount of II, it is felt that the dependence of log $1/\tau$ on $-D_o$ (Fig. 20) indicates the rate law $1/\tau = kd_o$ for the process causing the coalescence. This implies a simple protonation mechanism for this process. The slope of a plot of $1/\tau$ versus d_o (61) gives a value of $k = 4 \times 10^{-7} M^{-1}$ sec.$^{-1}$, as does the intercept in Figure 20.

For the purposes of the following mechanistic treatment, it will be assumed that k is subject only to medium effects and is not kinetically dependent on the concentration of the amidinium salt. This is assumed in part because of lack of appropriate data for the dependence of $1/\tau$ on the concentration of the amidinium ion, and secondly because of the reasonableness of the kinetic conclusions which are reached.

The kinetic dependence of the doublet coalescence in each $N\text{-}CH_3$ signal on acidity has not been determined. A kinetic treatment on this process would be practically impossible, since the separate $N\text{-}CH_3$ signals are broadening simultaneously with doublet coalescence due to the process which at a higher acidity will cause them to coalesce into a singlet. It is suggested, however, that the processes producing each of these effects can be represented by the same kinetic rate law. If this rate law is that previously given and

$$1/\tau = kho \qquad (12)$$

reproduced in equation 12, the following reasonable mechanistic steps shown in Figure 21 will account for the results. Protonation

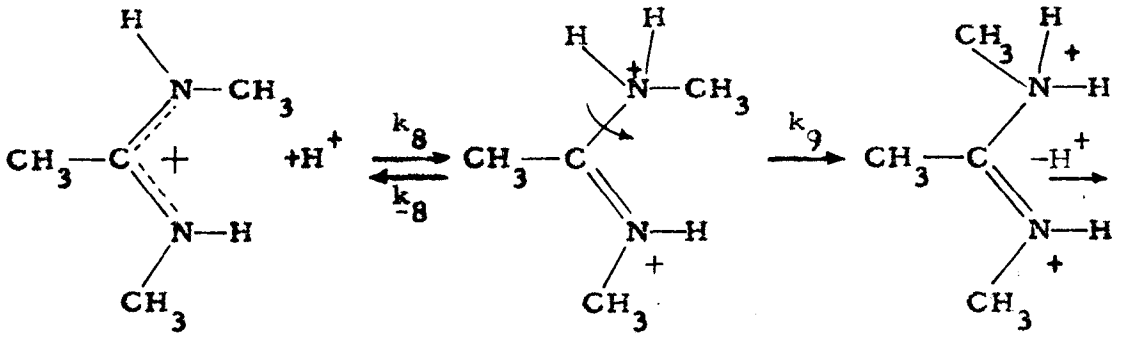

II IIa IIb

Fig. 21

of II followed by rapid deprotonation of IIa will cause the doublet N-CH_3 signal, corresponding to the nitrogen that is protonated, to coalesce into a singlet if the deprotonation step is random. That is, the protons on the tetrahedral nitrogen must lose their separate identities before the deprotonation step.

This process may occur at either nitrogen in II. The difference in the apparent rate of doublet coalescence for the two N-CH_3 signals implies a difference in the rates of protonation at the two conformationally different nitrogen atoms.

At a sufficiently high acidity ($-H_o > 8.0$), the mean-lifetime of IIa becomes long enough to allow rotation about the C_{CN}-$NH_2CH_3^+$ single bond in IIa to compete with deprotonation. Thus, through a series of protonation, rotation, and deprotonation steps such as those shown in Figure 21, the magnetically distinct "inside" and "outside"

$N\text{-}CH_3$ groups are averaged and only a single signal is observed.

The difference in the "coalescence acidity" of the high and low field $N\text{-}CH_3$ doublets has been explained by a conformational effect on the basicities of the two nitrogen atoms in II. Since the high field $N\text{-}CH_3$ doublet is broader than the low field doublet (Fig. 17) under non-exchanging conditions (14% H_2SO_4), it is important to demonstrate that the apparent coalescence of the former at a lower acidity than the latter is indeed meaningful and not an artifact of the difference in signal shape of the two doublets (45).

The apparent component separation within each doublet at a given acidity has been corrected for overlap by the method of Gutowsky and Holm (45). A value of T_2 for each of the $N\text{-}CH_3$ doublet signals was obtained (Table IV) from the average of the two values

TABLE IV

Kinetic Data. $N\text{-}CH_3$ Doublet Coalescence in Sulfuric Acid. 30°

$N\text{-}CH_3$ Group[3]	$\Delta\upsilon_{\frac{1}{2}}$ (cps)	T_2 (sec.)	$h_o \times 10^{-5}$	$\delta\upsilon_e/\delta\upsilon_\infty$	$1/2\pi\tau\delta\upsilon$	$1/\tau$ (sec.$^{-1}$)	$k \times 10^{6}$ sec.$^{-1}$ M^{-1}
High Field	2.0	0.16	4.79	0.84	0.25	7.85	16
Low Field	1.3	0.26	47.9	0.76	0.38	11.9	2.5

$\Delta\upsilon_{\frac{1}{2}}$ for the components of that doublet in 14% H_2SO_4-H_2O. Values of $\delta\upsilon_\infty$ for each doublet (in this case $\delta\upsilon_\infty = J_{H,CH_3}$) (Table VIII) were

also measured under the same conditions as $\Delta\nu_{\frac{1}{2}}$. Under the conditions such that $\tau \to \infty$ (14% H_2SO_4), the ratios $\delta\nu/\delta\nu_{\infty}$ are < 1.005, indicating that overlap does not cause the apparent splittings in these doublets to be significantly less than the true splitting. However, the values $2\pi T_2\delta\nu$ of 8.0 and 5.0 for the low and high field doublet indicate that corrections are important as the signals begin to coalesce (45).

Two sets of data are available for comparison of the relative rates of coalescence of the doublets. These are obtained from the partially coalesced high field doublet at $-H_o = 5.69$ and the partially coalesced low field doublet at $-H_o = 6.69$ (Fig. 17, Table VIII). Values of $1/\tau$ have been calculated for each of these spectra. If $1/\tau = kh_o$, a comparison of the quantities $1/(\tau h_o) = k$ for each doublet will indicate the difference between the rate constants k_{hf} and k_{lf} (TableIV) corresponding to protonation at the nitrogen atom belonging to the high field N-CH_3 and low field N-CH_3 signals, respectively. The ratio $k_{hf}/k_{lf} = 6.4$ establishing a difference in rates of protonation at the two different nitrogen atoms.

An independent conformation of $k_{hf} > k_{lf}$ has been obtained. In 28% sulfuric acid-d_2, it was found that the rate of nitrogen-proton replacement by deuterium in II was sufficiently slow to allow several n.m.r. spectra to be recorded before exchange was complete (Fig. 22). Only the N-CH_3 region of the spectrum has been reproduced. The first spectrum was recorded approximately 15 sec. after mixing

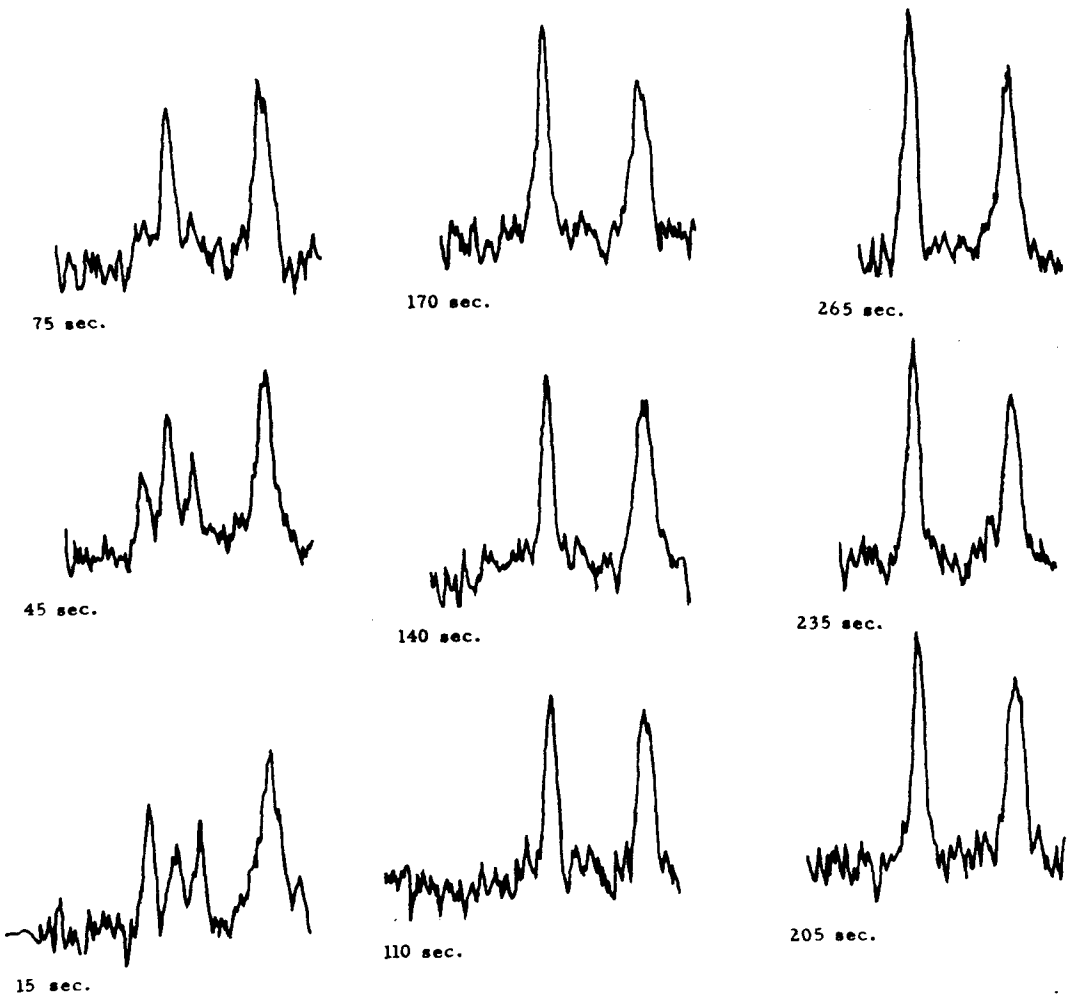

Fig. 22. Change in the N-CH_3 proton magnetic resonance signals for N,N'-dimethylacetamidinium chloride in 28% sulfuric acid-d_2 with time. 30°. 60 Mcps.

the solid II and the deuterated solvent. The low field doublet N-CH_3 pattern is still visible; however, the high field doublet pattern has almost completely disappeared due to deuterium incorporation. Over the interval of 15-170 sec., the singlet resonance signal in the low field N-CH_3 region increases in intensity as the outer doublet pattern simultaneously disappears. The singlet resonance in the high field N-CH_3 portion of the spectrum reaches maximum intensity approximately 45 sec. after mixing.

Since the lower field N-H signal for II, in H_2SO_4 solutions, disappears simultaneously with the coalescence of the high field N-CH_3 doublet (vide supra), it is reasonable to assume that these signals correspond to the proton and the methyl group attached to the same nitrogen atom. The low field nitrogen proton has already been tentatively assigned to the "outside" proton position (vide supra). This implies that the high field N-methyl proton signal corresponds to an "inside" position. The high field N-CH_3 signal has also been previously assigned to the "inside" methyl group on the basis of independent evidence. It may be concluded that the more basic nitrogen atom thus has the "outside" proton, "inside" methyl group conformation.

A consideration of the above process (Fig. 21) in terms of Grunwald's studies on ammonium ions in strong sulfuric acid (23) is

appropriate. The rates of proton exchange for ammonium, methylammonium, and trimethylammonium chloride have been measured as a function of h_o in sulfuric acid solutions ranging from 25-70% sulfuric acid. These rates are found to be directly proportional to the concentration of ammonium ion, but inversely proportional to h_o. A mechanism (23) which fits this data is represented in Figure 23 for the ammonium ion. The dotted lines in the formulae below indicate

$$H_3\overset{+}{N}\text{---}H^{*}\cdots OH_2 \underset{k'_{-4}}{\overset{k_4'}{\rightleftharpoons}} H_3N\cdots H^{*}\text{---}OH + H^{+}$$

$$H_3N\cdots {}^{*}H\text{---}OH \xrightarrow{k_H'} H_3N + H^{*}OH$$

Fig. 23

hydrogen bonds. The numbering system is that used by Grunwald. The resultant rate expression is represented in equation 13, which in

$$\text{Rate} = k_4'(NH_4^+)\, k_H'/(k_H' + k'_{-4}(H^+)) \qquad (13)$$

strong acid reduces to equation 14, and in dilute acid reduces to

$$\text{Rate} = k_4'\, k_H'\,(NH_4^+)/k'_{-4}(H^+) \qquad (14)$$

equation 15 (23). The rate law shown in equation 15 is part of the

$$\text{Rate} = k_4'\,(NH_4^+) \qquad (15)$$

general expression (eq. 5) considered for proton exchange in dilute aqueous acid (21, 23).

The rate-determining step for proton exchange in strong acid in the above reaction scheme (Fig. 23) is the breaking of the amine-water hydrogen bond in the step represented by k'_H (23). This can occur by either a rotation of the water molecule or a diffusion of this water molecule from the solvation shell. Calculated specific rate constants for these processes agree well with measured values of k'_H which have been corrected for viscosity (23).

No rate data for proton exchange have been obtained for solutions of II in the region pH < 3 to $-H_o$ < 5. It is thought that in this region a mechanism for proton exchange may be operative which has the same kinetic law as that for the exchange reaction of the ammonium ions in strong acid. The form of the rate law given in equation 14 is analogous to that for hydroxide ion catalyzed proton transfer. Grunwald has demonstrated that this process is too slow in the sulfuric acid-ammonium ion solutions that he has studied to account for the observed exchange rate. The importance of this process for strong sulfuric acid solutions of II cannot be estimated without data for rates of exchange in this region of acidity.

If the strong acid mechanism, Figure 23, is present in sulfuric acid solutions of II, a more detailed picture of the protolysis mechanism postulated in Figure 21 may be considered. The hydrogen bond

equilibrium represented in Figure 23 can be considered to be occurring throughout the total range of sulfuric acid concentration. As the acidity is increased, the rate of proton exchange due to breaking of these hydrogen bonds should decrease by analogy with ammonium ions. However, the nitrogen atoms in II are only formally bonded to three other atoms. The unshared pair of electrons on each nitrogen is somewhat delocalized due to resonance interactions, but is involved in π not σ bonding. Thus, weak hydrogen-bonded interactions probably exist directly between the nitrogen atom and a proton on an adjacent water molecule. As the acidity is increased, and more water molecules in the solvation shell are protonated, proton transfer from one of these protonated molecules weakly interacting with the nitrogen atom becomes more favorable. Since the other proton on the same nitrogen atom is already hydrogen-bonded to a water molecule, the removal of the extra proton (k_{-8}, Fig. 21) can be random if the nitrogen atom becomes tetrahedrally hybridized upon addition of the second proton. This process need not destroy the magnetic non-equivalence of the $N\text{-}CH_3$ groups if the mean-lifetime of the tetrahedral nitrogen configuration (Fig. 24) is sufficiently short. As the acidity of the

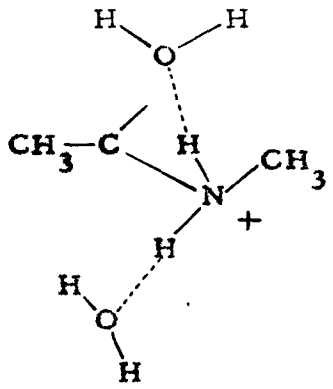

Fig. 24

solution is further increased, the mean-lifetime of the tetrahedral configuration increases to the point where rotation about the $C_{CN}\text{-}NH_2CH_3^+$ single bond may compete with the deprotonation process.

The rate constants k_{HF}, k_{LF}, and k_{rot} should be defined in terms of the specific rate constants shown in Figure 21. The quantity k_8 is the specific rate constant for protonation at a nitrogen atom. The quantities $k_{8(HF)}$ and $k_{8(LF)}$ are defined as the specific constants k_8 corresponding to protonation at the two different nitrogen atoms. Statistical corrections give $k_{8(HF)} = 4k_{HF}$ and $k_{8(LF)} = 4k_{LF}$. If a nitrogen atom with attached proton of spin $I = +1/2$ is designated N(+), then there is a 50% chance that a proton of spin $I = -1/2$ will add to give N(+, -). Assuming random deprotonation, there is then a 50% chance that N(+, -) will deprotonate to give N(-). Hence the protonation process

inverts spins on nitrogen (causing doublet coalescence) 25% of the time. This gives the statistical correction shown above. Thus, $k_{8(HF)} = 6.4 \times 10^{-5}$ sec.$^{-1}$M^{-1} and $k_{8(LF)} = 1 \times 10^{-5}$ sec.$^{-1}$M^{-1} (see Table IV). The constant k_{rot} is less easily defined. Referring to Figure 21, it may be seen that IIb equalizes the N-CH_3 groups. If $k_9 > k_{-8}$, k_{rot} should be approximately equal to the protonation constants k_8. If $k_9 < k_{-8}$, k_{rot} will be less than the protonation constants and $k_{rot} = k_8 k_9 / k_{-8}$. A direct comparison of $k_{8(HF)}$, $k_{8(LF)}$, and k_{rot} may not be proper since k_{rot} was determined in sulfuric acid-d_2. An isotope effect may be expected for k_8. No isotope effect is expected for k_9 nor for k_8/k_{-8}, since $D_o = H_o$ in this range of acidity. The ratio $k_{8(HF)}:k_{8(LF)}:k_{rot} = 160:25:1$. The difference between k_{rot} and the constants k_8 is sufficiently large to be outside of the range of an isotope effect. It may be concluded that $k_9 < k_{-8}$; the rotation step represented by k_9 is slower than deprotonation. No absolute estimates of k_{-8} and k_9 can be made.

Quadrupole Moment of ^{14}N in Amidinium Salts

It has been mentioned above that the nitrogen-proton resonance signals for the amidinium salts I-IV in anhydrous DMSO at room temperature do not show the characteristic coupling with the ^{14}N nucleus that is observed in many systems containing non-exchanging nitrogen-protons. This coupling with the nitrogen nucleus gives rise to a triplet

pattern for the proton signal with coupling constants on the order of 50-65 cps (27). Systems in which this splitting is observed are various ammonium salts under conditions in which proton exchange is very slow (21-26), anhydrous ammonia (62), and certain amides at elevated temperatures (30). Other systems which do not show this coupling are those in which nitrogen-protons can exchange rapidly (21-26, 62, 63), and certain amides under non-exchanging conditions at room temperature (30, 31).

Proton exchange cannot adequately explain the lack of ^{14}N coupling in the amidinium systems studied. The spin-spin splitting of N-CH_3 protons of N,N'-dimethylacetamidinium chloride (II) in DMSO (Fig. 11) by adjacent nitrogen-protons indicates that proton exchange is very slow or completely absent in this solvent system.

The second factor which determines whether or not a ^{14}N triplet coupling pattern is observed is the quadrupole moment of the ^{14}N nucleus and the fluctuating electric field gradient which this moment establishes around the nitrogen nucleus (27-31). If a nitrogen nucleus possesses a very symmetric electric field, molecular motions will cause this field to exert relatively little torque on the nucleus and hence mean-lifetimes of the three nuclear spin states of ^{14}N will be sufficiently long to allow detection of the triplet coupling pattern. On the other hand, an asymmetric electric field will exert a large torque on the nitrogen nucleus due to molecular motions, and transitions

between the three spin states for ^{14}N will occur sufficiently often so that only a singlet nitrogen-proton resonance will be observed.

The symmetry of the electric field at a nitrogen atom has been related to the hybridization of the atom (27). Tetrahedral, non-exchanging, ammonium ions possess relatively symmetric fields, and hence show the triplet pattern, while amides in which the hybridization at nitrogen approaches sp^2-p, possess more asymmetric fields and show only broad nitrogen-proton singlets at room temperature.

The nitrogens in the amidinium groups undoubtedly approach sp^2-p hybridization as closely as possible to permit maximum resonance stabilization. The electric field asymmetry associated with this hybridization could account for the lack of ^{14}N coupling in these salts.

The nitrogen-proton signal widths (cps) at half-height ($\Delta\nu_{\frac{1}{2}}$) for the various amidinium salts have been listed in Table I. Not only are the nitrogen-proton resonance signals singlets, but they are relatively sharp singlets as compared to amides in which the singlet proton resonances are on the order of 10-75 cps wide (40 mcps) at half-height (30). Tiers has examined a series of N-acyl-α-amino acids, and guanidinoacetic acid in trifluoroacetic acid in which nitrogen-proton exchange is very slow, as can be seen by the splitting of α-C-H protons by the nitrogen-protons (31). In these systems, values of

$\Delta\nu_{\frac{1}{2}}$ of the nitrogen-proton signals are on the order of 6-10 cps. These narrow lines are explained by very efficient relaxation of the ^{14}N nucleus due to a highly asymmetric electric field. The 9-16 cps line widths of the amidinium nitrogen-protons thus indicate that the nitrogens in these salts are also surrounded by highly asymmetric electric fields. Tiers (31) suggests that the degree of line narrowing may give an indication of the symmetry of the field. Thus it might be concluded that a more asymmetric electric field exists in the salts I and III than in II and IV. However, the broadness of the nitrogen-proton signal in II is in part due to unresolved coupling with adjacent $N\text{-}CH_3$ protons.

Roberts (30) has shown that the broad nitrogen-proton singlets observed in certain amides at room temperature become triplets (J = 50-60 cps) as the temperature of the sample is increased. The transition temperatures for these various amides are quite different, but in general are above 175°. The conclusion is reached that slow molecular motions are most effective for quadrupole relaxation of the ^{14}N dipole. The increased internal molecular motion in these amides with an increase in temperature appears to effectively symmetrize the electric field with respect to the nitrogen nucleus.

These results agree with the observations given above concerning the effect of temperature on the nitrogen-proton resonance signal of Ia in DMSO (Fig. 14). The broadened rather than sharp

singlet observed at 115° indicates that increased internal molecular motions are decreasing the efficiency of quadrupole relaxation of the ^{14}N nuclear moment. It would be predicted that this nitrogen-proton signal should continue to broaden and eventually become a triplet if the temperature were further increased.

Dihedral Angles and N-H, C-H Proton Coupling

Azo-bis-(N, N'-dimethylene)-isobutyramidinium nitrate (IV) deserves special mention. Spin-spin coupling between the nitrogen-protons and α-methylene groups in this molecule has not been observed in anhydrous DMSO or in sulfuric acid solutions. Rapid proton exchange does not explain these results since it has been demonstrated that nitrogen-proton exchange in sulfuric acid solutions of appropriate composition and in DMSO is extremely slow and that spin-spin coupling analogous to that in II would be expected. The fact that coupling is not observed requires a different explanation.

Karplus (64) has pointed out that vicinal proton-proton spin coupling in saturated ethane-type systems is strongly dependent on the dihedral angle φ between the two protons in question. Both Karplus (64) and Conroy (65) have calculated theoretical curves for the variation of J_{12} with dihedral angle for a saturated H-C-C-H system. They conclude that the maximum coupling is observed at $\varphi = 0°$ and 180° (8 and 11 cps, respectively) and that J_{12} becomes zero at about $\varphi = 80°$.

With the assumption that the amidinium group in IV is planar, it is possible to estimate a dihedral angle of 60° between a nitrogen-proton and either of the two protons on its adjacent methylene group. According to the "Conroy Curve" (65), a coupling constant of ~2 cps is predicted for the same dihedral angle in a saturated carbon system. Coupling constants between vicinal protons in ethyl groups are on the order of 7 cps, while those in isopropyl groups are about 6 cps (66). The coupling constant (2 cps) for $\varphi = 60°$ is thus about 30% of that expected in open-chain saturated carbon compounds. The N-H, $N-CH_3$ 1,2-coupling constant in II has been found to be 5 cps, while J_{12} for N-methylamides is about 4-5 cps. A rough approximation of the expected magnitude of coupling in IV (30% of that in II) gives a value $J_{12} = 1-1.5$ cps.

It is not necessary to discuss the lack of resemblance of an amidinium group to a saturated carbon system, but it is perhaps significant to observe that no resolvable coupling is observed in IV when it has a geometry that closely approaches that geometry lying in the region of minimum coupling in the saturated carbon system. The shape of a "Conroy Curve" for these nitrogen systems, when available, may well show $\varphi = 60°$ as the point where $J_{12} \sim 0$.

Experimental

Melting points were determined with samples of the compounds in thin-walled capillary tubes using a variable temperature circulating oil bath. Melting points are uncorrected. Microanalyses were done by the Elek Micro Analytical Laboratories, Los Angeles, California, and Spang Microanalytical Laboratory, Ann Arbor, Michigan.

Dimethylsulfoxide

Dimethylsulfoxide (DMSO), Crown-Zellerbach technical grade, was purified in the following manner. After a preliminary distillation at reduced pressure (0.2 mm), the distillate was shaken with Linde Co., Type 4A, molecular sieve in a glass-stoppered round-bottom flask. The dry DMSO was then filtered through Celite in a dry box under an atmosphere of dry nitrogen, and distilled at reduced pressure (0.2 mm) through a 12-inch Vigreux column. The middle fraction distilling at 45°/0.2 mm was collected. An n.m.r. spectrum of the neat solvent taken at high amplification showed no detectable water-proton resonance. The purified DMSO was stored in a glass-stoppered round-bottom flask.

Sulfuric Acid

Sulfuric acid, DuPont reagent grade, was used without further purification.

Sulfuric Acid-d_2

Sulfuric acid-d_2 (approximately 96.5 wt. %) was prepared according to the method of Best and Wilson (67) using Baker and Adamson "Sulfan B" and deuterium oxide (99.5%) obtained from General Dynamics Corporation.

Acetamidinium Chloride (Ia)

Acetamidinium chloride was prepared according to the method of Pinner (68, 69) and recrystallized from absolute ethyl alcohol; m.p. 165-168° (Lit. (68, 69), m.p. 164-166°, 166-167°). Molecular weight determined by gravimetric chloride analysis was 94.47; calculated for $C_2H_7N_2Cl$, 94.55. Ia is very hygroscopic.

Acetamidinium Nitrate (Ib)

Acetamidinium nitrate was prepared from an aqueous solution of the corresponding chloride (Ia) by addition with stirring of an equivalent amount of aqueous silver nitrate. The resultant silver chloride precipitate was filtered off, the amidinium nitrate was precipitated from solution by addition of a large quantity of acetone, and recrystallized from absolute ethyl alcohol. M.p. 189-190°. Ib is very hygroscopic. Calculated for $C_2H_7N_3O_3$: C, 19.83; H, 5.83; N, 34.70; O, 39.64. Found: C, 18.44, 18.22; H, 5.83, 5.97; N, 35.07, 34.88. The microanalyst (Spang) reported violent explosion during combustion under oxygen.

N,N'-dimethylacetamidinium Chloride (II)

N,N'-dimethylacetamidinium chloride was prepared according to the method of Pinner (70) and recrystallized from absolute ethyl alcohol; m.p. 214.5-215.5° (lit. (70) m.p. 218°). II is very hygroscopic. Hydrolysis of II in 1 N sodium hydroxide solution gave equivalent amounts of methylamine and N-methylacetamide. This was shown by n.m.r. analysis and confirms the symmetrical dimethyl structure.

Azo-bis-isobutyramidinium Nitrate (III)

Azo-bis-isobutyramidinium nitrate was prepared from the corresponding chloride by a procedure identical to that given for the preparation of acetamidinium nitrate (Ib). The chloride was obtained from the Yerkes Research Laboratory, E. I. duPont de Nemours and Co., and had been recrystallized from water. Calculated for $C_8H_{20}N_8O_6$: C, 29.63; H, 6.22; N, 34.55; O, 29.60. Found: C, 29.75; H, 6.30; N, 34.45. M.p. 162.5° dec.

Azo-bis-N,N'-dimethylene-isobutyramidinium Nitrate (IV)

A 10 g. sample of unrecrystallized azo-bis-isobutyramidinium chloride, obtained from duPont (see above), was dissolved in 100 ml. of 98% ethylenediamine, M. C. & B., with stirring. The chloride rapidly dissolved in the diamine to give a clear solution. Upon stirring the solution for several minutes at room temperature, a white solid precipitated. This was filtered off and recrystallized first from

chloroform and then absolute methyl alcohol. M.p. 122.5° dec. Calculated for azo-bis-N,N'-dimethylene-isobutyramidine ($C_{12}H_{22}N_6$): C, 57.56; H, 8.86; N, 33.57. Found: C, 57.65; H, 8.97; N, 33.46. The hydrochloride of $C_{12}H_{22}N_6$ was prepared by passing a stream of anhydrous hydrogen chloride through a chloroform solution of this compound. Calculated for $C_{12}H_{24}N_6Cl_2$: C, 44.58; H, 7.49; N, 26.00; Cl, 21.94. Found: C, 44.48; H, 7.51; N, 25.88; Cl, 21.86. The nitrate was prepared by addition of an equivalent amount of concentrated nitric acid to an absolute ethyl alcohol solution of the amidine, $C_{12}H_{22}N_6$. Upon addition of the nitric acid, a solid precipitated from solution, was filtered off, and recrystallized from water. M.p. 146.5° dec. Calculated for the nitrate, $C_{12}H_{24}N_8O_6$: C, 38.29; H, 6.43; N, 29.77; O, 25.51. Found: C, 38.27, 38.33; H, 6.29, 6.17; N, 29.82, 29.66. Thermal decomposition of this nitrate salt in DMSO gives a stoichiometric quantity of nitrogen gas based on the structural formula IV (molecular weight 376.38). The microanalyst (Spang) reported a violent explosion during combustion under oxygen.

N.m.r. Spectrometers

The nuclear magnetic resonance spectrometers used in this study were a Varian Model V-4300B (HR-60) spectrometer, equipped with a Super-stabilizer, operating at ν_o = 60 Mcps.; and a Varian A-60 spectrometer operating at ν_o = 60 Mcps. The majority of the spectra were taken with the A-60 spectrometer used without

modification. The studies of dilute aqueous acid solutions in Ia and variable temperature experiments were performed using the HR-60 spectrometer with suitable modifications as described below.

N.m.r. Sample Tubes

Standard Varian Analytical Sample Tubes (4.28 mm ID) were used for all spectra taken with the A-60 spectrometer. Sample tubes for use with the HR-60 spectrometer were made from Pyrex glass tubing (5 mm OD).

All sample tubes were cleaned in the following manner. The tubes were first filled with and immersed in a hot cleaning solution of 25% nitric acid, 75% sulfuric acid and allowed to stand for at least one hour, then rinsed with distilled water several times and filled with and immersed in concentrated ammonium hydroxide. They were again thoroughly rinsed with distilled water and dried in an oven above 110°. Upon removal from the oven the tubes were capped with small corks or plastic tops until used.

Temperature Dependence Study-Acetamidinium Chloride in DMSO

The sample used in this study was prepared by dissolving acetamidinium chloride (Ia), recrystallized from ethyl alcohol and dried in vacuo, in anhydrous DMSO. The solution contained approximately 15% of Ia and was sealed in a Pyrex n.m.r. tube. A variable temperature probe with a Pyrex dewar encasing the insert was used (71). The temperature within the probe was varied by first passing

HP nitrogen gas over a hot wire encased in a Pyrex glass vacuum jacketed tube, and then directing this stream of hot gas into the area around the probe insert. Stability of temperature was not easily obtained and was a critical function to the gas flow rate and the settings on the Variac used to control the temperature of the hot wire. The temperature in the probe insert was measured by means of a copper-constantan thermocouple placed within the probe insert, in conjunction with a Leeds-Northrup precision potentiometer. The temperature was determined both before and after the spectrum was taken. Only the spectrum of the nitrogen-protons was recorded. The peak separation was determined by the audio-sideband technique (72). A Hewlett-Packard Model 200AB audio oscillator and Model 521-C frequency counter were used for this purpose. After the experiment had been completed, it was found that a malfunction existed in the frequency counter which had been used to determine the audio-sideband positions in cps. A vacuum tube in the counter was faulty and this caused part of one decade to be inoperable. Thus, the cps reading on the counter for each sideband was not correct. However, the same values were observed on the counter for each of the sidebands from spectrum to spectrum. This shows that the absolute separation of the sidebands (determined by the audio oscillator) was constant from spectrum to spectrum. Although it is impossible to obtain values for peak separation in cps from these spectra, the

relative peak separations $\delta\nu_e/\delta\nu$ could still be determined. The signal separation $\delta\nu_\infty$ (cps) under non-exchanging conditions was obtained from spectra taken on the Varian A-60 spectrometer at room temperature.

The data are presented in Table V, along with estimated errors

TABLE V

Temperature Dependence Study of Acetamidinium Chloride in Anhydrous DMSO

			T_2=0.03 sec.		T_2=0.01 sec.	
T°K	$1/T \times 10^3$	$\delta\nu_e/\delta\nu_\infty$	$1/2\pi\tau\delta\nu$	$\log 1/2\pi\tau\delta\nu$	$1/2\pi\tau\delta\nu$	$\log 1/2\pi\tau\delta\nu$
310.6	3.22	1.00	0		0	
344.0	2.91	0.85±.03	0.24±.03	1.38±.05	0.02±.03	0.3±0.4
350.8	2.85	0.82±.03	0.28±.03	1.45±.04	0.06±.02	0.7±0.2
358.4	2.79	0.68±.03	0.37±.02	1.58±.02	0.14±.01	1.14±.04
361.2	2.77	0.62±.03	0.42±.02	1.62±.01	0.17±.01	1.23±.03
368.8	2.71	-	-		-	

in the measurements. The values $1/2\pi\tau\delta\nu$ were calculated by the method of Gutowsky and Holm (45) using the parameters $\delta\nu_\infty$ = 29 cps, a) T_2 = 0.03 sec., and b) T_2 = 0.01 sec. The two values of T_2 were obtained from the relationship $2/T_2 = 2\pi\Delta\nu_{\frac{1}{2}}$, where $\Delta\nu_{\frac{1}{2}}$ is the width at half-height of the nitrogen-proton resonance signal. The value T_2 = 0.03 sec. was calculated from the average value $\Delta\nu_{\frac{1}{2}}$ =10.5±0.5

cps for the two signals at 37°, and the value T_2 = 0.01 sec. was calculated from the value $\Delta\nu_{\frac{1}{2}}$ = 30 cps for the coalesced signal at 115°. The rate expression used for calculating activation parameters is that given in equation 16 (45).

$$\text{Log } 1/2\pi\tau\delta\nu = \log k_o/\pi\delta\nu - E_a/2.3\,RT \qquad (16)$$

Plots of $1/2\pi\tau\delta\nu$ for T_2 = 0.03 sec. and T_2 = 0.01 sec. are shown in Figures 25 and 26. For T_2 = 0.03 sec., E_a = 9±2 kcal/mole and $k_o = 10^5 - 10^7$. For T_2 = 0.01 sec., E_a = 25± 8 kcal/mole and $k_o = 10^{11} - 10^{21}$.

T_2 for Water Protons in Aqueous Acid Solutions of Acetamidinium Ion

Preparation of Samples. Acetamidinium chloride (Ia) recrystallized from ethyl alcohol and dried in vacuo over P_2O_5, was weighed into a 100-ml. beaker. A 50-ml. sample of deionized water was added to the solid chloride (Ia) and the solution (A) was stirred with a magnetic stirrer. A 10.0-ml. aliquot of (A) was then pipetted into a 50.0-ml. volumetric flask which was stoppered and stored in the refrigerator. This sample, after dilution to 50.0 ml. (B), was used for determination of the concentration of amidinium salt (Ia) in the initial aqueous solution (A) (see below). A 5.0-ml. aliquot of (A) was pipetted into a small glass-stoppered Erlenmeyer flask which was also stored in the refrigerator. Density measurements were made on this sample (see below).

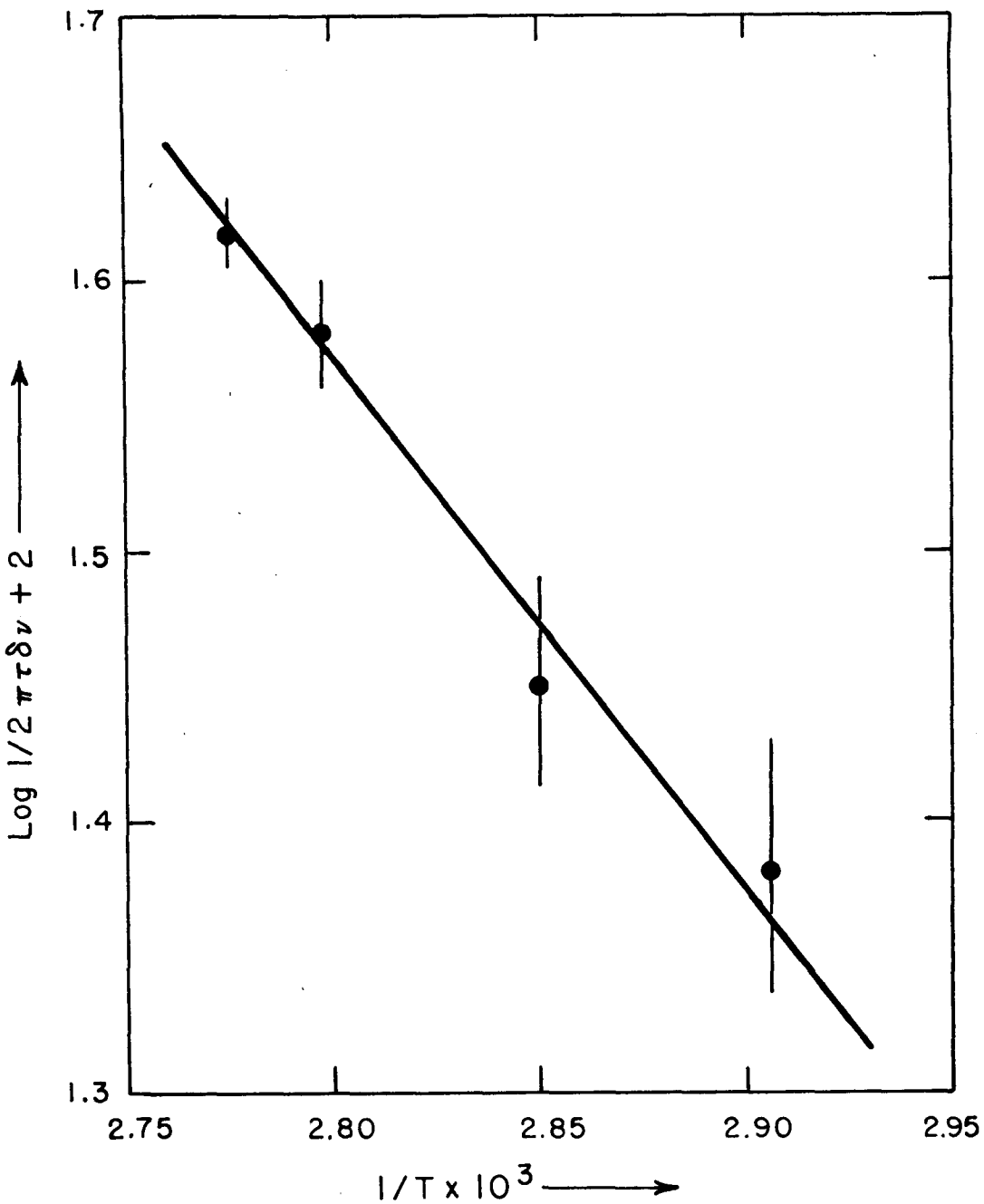

Fig. 25. Log $1/2\pi\tau\delta\nu$ vs. 1/T. Acetamidinium chloride in DMSO. T_2 = 0.03 sec.

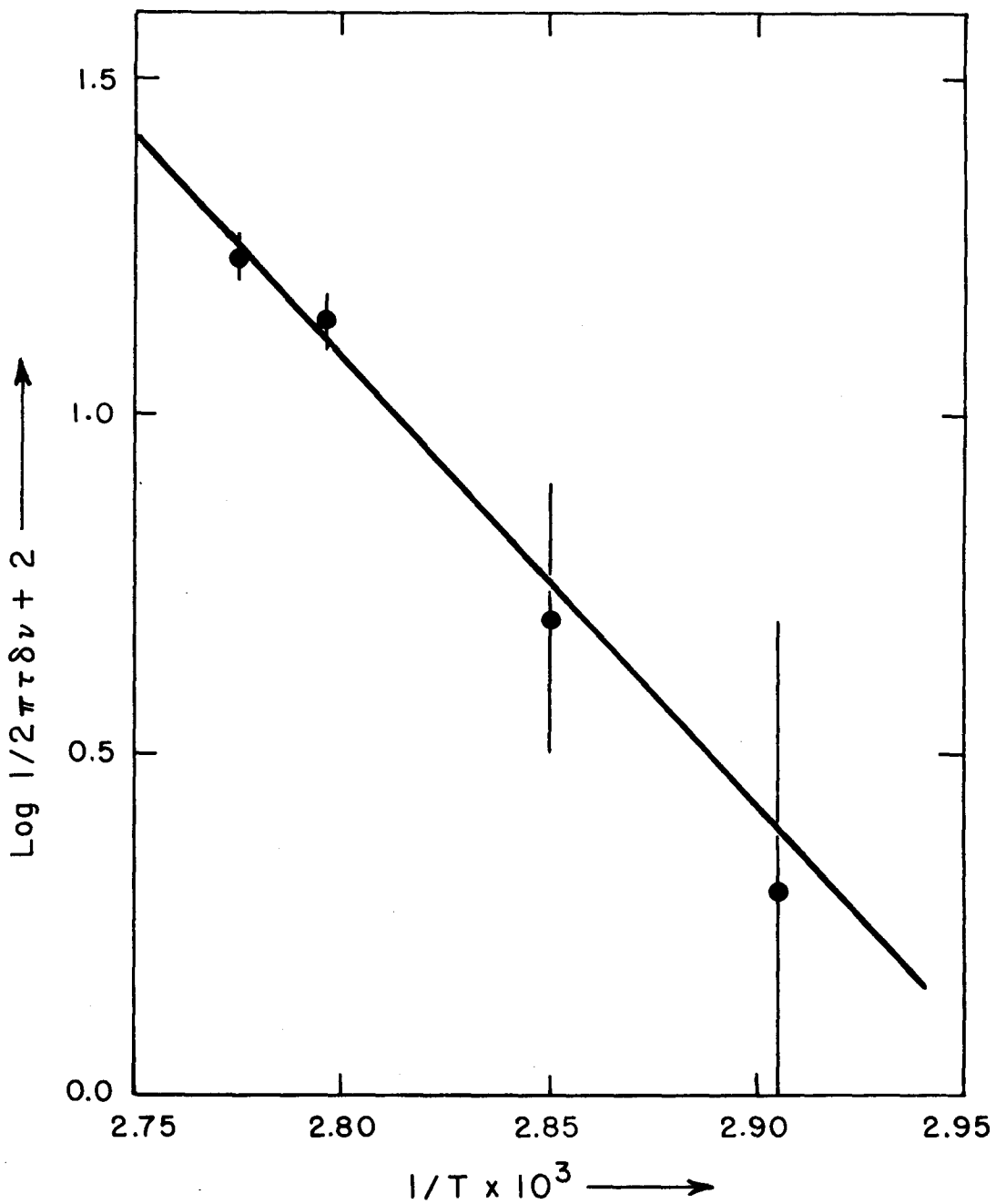

Fig. 26. Log $1/2\pi\tau\delta\nu$ vs. $1/T$. Acetamidinium chloride in DMSO. $T_2 = 0.01$ sec.

Hydrochloric acid (0.1 N) was then added dropwise by means of a fine capillary dropper to the remaining solution (A) with stirring. Approximately 0.5 ml. aliquots of this solution were taken at appropiate pH values and placed in n.m.r. sample tubes which were immediately immersed in a Dry Ice-isopropyl alcohol slurry. After the liquid content of the tubes was frozen, the tubes were sealed in an oxygen torch flame and again placed in the slurry until the spectra were taken. All spectra were recorded within 8 hours after the samples were prepared. No evidence of hydrolysis reactions was observed. The pH measurements were made using a Beckman Model G pH meter equipped with Beckman Glass and Calomel electrodes. The pH meter was standardized with Beckman pH 4 buffer immediately preceding the measurements on the amidinium chloride solutions. Standardization of the pH meter was done under identical conditions to the actual pH determinations. Samples were taken in the pH range 3-5. The amount of hydrochloric acid added to the amidinium salt solution (A) was negligible in comparison to the total volume of the solution and no correction was made for the extremely small change in amidinium chloride concentration. The capillary droppers employed were cleaned in a manner analogous to the cleaning of the n.m.r. sample tubes.

The above procedure was used for a 9.42 g. sample and an 18.90 g. sample of acetamidinium chloride (Ia).

Acetamidinium Chloride Concentrations. The concentrations of acetamidinium chloride (Ia) in the water solutions containing 9.42 g. (A_1) and 18.90 g. (A_2) of Ia were determined by an absorption indicator method for the volumetric determination of chloride ion in aqueous solution (73).

A 4.03218 g. sample of sodium chloride, dried at 100° for several hours, was dissolved in distilled water in a 500-ml. volumetric flask. Three 25.0-ml. aliquots of this standard solution were titrated to a pink end point with a freshly prepared aqueous solution of silver nitrate (17 g. diluted to 1 l.) using several drops of 1% dichlorofluoroescein (70% ethyl alcohol) indicator. The volume of silver nitrate solution required per 25.0 ml. sample was 33.53±0.02 ml. The concentration of the silver nitrate solution is calculated to be 0.10287 ± 0.00007 N. The concentrations of chloride ion in the solutions (A_1) and (A_2) were determined by titrating three 10.0-ml. samples of (B_1) and three 5.0-ml. samples of (B_2) (see Preparation of Samples) to a dichlorofluorescein end point with the same silver nitrate solution. Volumes of silver nitrate solution required for the sample volumes titrated were: (B_1), 34.03 ± 0.01; (B_2), 29.74 ± 0.03 ml. The concentrations of Ia in (A_1) and (A_2) are calculated to be 1.750 ± 0.002 M and 3.059 ± 0.005 M, respectively.

Density of Acetamidinium Chloride Solutions. Densities of the two aqueous acetamidinium chloride solutions, (A_1) and (A_2),

were determined with the 5-ml. aliquots described under Preparation of Samples. Two determinations were made at each of the two concentrations. A pychnometer of 1.9978 ± 0.0002 cc volume (determined from measurements on pure water) was used. The measurements were made at 25° with a Mettler Analytical Balance. Densities of the solutions at 25° are: (A_1), 1.0245 ± 0.0002 g./cc ; and (A_2), 1.0449 ± 0.0002 g./cc.

Procedure for Recording N.m.r. Spectra. The nuclear magnetic resonance spectra of water-protons in the previously described samples of aqueous acetamidinium chloride solutions at various pH values, as well as the spectrum of pure water, were recorded under fast passage (74) conditions in the following manner.

The HR-60 spectrometer in conjunction with a Sanborn High-Speed recorder was employed. The Saw-Tooth sweep unit on the spectrometer was used in order to continuously sweep through the water resonance signal. Settings on this unit were: Sweep Frequency, 4x6, and Sweep Field, 1x7. The transmitter power level was 17 decibels out. The Integrator Function was set on Scope. The recorder chart paper feed rate was set at 20 mm per second. All other settings on the spectrometer were "routine." Sample tubes were spun to improve field homogeneity.

The probe was balanced by adjustment of the fine and coarse paddles, and maximum resolution was obtained on a pure water sample by appropriate adjustments of the X, Y, Z, and Curvature Shim Coils.

Resolution was maintained by continuous adjustment of the Y Gradient Shim Coil to give the most symmetric decay envelope with the longest "ringing" time for the water resonance as observed on the oscilloscope.

A series of water signals were recorded for a given sample while the Y Gradient Shim Coil was adjusted to give maximum resolution. Before each amidinium chloride sample, a pure water sample was run to assure that resolution was not changing.

Calculations of Transverse Relaxation Times (T_2). Under the fast passage conditions used to obtain the resonance signals for water protons, the shape of the decay envelope can be approximated by equation 17 (74). The decay envelope is generated by a series of

$$f(t) = A\, e^{-t/T_2} \qquad (17)$$

maximum pen deflections which decrease in amplitude with time. Each maximum deflection gives a value of $f(t_i)$ corresponding to a time t_i. The initial resonance absorption corresponds to $t = 0$. A plot of log $f(t_i)$ versus t_i theoretically generates a straight line of slope $-1/2.303\,T_2$.

The complete series of water-proton signals obtained for each sample was first visually inspected and several signals from each sample series which appeared to have the most symmetric decay envelopes and the longest "ringing" time were chosen for analysis. Values of $f(t)$ and t were measured in chart paper units with the aid of a magnifying glass. An auxiliary stylus on the Sanborn recorder

marked one-second intervals on the chart paper and thus it was possible to convert time values in chart paper units to seconds. Each signal analyzed was considered valid only if the first four or five values of log f(t) versus time generated a reasonable straight line. These representative values of $1/T_2$ are given in Table VI. The final value of $1/T_2$ chosen for each of the samples was the smallest value obtained in the series of curves analyzed for that sample (Table VI). The rationale for this choice was that the larger the value of T_2 (the smaller the value of $1/T_2$), the better the resolution at the time that the signal was recorded. Each complete series of water-proton signals for the pure water sample was analyzed in the same manner. The smallest value of $1/T'_2$ obtained in each series is shown in Table VII. The consistency of these values demonstrates that the

TABLE VII

Transverse Relaxation Times for Protons of Pure Water. 33°

Run	$1/T'_2$	Deviation from the mean, $\overline{1/T'_2} = 2.039$	Deviation from the mean, $\overline{1/T'_2} = 2.0012$
1	2.0225	-0.0165	+0.0213
2	1.9994	-0.0396	-0.0018
3	1.9990	-0.0400	-0.0022
4	2.1030	+0.0640	
5	1.9839	-0.0551	-0.0173
6	2.1263	+0.0873	

TABLE VI

Transverse Relaxation Times of Water-Protons in Aqueous Solutions of Acetamidinium Chloride. 33°

(AH^+) moles/ℓ.	pH	$1/T_2$ (sec.$^{-1}$) Representative Values	Value Chosen
1.750	5.13	4.2606	
		4.6721	
		4.4257	
		4.1807	4.18
		4.8498	
1.750	4.95	3.5622	
		3.2099	
		3.1618	3.16
1.750	4.81	3.2700	
		3.5720	
		2.9310	2.93
3.059	5.08	6.6250	
		5.8630	5.86
		6.5370	
		6.3250	
3.059	4.95	4.1096	
		3.5245	
		3.6641	
		3.1511	3.15
3.059	4.29	2.6406	
		2.5892	2.59

values $1/T_2$ for each sample of acetamidinium chloride may be reasonably compared and allows an estimate of the possible error in these values. Considering all six values for $1/T'_2$ gives the value $1/T'_2 = 2.04 \pm .06$. For lack of a better estimate, the error ± 0.06 was given to each value of $1/T_2$ (Table VI). However, this value of $1/T'_2$ was not used in calculations of $1/\tau_{H_2O}$. An inspection of Table VII shows that deviations using $1/T'_2 = 2.04$ are positive for the runs 4) and 6), and of the same order of magnitude but negative for runs 1), 2), 3), and 5). A determination of $1/T'_2$ using these latter four runs gives the value $1/T'_2 = 2.00 \pm .02$ which was used in the calculations of $1/\tau_{H_2O}$.

N,N'-dimethylacetamidinium Chloride. Sulfuric Acid Solutions

Determination of Sulfuric Acid Concentrations. The sulfuric acid solutions were prepared in the approximate percent compositions desired on a volumetric basis using 1.83 as the specific gravity for 93% sulfuric acid (75). The density of 100% sulfuric acid-d_2 (1.857) (76) was corrected to an approximate density of 1.862 for 96% acid by using the same increment of density change as that for 100% to 96% sulfuric acid (75). The density of deuterium oxide (99.5%) is 1.10769 at 27° (77).

The compositions of these various sulfuric acid-water solutions were determined by titration of known weights of the mixtures with standardized 1N sodium hydroxide solution to a methyl red end

point. Two titrations were performed on each solution and the weight-percent sulfuric acid was taken as an average of these two determinations. Values of H_o corresponding to the various mixtures were interpolated from data given by Paul and Long (61). Bigeleisen (61) has demonstrated that H_o is a good approximation to D_o except in the range 10^{-3} to 10^{-1} M. Thus, values of D_o were obtained from tables of computed H_o values.

Preparation of Samples. The procedure used for preparing samples and taking the n.m.r. spectra was identical for both the sulfuric acid and sulfuric acid-d_2 experiments. Samples were prepared by placing approximately 0.05-g. amounts of N,N'-dimethylacetamidinium chloride in 1-ml. volumetric flasks. Because the amidinium salt was extremely hygroscopic, the weights of the samples were not accurately determined. These volumetric flasks containing the salt were then placed unstoppered in a vacuum desiccator and dried for several hours in vacuo over phosphorous pentoxide. The flasks were immediately stoppered after removal from the desiccator. The previously prepared solutions of sulfuric acid were then added quickly to the flasks which had been cooled on Dry Ice. Sufficient acid was added to bring the level of the solution to the 1-ml. mark. Each flask was shaken until all of the salt had dissolved and the solution was then quickly transferred to a standard Varian n.m.r. tube which was stoppered and placed in Dry Ice. It was necessary to exercise

particular care with the solutions above 60% sulfuric acid because the insolubility of hydrogen chloride caused rapid gas evolution upon addition of the acid to the amidinium salt. This was minimized by the cooling procedures mentioned above. Spectra were recorded using the A-60 spectrometer.

The spectral data are summarized in Tables VIII and IX.

TABLE VIII

Spectral Data for N,N'-dimethylacetamidinium Chloride in Sulfuric Acid (30°)

		J_{NH,NCH_3} (cps)			$\nu_{C-CH_3}-\nu_{N-CH_3}$ (cps)	
$\%H_2SO_4$	$-H_o$ (61)	low field	high field	$\delta\nu$(N-CH_3) (cps)	low field	high field
14	0.6	5.0	5.0	9.5	47.5	38.0
30	1.7	5.0	5.0	9.5	48.5	38.5
40	2.4	5.0	5.0	9.5	48.5	39.0
52	3.6	5.0	5.0	9.5	49.0	39.5
62.18±.03	4.71	5.0	5.0	9.5	49.0	39.5
70.26±.05	5.69	5.0	4.2	9.9	49.5	39.5
77.9± .2	6.69	3.8	-	7.5	48.0	40.5
84.67±.02	7.62	(1.6)	-	7.4	48.4	41.0
90.67±.04	8.35	-	-	-	45.5	
90.86±.07	8.37	-	-	-	45.7	

TABLE IX

Spectral and Kinetic Data for N,N'-dimethylacetamidinium Chloride in Sulfuric Acid-d_2. (30°)

$\%D_2SO_4$	$-D_o$ (61)	$\delta\nu$(N-CH_3) (cps)	$\delta\nu/\delta\nu_\infty$	$1/\tau$ ($sec.^{-1}$)	log $1/\tau$
60	4.5	9.8($\delta\nu_\infty$)	1.00	0	-
83.9±.2	7.51	9.2	0.94	10.7	1.02
84.70±.05	7.62	8.4	0.86	17.8	1.25
85.11±.06	7.67	8.6	0.88	16.2	1.21
87.0 ±.2	7.90	4.2	0.43	34.6	1.54
88.0 ±.1	8.03	3.0	0.31	37.1	1.57

REFERENCES

1. R. L. Shriner and F. W. Neumann, Chem. Rev., 35, 351 (1944).
2. R. Delaby, J. V. Harispe, and S. H. Renard, Bull. soc. chim. France, 11, 227 (1944).
3. D. C. Prevorsek, J. Phys. Chem., 66, 769 (1962).
4. E. B. Schoenbach and E. M. Greenspan, Medicine, 27, 327 (1948).
5. O. Gisvold, J. Am. Pharm. Assoc., 42, 372 (1954).
6. T. J. Dougherty, J. Am. Chem. Soc., 83, 4849 (1961).
7. This Dissertation, p. 100.
8. T. J. Dougherty, private communication.
9. This Dissertation, p. 29.
10. J. A. Pople, W. G. Schneider, and H. J. Bernstein, "High-resolution Nuclear Magnetic Resonance," McGraw-Hill, Inc., New York, 1959, p. 366.
11. M. T. Rogers and J. C. Woodbrey, J. Phys. Chem., 66, 540 (1962).
12. B. Sunners, L. H. Piette, and W. G. Schneider, Can. J. Chem., 38, 681 (1960).
13. D. G. de Kowalewski and V. J. Kowalewski, Ark. Kem., 16, 373 (1961).
14. J. V. Hatton and R. E. Richards, Molec. Phys., 3, 253 (1960).
15. J. V. Hatton and R. E. Richards, ibid., 5, 139 (1962).

16. J. C. Woodbrey and M. T. Rogers, J. Am. Chem. Soc., 84, 13 (1962).

17. A. Berger, A. Lowenstein, and S. Meiboom, ibid., 81, 62 (1959).

18. A. Saika, ibid., 82, 3540 (1960).

19. G. Fraenkel and C. Franconi, ibid., 82, 4478 (1960).

20. G. Fraenkel, A. Lowenstein, and S. Meiboom, J. Phys. Chem., 65, 700 (1961).

21. M. T. Emerson, E. Grunwald, and R. A. Kromhout, J. Chem. Phys., 33, 547 (1960).

22. E. Grunwald, P. J. Karabatsos, R. A. Kromhout, and E. L. Purlee, ibid., 33, 556 (1960).

23. M. T. Emerson, E. Grunwald, M. L. Kaplan, and R. A. Kromhout, J. Am. Chem. Soc., 82, 6307 (1960).

24. E. Grunwald, A. Lowenstein, and S. Meiboom, J. Chem. Phys., 25, 382 (1956); 27, 630 (1957).

25. A. Lowenstein and S. Meiboom, ibid., 27, 1067 (1957).

26. S. Meiboom, A. Lowenstein, and S. Alexander, ibid., 29, 969 (1958).

27. L. M. Jackman, "Nuclear Magnetic Resonance Spectroscopy," Pergamon Press, Inc., New York, 1959, p. 72.

28. J. A. Pople, W. G. Schneider, and H. J. Bernstein, op. cit., pp. 102, 227.

29. J. D. Roberts, "Nuclear Magnetic Resonance," McGraw-Hill, Inc., New York, 1959, Chapter 5.

30. J. D. Roberts, J. Am. Chem. Soc., 78, 4495 (1956).

31. G. V. D. Tiers and F. A. Bovey, J. Phys. Chem., 63, 302 (1959).

32. An excellent discussion of nuclear magnetic resonance and its applications is given by J. A. Pople, W. G. Schneider, and H. J. Bernstein, op. cit.

33. R. C. Neuman, Jr., G. S. Hammond, and T. J. Dougherty, J. Am. Chem. Soc., 84, 1506 (1962).

34. This Dissertation, Part II.

35. H. L. Schläfer and W. Schaffernicht, Angew. Chem., 72, 618 (1960).

36. E. J. Corey and M. Chaykovsky, J. Am. Chem. Soc., 84, 866 (1962).

37. P. Nylen, Z. anorg. allgem. Chem., 246, 227 (1941).

38. J. A. Pople, W. G. Schneider, and H. J. Bernstein, op. cit., p. 272.

39. L. M. Jackman, op. cit., p. 73.

40. J. D. Roberts, "Nuclear Magnetic Resonance," McGraw-Hill, Inc., New York, 1959, p. 43.

41. A qualitative review of spin-spin splitting is given in reference 32. See page 91.

42. L. Jackman, op. cit., p. 56.

43. This Dissertation, p. 29.

44. H. C. Brown, G. K. Barbaras, H. L. Berneis, W. H. Bonner, R. B. Johannesen, M. Grayson, and K. L. Nelson, J. Am. Chem. Soc., 75, 1 (1953).

45. H. S. Gutowsky and C. H. Holm, J. Chem. Phys., 25, 1228 (1956).

46. L. Pauling, "The Nature of the Chemical Bond," Third Ed., Cornell University Press, New York, 1960, p. 239.

47. M. Karplus, J. Chem. Phys., 30, 11 (1959).

48. R. R. Fraser and D. E. McGreer, Can. J. Chem., 39, 505 (1961).

49. C. C. Costain and J. M. Dowling, J. Chem. Phys., 32, 158 (1960).

50. V. J. Kowalewski and D. G. de Kowalewski, ibid., 32, 1272 (1960).

51. S. I. Mizushima, "Structure of Molecules and Internal Rotation," Academic Press, Inc., New York, 1954, pp. 117-152.

52. R. R. Fraser, Can. J. Chem., 38, 549 (1960).

53. J. H. Richards and W. F. Beach, J. Org. Chem., 26, 623 (1961).

54. J. A. Pople, W. G. Schneider, and H. J. Bernstein, op. cit., p. 221.

55. Idem., p. 219.

56. Idem., p. 29.

57. Idem., p. 46.

58. This Dissertation, p. 176.

59. L. Meites and H. C. Thomas, "Advanced Analytical Chemistry," McGraw-Hill, Inc., New York, 1958, p. 91.

60. M. Eigen and J. Schoen, Z. Electrochem., 59, 483 (1955).

61. D_o and d_o are the acidity functions for deutero-acids corresponding to the Hammett acidity functions H_o and h_o. See M. A. Paul and F. A. Long, Chem. Rev., 57, 1 (1957); E. Hogfeldt and J. Bigeleisen, J. Am. Chem. Soc., 82, 15 (1960).

62. R. A. Ogg, J. Chem. Phys., 22, 560 (1954).

63. R. A. Ogg, Disc. Faraday Soc., 17, 215 (1954).

64. M. Karplus, J. Chem. Phys., 30, 11 (1959).

65. H. Conroy, Adv. in Org. Chem., II, 308 (1960).

66. R. E. Glick and A. A. Bothner-By, J. Chem. Phys., 25, 362 (1956).

67. A. P. Best and C. L. Wilson, J. Chem. Soc., 239 (1946).

68. A. W. Dox, Org. Syn., Col. Vol. I, J. Wiley and Sons, Inc. 1941, p. 5.

69. A. Pinner, Ber., 16, 1654 (1883); 17, 178 (1884).

70. A. Pinner, "Die Imidoäther und ihre Derivate," Berlin, 1892, p. 112.

71. C. Franconi and G. Fraenkel, Rev. Sci. Instr., 31, 657 (1960).

72. J. T. Arnold and M. E. Packard, J. Chem. Phys., 19, 1608 (1951).

73. A. R. Olsen, C. W. Koch, and G. C. Pimental, "Introductory Quantitative Chemistry," Freeman and Co., San Francisco, 1956, p. 272.

74. J. A. Pople, W. G. Schneider, and H. J. Bernstein, op. cit., p. 40.

75. Handbook of Chemistry and Physics, Fortieth Ed., Chemical Rubber Publishing Co., 1959, p. 2051.

76. R. H. Flowers, R. J. Gillespie, J. V. Oubridge, and C. Solomons, J. Chem. Soc., 667 (1958).

77. H. L. Johnston, J. Am. Chem. Soc., 61, 878 (1939).

II. THE KINETICS OF THE THERMAL DECOMPOSITION OF AZOBISISOBUTYRAMIDINES AND THEIR SALTS IN SOLUTION

Introduction

Studies of the thermal decomposition reactions of aliphatic azo-nitriles with special emphasis on the mechanism of inefficient radical production in these reactions has been a major interest in this research group. The "cage effect" or geminate recombination of radicals has been carefully studied for 2,2'-azobisisobutyronitrile (ABN) (1) and 1,1'-azocyanocyclohexane (ACC) (2). Thermal decomposition of these aliphatic azo-nitriles involves as a first step the homolytic cleavage (3,4) of the carbon-nitrogen bonds in the C-N=N-C portion of the molecule giving nitrogen and two radicals which are nearest neighbors in a "cage" (5) of solvent molecules. Two subsequent processes may then occur (6). These are: 1) Primary recombination of these geminate radicals within the "cage"; or 2) Diffusion of these fragments from their initial lattice sites. If process 2) occurs, there is a high probability that these two original nearest neighbors may again become nearest neighbors if diffusion has only separated them by one or two lattice sites. Recombination of these fragments which have begun to separate, but diffuse together again, is designated as secondary recombination (6). When diffusion has proceeded to such an extent that the probability of encounter between original geminate radicals approaches the probability of encounter between any two given radical fragments, the radicals are said to be "free" in solution.

The choice of the word encounter, as opposed to collision of these fragments, is important in understanding "cage effects." Any model of a liquid predicts that once two species A and B have become nearest neighbors, they will exist in that situation for a time which is long compared to molecular vibration frequencies (7). This time of encounter is on the order of 10^{-11} sec. for non-interacting fragments in solution. The analogous collision time for two species in the gas phase is on the order of 10^{-13} sec. The time of encounter for species in solution is also dependent on any specific interactions which may exist between A and B, or between A or B and solvent molecules (7). Thus attractive interactions between A and B would be expected to lengthen encounter times, while repulsive interactions will shorten this time. Solvent viscosity and dielectric constant might be considered to be important factors in determining these encounter times. However, specific interactions between solvent molecules and A or B may have no relation to bulk solvent properties and the meaning of such correlations or lack of correlations is to be seriously questioned.

The amount of primary and secondary recombination is considered to constitute the "cage effect" (6). The fraction of initially formed radicals which survive these reactions is designated as the efficiency of radical production. Of course, coupling of radicals is not the only primary or secondary process which decreases the efficiency of radical production. Disproportionation of radical fragments

may also occur, and will be just as effective in removing radicals from solution.

Initially formed radicals may possess some extra vibrational energy (1) which will be rapidly dissipated on encounters with solvent molecules. However, it might also be expected the the frequency factor for reactions between these "hot" radicals, produced as nearest neighbors, would be greater than that for reaction between fragments which have diffused apart and have had the opportunity for deactivation by solvent molecules. The degree of primary recombination may thus be influenced by the extra energy which these radicals possess. There is, however, no indication that the chemistry which these radicals undergo after formation is affected by any extra energy which they may possess.

In order to extend the studies of azo-compounds and geminate recombination processes, the thermal decomposition reactions of azo-amidines and their salts have been investigated. Azobisisobutyramidinium chloride (ABA-2HCl), shown in Figure 1, was first reported by Upson (8) in 1952, and is in current use industrially as a

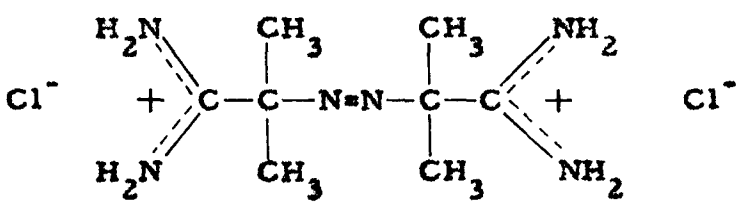

Fig. 1

water soluble polymerization initiator (9). It is easily synthesized from the well known polymerization initiator azobisisobutyronitrile (ABN) by the method of Pinner (8, 10). This compound was considered to decompose in a manner analogous to that of azo-nitriles giving quantitative nitrogen evolution and 2-isobutyramidinium radicals (11). Preliminary measurements of its rate of decomposition in water showed that it decomposed more rapidly than ABN at comparable temperatures (12).

The azo-amidinium salt (Fig. 1) presented an interesting system since the possibility existed that the mono-protonated (ABA-HCl) and unprotonated (ABA) forms of this compound could be similarly studied (13). The major interest in studying these three forms of this azo-amidine was to determine the effect of the positively charged amidinium groups on the amount of geminate recombination. Schematically, the decomposition reactions of these variously protonated amidines was visualized as shown in equations 1-3 (13). The bars across the top of the radical pairs symbolize that these radicals are

$$A\text{-}N_2\text{-}A \xrightarrow{k_0} N_2 + \overline{A\cdot\ \cdot A} \xrightarrow[k_{D0}]{k_{R0}} \qquad (1)$$

$$A\text{-}N_2\text{-}\overset{+}{A}H \xrightarrow{k_1} N_2 + \overline{A\cdot\ \cdot AH}^{+} \xrightarrow[k_{D1}]{k_{R1}} \qquad (2)$$

$$\overset{+}{H}A\text{-}N_2\text{-}\overset{+}{A}H \xrightarrow{k_2} N_2 + {}^{+}\overline{HA\cdot\ \cdot AH}^{+} \xrightarrow[k_{D2}]{k_{R2}} \qquad (3)$$

initially formed as nearest neighbors. The constants k_R and k_D refer to the primary and secondary reactions, and the competing diffusion process, respectively. The constants k_0, k_1, and k_2 are, respectively, the specific rate constants for decomposition of the unprotonated, monoprotonated, and diprotonated azo-amidines. The efficiency of radical production is equal to the ratio k_D/k_R. Since the geminate pair in equation 3 involves two positively charged species, it would be expected that k_{D2}/k_{R2} would be greater than k_{D0}/k_{R0} or k_{D1}/k_{R1}. In particular, it was of interest to determine the absolute magnitude of this ratio for ABA-2HCl (13). The effect of protonation on the rate of the decomposition reaction was also of interest (13).

The originally conceived research problem involved studies of the rate of decomposition and efficiency of radical production of ABA-2HCl in aqueous solution as a function of pH (13). It was shortly determined that aqueous base was not sufficiently strong to neutralize the diprotonated azo-amidinium salt, and that hydrolysis of the amidinium groups occurred rapidly in strong aqueous alkali solutions. Potentiometric titration curves obtained from the addition of aqueous sodium hydroxide to solutions of ABA-2HCl showed no inflection point characteristic of neutralization of the weakly acidic amidinium groups (see Experimental).

A suitable non-aqueous solvent system was desired. Several requirements had to be met by this solvent. The three species ABA,

ABA-HX, and ABA-2HX had to be soluble. Further, the solvent could not be so acidic that ABA would be protonated, or so basic that ABA-2HX would be deprotonated. Nor could it be a solvent that would readily solvolyze the amidine or amidinium groups. A fourth requirement was that it be inert to the radicals produced in the decomposition reactions. No suitable non-aqueous solvents could be found that would dissolve ABA-2HCl. However, it was found that the dinitrate ($ABA\text{-}2HNO_3$) (14) was readily soluble in anhydrous dimethyl sulfoxide (DMSO). DMSO also met the other requirements in that it is a weak base (15) and less acidic than triphenylmethane (16). The stability of DMSO toward radicals was not known. To check this point, ABN was thermally decomposed in DMSO (see Experimental). Tetramethylsuccinodinitrile was isolated in > 85% yield. It is thus assumed that DMSO is relatively inert to the radicals which would be produced by thermal decompositions of the azo-amidines. Unfortunately, DMSO is thermally unstable. Decomposition is not visually noticeable in reactions which are run for periods of less than 10 hours below 80°. However, the reaction mixture develops the characteristic odor of dimethyl sulfide after even short reaction periods (1-3 hours) at temperatures as low as 60°. On evaporation of the solvent after a reaction time of several hours at 70-80°, viscous yellow or orange decomposition products are present. These make quantitative product analyses difficult and unpleasant.

At the time that this study was begun, the only available azoamidine was ABA-2HCl. Syntheses of the free base ABA, and the dinitrate salt ABA-$2HNO_3$ are described in the Experimental section. In the process of looking for suitable solvents for ABA-2HCl, a reaction between ABA-2HCl and ethylenediamine was discovered which gives excellent yields of azobis-N,N'-dimethyleneisobutyramidine (ADEBA) shown in Figure 2. The procedure for the preparation of this azo-

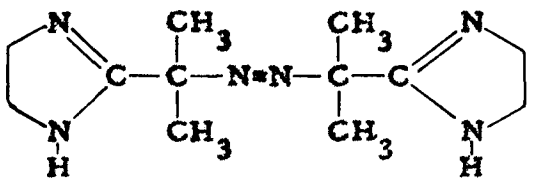

Fig. 2

amidine and its dinitrate (ADEBA-$2HNO_3$) are given in the Experimental section.

The majority of the kinetic studies have been performed with the ADEBA system which is analogous to the ABA system. The reason for this switch in compounds was necessitated by two annoying properties of ABA (free base). The half-life of ABA at 70° is on the order of 50 hours, making studies in the thermally unstable DMSO quite difficult. Secondly and most important, thermal decomposition of ABA yields not only nitrogen, but also ammonia. This feature adds no apparent complications to the chemistry of the decomposition reaction, as will be discussed later, but makes rate studies by gas evolution techniques

very tenuous. Accurate rate constants have not been obtained for either nitrogen or ammonia evolution. At the time that this research was being carried out it seemed much more advisable to study the ADEBA system which would yield the same information as the originally conceived problem involving ABA.

The results have been divided into several broad categories. These deal basically with the chemistry, the rates, and the efficiencies of the decomposition reactions. The Experimental section is similarly categorized. In addition, the synthesis of a new azo-nitrile is described.

I wish to thank Drs. C. S. Wu and B. Seidel for their time and efforts in design and construction of an improved gas apparatus which has been invaluable for these studies. I also wish to thank Dr. U. S. Nandi and Mr. Richard Tunder for the time which they spent helping me to learn the manometric technique and for cleaning up the mess when I turned the wrong stopcock.

Results and Discussion

Products of the Thermal Decomposition Reactions

No material balance has been obtained in any product analysis of thermal decomposition reactions of the azo-amidines or azo-amidinium salts in water or DMSO. A series of products from the thermal decomposition of ABA-2HCl in water have been reported by Dougherty (17). All of these products can be considered to arise from tetramethylsuccinamidinium chloride (Fig. 3) or tetramethylsuccinimidinium chloride (Fig. 4). Since the decomposition reaction is studied in water, hydrolysis of these

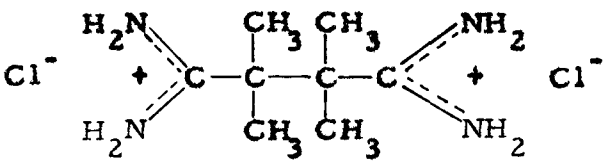

Fig. 3

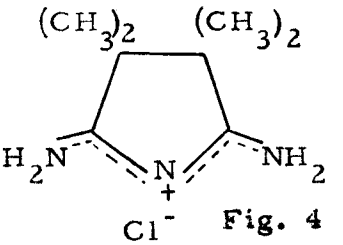

Fig. 4

first formed products leads to a series of products such as imides, anhydrides, and mixed amide-amidinium compounds. All of these products are derived from carbon-carbon coupling of the first formed radicals.

Similarly, the thermal decomposition reactions of ABA-2HNO$_3$ and ADEBA-2HNO$_3$ in anhydrous dimethyl sulfoxide give 35% and 29% yields, respectively, of products which are identified as tetramethylsuccinimidinium nitrate (analogous to the chloride in Fig. 4) and N,N'-dimethylene-tetramethylsuccinamidinium nitrate (Fig. 5). Dougherty (17)

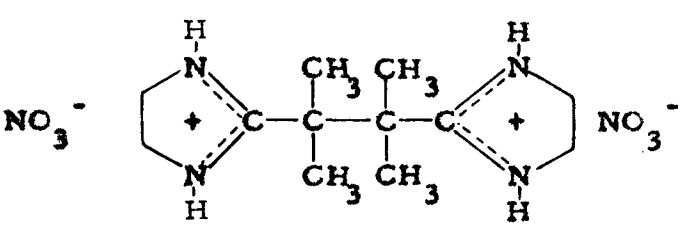

Fig. 5

discusses the possibility of two tautomeric forms of the imidinium salt (Fig. 4).

A complete description of the imidinium salt (Fig. 4) is given in the Experimental section.

The structure of the imidinium salt (Fig. 4) has been confirmed by microanalysis, and hydrolysis to tetramethylsuccinimide. The structure of the diamidinium salt in Figure 5 agrees with microanalytical results and is suggested by the fact that n.m.r. spectra in water, and infrared spectra (nujol mull) of this salt and ADEBA-$2HNO_3$ are practically identical.

Products from the thermal decomposition reactions of ABA and ADEBA in DMSO have not been characterized. Thermal decomposition of ADEBA in DMSO gives a solid product in 34% yield whose n.m.r. and infrared spectra in chloroform differ markedly from those of ADEBA. The n.m.r. spectrum of this product in 15% sulfuric acid, however, is practically superimposable on that of ADEBA in 15% sulfuric acid. The n.m.r. spectrum of this product in dilute aqueous acid initially resembles that in chloroform, but slowly changes to the very simple two component spectrum observed in sulfuric acid. It has been found that hydrolysis of the amidinium groups to give ethylenediamine cannot account for these simple spectra in sulfuric acid. The resonance signal of the methylene protons of added ethylenediamine is quite distinct from those of the product or ADEBA in these sulfuric acid solutions. It is postulated that the product isolated in 34% yield may be one of those represented in Figure 6, and that addition of this material to sulfuric acid brings about acid catalyzed

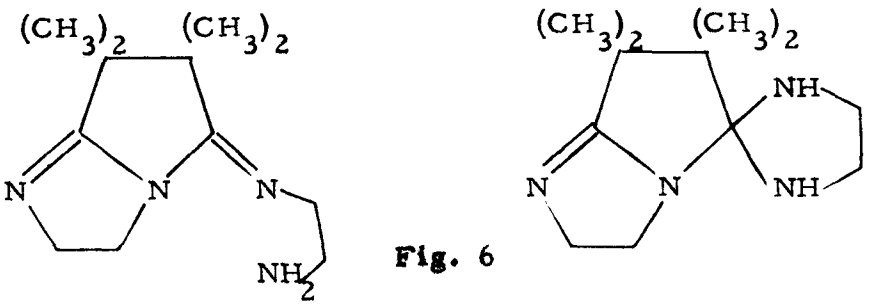

Fig. 6

conversion to the diamidinium ion shown in Figure 5. The n.m.r. spectrum of the product in sulfuric acid is practically identical to the n.m.r. spectrum of the diamidinium salt (Fig. 5) in water except for minor variations in chemical shift of the methyl group and methylene group signals (see Experimental).

No products from thermal decomposition of ABA have been examined. However, it is known that ammonia evolution accompanies the decomposition reaction in relatively high yield. Rates of ammonia evolution in decomposition reactions of ABA will be discussed below. Ammonia evolution leads to the conclusion that a cyclized product analogous to the imidine (Fig. 4) may be formed in this decomposition reaction.

The fact that the cyclized imidines rather than open chain diamidines are produced in these decomposition reactions (with the exception of ADEBA-2HNO$_3$) may be considered to be due to unfavorable steric interactions in the open-chain compounds. Eberson (18) has synthesized a series of tetraalkyl succinic acids and notes that in aqueous solution, conversion to the anhydrides is quite facile. That

the product from decomposition of ADEBA-$2HNO_3$ is apparently an acyclic diamidinium salt is somewhat surprising. However, this may arise from a combination of factors. The amidinium groups in the diamidinium salt (Fig. 5) are favorably resonance stabilized. Cyclisation to form an imidine structure would destroy at least one of these groups. However, the ring systems in ADEBA possess no analogous stabilization. Further, the base or nucleophile strengthening effect of DMSO is well known. Hence the formation of the imidine type product from ADEBA by nucleophilic attack at carbon may somehow lower the energy of the molecule. When this imidine (Fig. 6) is dissolved in acid, imidine ring opening may be rapid due to the resultant favorable amidinium resonance. Cyclisation of tetramethylsuccinamidinium ions to give the imidinium ions (Fig. 4) destroys one amidinium group, but on the other hand can give the tautomeric form shown in Figure 4, in which amidinium-type resonance is maintained. This is not possible for the analogous imidinium salt corresponding to cyclisation of the diamidinium salt shown in Figure 5.

No products other than those arising from carbon-carbon coupling reactions have been isolated. Acid catalyzed hydrolysis of the reaction mixture from a thermal decomposition of ADEBA-$2HNO_3$ in DMSO, and subsequent vapor phase chromatographic analysis of an ether extract of the hydrolysate, suggests that isobutyric acid is present. Bickel and Waters (19) have studied the thermal decomposition

reaction of dimethyl azobisisobutyrate in benzene and have isolated methyl isobutyrate in 14% yield. Other products isolated were dimethyl tetramethylsuccinate (41%), methyl methacrylate (4%), and dimeric and trimeric products (37%) arising from disproportionation and coupling reactions of carbmethoxy-isopropyl radicals with radicals produced by addition of carbmethoxy-isopropyl radicals to methyl methacrylate. A part of the methyl methacrylate, and all of the methyl isobutyrate, are undoubtedly formed in a disproportionation reaction in competition with the coupling reaction giving dimethyl tetramethylsuccinate. Dimethyl azobisisobutyrate is structurally analogous to the azo-amidines and their salts and similar reactions may well occur in these systems. Isobutyric acid would arise from acid hydrolysis of N,N'-dimethylene-isobutyramidinium nitrate, produced as a result of disproportionation of the amidinium-isopropyl radicals.

It has been shown that two types of radical coupling reactions occur in thermal decomposition reactions of ABN and ACC. These give rise to the carbon-carbon coupled products tetramethylsuccinodinitrile (in the case of ABN) (20) and a carbon-nitrogen coupled product which is a keteneimine (21). The keteneimine thermally decomposes to give the original cyano-propyl radicals (in the case of ABN) which may again couple to give the dinitrile or the keteneimine (1). No analogous carbon-nitrogen coupled products have been isolated in

decomposition reactions of the azo-amidines or their salts. This possibility has been discussed by Dougherty (17).

Rates of Thermal Decomposition Reactions

The rates of thermal decomposition of the various azo-compounds have been studied by measuring rates of nitrogen evolution. The majority of the rate studies have been performed in pure anhydrous dimethyl sulfoxide or mixtures of DMSO and cumene or tetralin. Some preliminary experiments were done to measure the rates of decomposition of ABA-2HCl and ABA-2HNO_3 in water; however, the rate study by Dougherty (17) on ABA-2HCl in water is much more complete, and will be used to supplement these studies in DMSO.

The gas evolution method has been highly developed in these laboratories and offers the most useful technique for kinetic studies on azo-compounds. These studies have been done using two gas apparatus. The preliminary experiments on ABA, ABA-2HNO_3, and ABA-2HCl, were performed on a gas apparatus previously described in the literature (22). The majority of the studies which are reported here have been done on a new apparatus which is based on the design of the original gas apparatus, but incorporates some very helpful modifications. This latter apparatus is described in the Experimental section. The older apparatus will be noted as GA-I, and the newer apparatus as GA-II.

Two basic methods have been used to evaluate rates of gas evolution. These are represented by equations 4 and 5.

$$\log(V_\infty - V_t)/V_\infty = -kt/2.303 \tag{4}$$

$$(dN_2/dt)_t/A_o = ke^{-kt} \tag{5}$$

Equation 4 is readily derived from an integrated first order rate equation, and equation 5 is the differential form of this same rate equation. Equation 4 requires that the decomposition reaction be studied at constant pressure, that the final total volume of gas be known or measurable, and that a series of volumes be determined as a function of time. The gas apparatus are constructed so that the readings V_∞ and V_t are made at identical pressures. The quantity V_∞ has been experimentally measured in most of the rate studies and is taken as the volume of gas evolved after 7-10 half-lives of reaction. V_∞ may also be calculated if the initial amount of azo-compound, and the absolute pressure in the system are known. In all cases where V_∞ has been measured and calculated for the same run, the correspondence is good. The reference pressure in the apparatus is made equal to atmospheric pressure and hence a barometric reading made at the time of the run allows for the pressure determination.

The use of equation 5 requires a knowledge of the initial amount of azo-compound A_o, and the reference pressure. When the reaction is sufficiently slow so that several volume readings may be made while

$e^{-kt} \approx 1$, the rate may be determined from the slope of the volume versus time readings. Otherwise, the rate of gas evolution is determined from a tangent to the curve, generated by the volume versus time readings, at time t.

The rate constants reported in this section (with the exception of those for ABA) have been determined by the V_∞ method. Where rate constants have been calculated by both methods, agreement is quite good. The data are reported in Table I. The column entitled Code gives the gas apparatus used, GA-I or GA-II; the method of analyzing the results; V_m or V_c for measured or calculated V_∞, and V_i for initial rate of gas evolution. The results for ABA are tentative and will be discussed below in conjunction with studies on attempts to measure the rate of ammonia evolution in this decomposition reaction. All rate constants were determined graphically from the best visual straight line through the data.

Enthalpies and entropies of activation have been determined for ADEBA-$2HNO_3$ and ADEBA in DMSO and DMSO-cumene, respectively, from the rate constants in Table I. The activation parameters are: ADEBA-$2HNO_3$, $\Delta H^\ddagger$ = 26 kcal. $mole^{-1}$, $\Delta S^\ddagger$ = +1 cal. $mole^{-1}$ $deg.^{-1}$; and ADEBA, $\Delta H^\ddagger$ = 29 kcal. $mole^{-1}$, $\Delta S^\ddagger$ = +7 cal. $mole^{-1}$ $deg.^{-1}$. Due to the narrow temperature range, these parameters must be considered tentative.

An inspection of Table I shows that the rates of decomposition

TABLE I

First Order Rate Constants for Nitrogen Evolution for a Series of Azo-Amidines

Run[a]	Azo Compound	T (°C)	Solvent[b]	k_{-1} (sec.$^{-1}$ x 10^5)		Code[c]	
147	ADEBA-2HNO$_3$	60	D-T	21.29		GA-II,	Vm
216	" "	"	D-C	19.11		"	"
219	" "	"	D-C	20.81	20.0±.9	"	"
93	" "	"	D	20.32		"	"
94	" "	"	D	21.11		"	"
95	" "	"	D	20.37	20.6±.4	"	"
217	" "	70	D-C	70.87		"	"
218	" "	"	D-C	68.44	69.7±1.2	"	"
87	" "	"	D	66.46		"	"
88	" "	"	D	66.95		"	"
91	" "	"	D	65.86	66.4±.4	"	"
97	" "	75	D	108.0		"	"
152	ADEBA	60	D-T	1.085		"	"
126	"	75	D-C	8.188		"	"
127	"	"	D-C	7.896	8.04±.14	"	"
114	"	80	D-C	13.78		"	"
117	"	"	D-C	13.96		"	"
118	"	"	D-C	13.90	13.9±.1	"	"
105	"	"	D	17.91		"	"
111	"	85	D-C	27.15		"	"
112	"	"	D-C	25.09	26±1	"	"
221	ABA-2HNO$_3$	60	D-C	4.86		"	"
82	" "	70	D-C	15.3		"	"
83	" "	"	D	17.6		"	"
1	ABA-2HCl	70	H_2O	14.8		GA-I,	Vm
2	" "	"	"	15.5		"	"

TABLE I (continued)

Run[a]	Azo Compound	T (°C)	Sol-vent[b]	k ($sec.^{-1} \times 10^5$)		Code[c]
13	ABA[d]	70	D	0.3588		GA-I, VI
16	"	"	D	0.3696		" "
17	"	"	D	0.3728		" "
19	"	"	D	0.3697	0.368±.003[d]	" "
181	ABN	70	D-C	4.871		GA-II, Vm
183	"	"	D-C	4.934	4.90±.03	" "
161	AACC[e]	90	CB	3.308		" "

(a) Run number refers to notebook experiment number.

(b) D-T is 2:1 DMSO-tetralin (by vol.); D-C is 2:1 DMSO-cumene (by vol.); D is anhydrous DMSO; CB is chlorobenzene.

(c) See text prior to Table I.

(d) Rate constant for total gas evolution (NH_3 and N_2).

(e) 1,1'-Azocyano-(N-methyl)-4-azacyclohexane.

of ADEBA-2HNO$_3$ and ABA-2HNO$_3$ are greater than those of ADEBA and ABA, respectively, at comparable temperatures. This is reflected in the enthalpies of activation which have been determined for ADEBA-2HNO$_3$ and ADEBA. These rate differences are in accord with the expected stabilities of the radicals which are produced in the decomposition reactions. A simple resonance treatment applied to the amidinium and amidine radicals is shown in Figure 7.

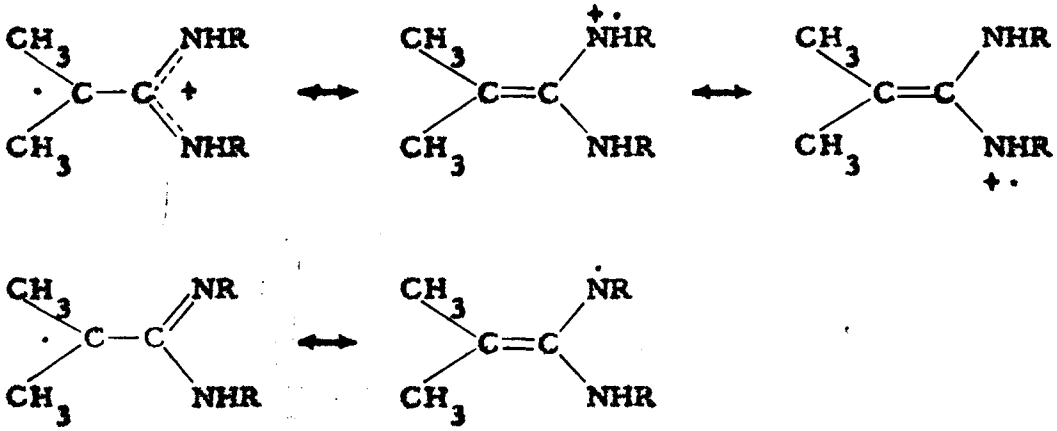

Fig. 7

Rates of decomposition of other aliphatic azo-compounds are similarly discussed in terms of stabilities of the resultant radicals (4). Representative activation parameters for azo-compounds are: azobisdiphenylmethane (toluene) (23), $\Delta H^{\ddagger}$ = 26.6 kcal. mole^{-1}, $\Delta S^{\ddagger}$ = +2 cal. mole^{-1} deg.$^{-1}$; ABN (toluene) (24), $\Delta H^{\ddagger}$ = 31.1, $\Delta S^{\ddagger}$ = +3; ABA-2HCl (water) (17), $\Delta H^{\ddagger}$ = 29.1, $\Delta S^{\ddagger}$ = +9; and azobis-γ,α'-diphenylethane (toluene) (25), $\Delta H^{\ddagger}$ = 32.6, $\Delta S^{\ddagger}$ = +7. The similarity of these activation parameters to those of the azo-amidines implies

that simple homolytic fission takes place in the rate determining step. The fact that imidine-type products are obtained might have led to the conclusion that cyclization occurs before homolytic cleavage to give nitrogen. This process would require that the azo-compounds (presumably having a trans configuration about the azo-linkage) isomerise to the cis configuration, and cyclize to form a seven membered ring. The entropies of activation are not in accord with such a process; the less positive entropy of activation being associated with ADEBA-$2HNO_3$, which does not give cyclic products.

The greater rates of decomposition for the ADEBA system, compared to the ABA system, imply that the methylene bridge in the amidine groups of ADEBA and ADEBA-$2HNO_3$ increases the stabilities of the resultant radicals, perhaps by restricting the geometry in these groups or through a hyperconjugative mechanism.

Ammonia Evolution from ABA

Insufficient data are available to determine either the true rate of nitrogen, or ammonia evolution in thermal decompositions of ABA. Three attempts have been made to determine the rate of decomposition of ABA by gas evolution techniques. These procedures are described in the Experimental section. Since it was known that ammonia was being evolved simultaneously with nitrogen, each of these procedures attempted to remove ammonia from the evolving gas and thus allow only nitrogen to determine the gas buret volume readings. Rate constants

were calculated from the expression $(dGas/dt)_o = kA_o$. Two rate constants were obtained which were smaller than the rate constant $k = 3.6 \times 10^{-6}$ sec.$^{-1}$, determined for total gas evolution (Table I). However, it is not known if all ammonia was trapped in the experiment giving the smallest rate constant (2.6×10^{-6} sec.$^{-1}$). Hence, these experiments are of little value except to confirm that ammonia was produced.

In an alternate experiment, the ammonia evolution from a solution of ABA in DMSO was monitored at 70°. The detailed procedure is given in the Experimental section. Unfortunately, reliable data were obtained only after the reaction had proceeded for > 100 hours. The data are given in Table XII. A kinetic treatment of ammonia evolution with this limited data is complicated. It is not known if a stoichiometric amount of ammonia is evolved in the decomposition reaction. It is assumed that ammonia arises from cyclization of diamidines which are produced as a result of coupling reactions. Disproportionation reactions would be expected to decrease the yield of ammonia. If cyclisation of the resultant diamidines occurs in a sufficiently rapid process, the rate of ammonia evolution will then be determined by the rate of the primary azo scission process. However, if cyclisation is slow in relation to the homolytic decomposition step, the rate of ammonia evolution will be given by a more complex kinetic expression (26). Insufficient data are available for a treatment of this type. If it is assumed that the rate of ammonia evolution may be

expressed by equation 6

$$R = dNH_3/dt = k_{NH_3} ABA \tag{6}$$

and that the rate constant for decomposition of ABA may be expressed in the normal manner as shown in equation 7, it is then possible to

$$\log(ABA/ABA_o) = -kt/2.303 \tag{7}$$

obtain equation 8, which allows the determination of the rate constant

$$\log R = \log R_o - kt/2.303 \tag{8}$$

k for thermal decomposition of ABA. Using the data in Table XII, a value of $k = (1.7 \pm .2) \times 10^{-6}$ sec.$^{-1}$ has been calculated from a slope of a plot of log R versus t. If equation 6 is valid, it may be rewritten in the form shown in equation 9, where k is the value of the rate constant for azo decomposition determined from equation 8.

$$R/ABA_o = k_{NH_3} e^{-kt} \tag{9}$$

Values of k_{NH_3} have been calculated from this equation and the data in Table XII. These results are given in Table II. The interesting result derived from Table II is that the specific rate constant for ammonia evolution is greater than the derived value of k for decomposition of ABA. This probably means that ammonia evolution does not occur by a process which is rapid compared to the thermal decomposition process. This conclusion invalidates equations 6, 8, and 9, and requires that a greater amount of data on ammonia evolution be accumulated for this reaction.

TABLE II

Rate Constants for Ammonia Evolution.

ABA in DMSO. 70°

Reaction Time[a] (hrs.)	R/ABA ($hr.^{-1} \times 10^{3}$)	e^{-kt}[b]	k_{NH_3}[c] ($sec.^{-1} \times 10^{-6}$)
104	4.3	0.517	2.3
123	3.9	0.472	2.3
126	3.7	0.463	2.2
148	3.3	0.403	2.3
196	2.4	0.298	2.2

(a) Average values of closely spaced determinations (see Table XII). $ABA_o = 1.01 \times 10^{-2}$ moles

(b) $k = 1.7 \times 10^{-6}$ $sec.^{-1}$

(c) Calculated from equation 9.

Rates of Decomposition of Monoprotonated Azo-amidines

It has been possible to study the rates of thermal decomposition and efficiencies (vide infra) of the unprotonated azo-amidines and the diprotonated azo-amidinium salts in DMSO, and DMSO-hydrocarbon solvents. The monoprotonated salts of ABA or ADEBA represented in Figure 8 cannot be studied separately in solution. If it were possible to prepare and isolate one of these mono-salts, an equilibrium would be established between it and the unprotonated and diprotonated species

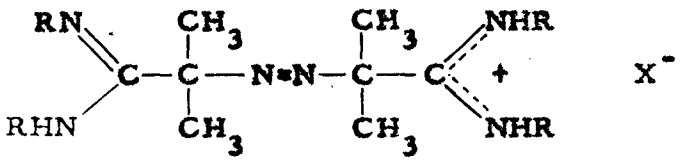

Fig. 8

as soon as it was dissolved in solution. The diamidines are analogous to dicarboxylic acids in that an acid-base equilibrium can be formulated as shown in Figure 9. A_0, A_1, and A_2 refer to ABA, ABA-HX,

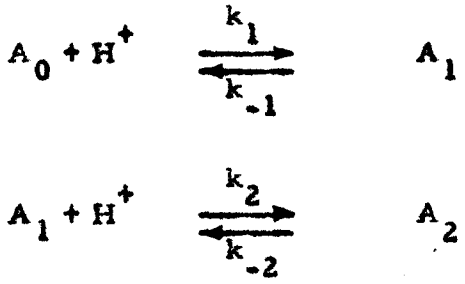

Fig. 9

and ABA-2HX (or ADEBA, ADEBA-HNO_3, and ADEBA-$2HNO_3$), respectively. The ratios of the various species in solution can then be represented by the expression given in equation 10, where

$$(A_1)^2/(A_0)(A_2) = K_1/K_2 \qquad (10)$$

$K_1 = k_1/k_{-1}$, and $K_2 = k_2/k_{-2}$.

It has been found (see Experimental) that a potentiometric titration curve, obtained on addition of methanolic hydrogen chloride to a solution of ABA in methanol, shows only a single inflection point

corresponding to two equivalents of acid. This observation indicates that the magnitudes of K_1 and K_2 are similar (27). It is possible to qualitatively estimate this ratio (K_1/K_2) using a method analogous to that applied to dicarboxylic acids by Bjerrum (28, 29). This has been done and is discussed at the end of this section. It will be shown that the statistical lower limit to the ratio K_1/K_2 is equal to 4, analogous to that of dicarboxylic acids. Since ABA is synthesised in good yield by the addition of an equivalent amount of ABA-2HCl to a sodium methoxide-methyl alcohol solution, the possibility of the amidine groups being sufficiently basic to remove protons from methyl alcohol is discounted. Thus the titration curve cannot be accounted for by assuming titration of methoxide ion.

In order to determine the rate constants for decomposition of the monoprotonated amidines ABA-HCl and ADEBA-HNO_3, two different techniques have been utilized. The first method involved addition of known amounts of concentrated hydrochloric acid to DMSO solutions containing known amounts of ABA. The initial rates of gas evolution were monitored and,with appropriate kinetic equations to be described below, an estimation of the rate of decomposition of ABA-HCl was possible. The second method involved mixing known amounts of ADEBA and ADEBA-$2HNO_3$ in DMSO. The rate of gas evolution was monitored and together with the appropriate expressions an estimation of the rate of decomposition of ADEBA-HNO_3 was obtained.

Discussion of results will be deferred until each method has been separately described and the results given.

ABA in DMSO. The rate of nitrogen evolution in a three component system consisting of ABA, ABA-HCl, and ABA-2HCl is shown in equation 11. The rate constants k_0, k_1 and k_2 refer to the rate of

$$dN_2/dt = k_0A_0 + k_1A_1 + k_2A_2 \qquad (11)$$

decomposition of ABA(A_0), ABA-HCl (A_1) and ABA-2HCl (A_2), respectively. Known amounts of concentrated hydrochloric acid have been added to DMSO solutions containing known amounts of ABA. It is expected that an equilibrium distribution of the three components A_0, A_1, and A_2 is established. The data for gas evolution studies on these mixtures at 70° are reported in Table XIII.

The problem of ammonia evolution in the thermal decomposition of ABA has been discussed previously. It should be pointed out that in these three component systems containing an excess of ABA, ammonia may be expected to be a product of the decomposition of each component. Any ammonium ion that is produced in the decomposition reactions will act like a strong acid to the amidine groups of ABA. Since neither the amount nor the rate of ammonia evolution is known, a maximum correction will be made. It is assumed that each azoamidine will decompose to give stoichiometric amounts of nitrogen and ammonia. This means that the rate of nitrogen evolution in

equation 11 will be taken as half of the observed rate of gas evolution (Table XIII).

In these experiments, the rates of gas evolution varied with the amount of added acid (Table XIII), but were constant for at least 100 minutes of each decomposition reaction. This implies that the concentrations of A_0, A_1, and A_2 remained "kinetically" constant over this period of reaction. A relatively small amount of acid was added in relation to the initial amount of ABA in solution. Thus the major species in solution was ABA. The rate of gas evolution from ABA in DMSO has been previously determined (Table I) and shows that ABA has a half-life of at least 50 hours at 70°. Hence, the loss of ABA due to thermal decomposition is negligible. The half-life of ABA-2HCl is approximately 1.1 hours at 70°. Its concentration should decrease by approximately a factor of 2 over this period. The half-life of ABA-HCl is unknown, but should be no less than that of ABA-2HCl. If the amidine groups of ABA are more basic than the products of decomposition, it would be expected that proton transfer between ABA and these products would approximately re-establish the initial equilibrium distribution of the three components. Thus the observed linearity of gas evolution with time over a 100 minute period is not unreasonable.

The rate constant k_1 has been determined in three separate runs using equation 11. The rates of nitrogen evolution are taken as half of the observed rates of gas evolution given in Table XIII. The

rate constant k_0 is taken as 1.8×10^{-6} sec.$^{-1}$ (see Table I) in accord with the assumption of stoichiometric nitrogen and ammonia evolution, and k_2 is taken as 1.7×10^{-4} sec.$^{-1}$ (Table I). The amounts of the three azo-compounds have been determined from the known initial amount of ABA, and the amount of added acid, for two different values of K_1/K_2 using equation 10. The data are presented in Table III. The detailed procedure for this study is given in the Experimental section.

TABLE III

Rate Constant for Decomposition of ABA-HCl in DMSO. 70°

Run	K_1/K_2	A_o (a,b) (moles x 10^5)	A_1 (a,b) (moles x 10^5)	A_2 (a,b) (moles x 10^5)	k_1 (a,c,d) (sec x 10^6)
5	4.0	23.14	2.070	0.046	71
1	"	20.73	4.135	0.205	49
2	"	18.96	5.804	0.444	47
5	17.4	23.15	2.109	0.011	72
1	"	20.73	4.279	0.051	53
2	"	18.96	6.136	0.114	53

(a) Initial concentration of ABA and added acid as well as values of $(dG/dt)_0$ are given in Table XIII.

(b) Calculated from equation 10 using an iterative procedure and the values K_1/K_2 given in column 2.

(c) Calculated from equation 11.

(d) Rate constants used were $k_0 = 1.8 \times 10^{-6}$ sec.$^{-1}$ and $k_2 = 1.7 \times 10^{-4}$ sec.$^{-1}$

ADEBA-ADEBA-$2HNO_3$ in DMSO. This study differs from that just described in that a mineral acid was not added to a DMSO solution of ADEBA, but known amounts of both ADEBA and ADEBA-$2HNO_3$ were mixed together in DMSO. The equilibrium shown in equation 12

$$A_0 + A_2 \rightleftharpoons A_1 \qquad (12)$$

describes the system. The symbols A_0, A_1, and A_2 refer to ADEBA, ADEBA-HNO_3, and ADEBA-$2HNO_3$, respectively. The ratio of these species is given by equation 10 shown above. The rates of gas evolution from the mixed solution were determined and are reported in Table XIV, along with the initial amounts of ADEBA and ADEBA-$2HNO_3$. The rate of gas evolution from these mixtures is that given in equation 11. No ammonia is evolved in these decomposition reactions and hence the observed rate of gas evolution is equal to the rate of nitrogen evolution. The rates of gas evolution reported in Table XIV were evaluated at a finite time t. This value of t was taken as close to t = 0 as possible within the limits of initial solvent equilibration in the gas apparatus. For the purpose of this calculation, it must be assumed (as in the prior treatment) that the initial equilibrium distribution of the three components is not significantly changed over the time t.

The rate expression given in equation 13 describes the rate of

$$(dN_2/dt)_t = k_0 e^{-k_0 t} A_0 + k_1 e^{-k_1 t} A_1 + k_2 e^{-k_2 t} A_2 \qquad (13)$$

gas evolution at time t for the resultant three component system. The

initial amounts of the three species have been calculated assuming $K_1/K_2 = 4$, and $K_1/K_2 \rightarrow \infty$, and are given in Table IV. The rate constant k_1 has been calculated from data in Tables IV and equation 13.

Discussion. The rates of decomposition of the monoprotonated azo-amidines ABA-HCl, and ADEBA-HNO_3, determined by the above procedures are summarized in Table V, along with the rates of decomposition of the unprotonated and diprotonated compounds.

TABLE V

Rate Constants for Decomposition of Unprotonated, Monoprotonated, and Diprotonated Azo-Amidines in DMSO

Compound	T (°C)	K_1/K_2	k_{-1} (sec.$^{-1}$ x10^5)	Ref.
ADEBA	60	-	1	a,b
ADEBA·HNO_3	"	4	25±3	c
"	"	∞	20±1	c
ADEBA·$2HNO_3$	"	-	20.6±.4	a,b
ABA	70	-	0.2	a,d
ABA·HCl	"	4	6±1	e
"	"	17.4	6±1	3
ABA·$2HNO_3$	"	-	17	a

(a) Table I (c) Table IV (e) Table III

(b) Table XIV (d) Page 110.

TABLE IV

Rate Constant for Decomposition of ADEBA·HNO_3 in DMSO. 60°

Run	K_1/K_2	t (sec.)	A_0 [a] ($moles \times 10^5$)	A_1 [a] ($moles \times 10^5$)	A_2 [2] ($moles \times 10^5$)	$k_0 e^{-k_0 t} A_o$ [b] ($moles\ sec.^{-1} \times 10^9$)	$k_2 e^{-k_2 t} A_2$ [b] ($moles\ sec.^{-1} \times 10^9$)	$k_1 e^{-k_1 t}$ ($sec.^{-1} \times 10^4$)	k_1 [c] ($sec.^{-1} \times 10^4$)
1	4	600	1.21	6.99	10.06	0.1203	18.314	1.96	2.2
2	"	"	0.415	4.29	11.17	0.0413	20.335	2.11	2.4
4	"	"	3.62	9.24	5.89	0.3598	10.723	2.44	2.9
5	"	"	3.57	7.76	4.22	0.3549	7.683	2.27	2.7
6	"	1200	5.41	5.35	1.32	0.5345	2.124	1.99	2.5
								(Avg.) =	2.5±0.3
1	∞	600	~0	9.43	8.84	~0	16.093	1.70	1.9
2	∞	"	~0	5.11	10.75	~0	19.570	1.93	2.2
4	∞	"	~0	16.48	2.27	~0	4.133	1.79	2.0
5	∞	"	~0	14.89	0.65	~0	1.183	1.65	1.8
6	∞	1200	4.09	7.99	~0	0.4041	~0	1.62	2.1
								(Avg.) =	2.0±0.1

(a) Evaluated from data in Table XIV and equation 10.

(b) $k_0 = 1 \times 10^{-5}$ sec.$^{-1}$ and $k_2 = 2.06 \times 10^{-4}$ sec.$^{-1}$ at 60° (Table I). Data in Table XIV, runs 7 and 8, show that rates of initial gas evolution give the same results.

(c) Evaluated from plots of $k_1 e^{-k_1 t}$ vs. k_1 for appropriate values of t.

The ratios of the rate constants k_0, k_1, and k_2 for each azo-compound are: ABA, $k_1/k_0 = 30$, $k_2/k_0 = 85$, $k_2/k_1 = 2.8$; ADEBA, $k_1/k_0 \simeq 20$, $k_2/k_0 \simeq 20$, $k_2/k_1 \simeq 1$. These results are quite surprising.

It is generally considered that the transition state for decomposition reactions of aliphatic azo-compounds involves simultaneous cleavage of both C-N bonds to the azo linkage (4). The rates of thermal decomposition of azomethane and azoisopropane differ considerably, and the rate of decomposition of the unsymmetrical methylisopropyl azo compound is approximately the geometric mean of the rates of the symmetric compounds (30). This implies that two bond cleavage is occurring (30). If one bond cleavage was occurring, it would be expected that the rate of decomposition of the unsymmetrical compound would be only approximately a factor of two less than that of the diisopropyl compound; the rate being determined by cleavage of the C-N bond giving the most stable radical. Even in the case of the unsymmetrical, substituted phenylazotriphenylmethanes, simultaneous two bond cleavage is indicated by studies of substituent effects (31). Also, no experiment has yet been run in which $R_3C\text{-}N{=}N\cdot$ radicals have been trapped. This, however, by itself, does not require synchronous bond cleavage since these azo-radicals might be expected to lose nitrogen quite rapidly.

An inspection of the ratios k_1/k_0, and k_2/k_1, for the ABA,

and ADEBA systems thus leads to a startling conclusion. The rate constant for thermal decomposition of the monoprotonated species ADEBA-HNO_3 is identical within experimental error to that of the diprotonated species ADEBA-$2HNO_3$, each being larger than that for unprotonated ADEBA by a factor of 20. Further, $k_2/k_1 = 2.8$ for the ABA system, while $k_1/k_0 \simeq 30$. It should be remembered that assumptions concerning ammonia evolution for the ABA system have been made in such a way as to minimize k_1. On the basis of the preceding argument against non-simultaneous bond cleavage, it may be reasoned that the rate determining step in the decomposition of these azo-compounds (at least in the mono- and diprotonated species) involves cleavage of a single C-N bond; the identity of that bond being determined by the greater stability of the amidinium-isopropyl radical as compared to the amidine-isopropyl radical (vide supra).

The nature of these experiments in which the rate constants k_1 have been determined requires approximations, but a critical analysis leads to the conclusion that the rate ratios given above must be qualitatively correct. If equilibration between ADEBA and ADEBA-$2HNO_3$ does not occur, the rates of gas evolution will be due only to these two components. An inspection of the data in Table XIV makes this conclusion untenable. Since k_0 and k_2 have been separately determined and give the ratio $k_2/k_0 = 20$, it may be concluded that the

major contribution to gas evolution would be due to ADEBA-$2HNO_3$. In order to make the maximum correction, it will be assumed that the concentration of ADEBA-$2HNO_3$ at time t is equal to the initial concentration. The data in Table XIV give values of k_2 ranging from 2.2×10^{-4} sec.$^{-1}$ to 3.3×10^{-4} sec.$^{-1}$ Since the rate of gas evolution is observed to decrease with time in these studies, a more reasonable assumption would be that the amount of ADEBA-$2HNO_3$ was less than the initial amount by a factor of $e^{-k_2 t}$. Values of k_2 calculated on this basis range from 2.6×10^{-4} sec.$^{-1}$ to $\sim 4.5 \times 10^{-4}$ sec.$^{-1}$ for runs 1, 2, 4, and 5. In run 6, the value of $k_2 e^{-k_2 t} = 3.3$ which is obtained is physically impossible at t = 1200 sec. The exponential function just given reaches a maximum of ~ 3.1 for $k_2 \simeq 1 \times 10^{-3}$ sec.$^{-1}$.

The effect of added nitrate ion on the rates of decomposition of ADEBA, and ADEBA-$2HNO_3$ has been determined. Separate solutions of ADEBA-$2HNO_3$ and ADEBA in DMSO were prepared containing a 10 fold and 15 fold molar excess of potassium nitrate, respectively. The rate constants obtained from rates of nitrogen evolution at 60° were 2.13×10^{-4} sec.$^{-1}$ (ADEBA-$2HNO_3$) and $\sim 1.4 \times 10^{-5}$ sec.$^{-1}$ (ADEBA). Within experimental error, the rate of decomposition of ADEBA-$2HNO_3$ is practically invariant to added salt, while the rate of decomposition of ADEBA increases by a factor of about 1.4. The increase in rate for ADEBA is too small to account for the results. Also, the amount of nitrate ion in comparison to

ADEBA in the mixed experiments is much less than that giving rise to the observed rate increase.

The assumption has been made that the amounts of the three components at time t can be calculated assuming the initial equilibrium distribution. Since $e^{-k_0 t} = 0.99$, and $e^{-k_2 t} = 0.88$ for runs 1, 2, 4, and 5, any equilibrium adjustment will be very slight and will not affect these results significantly.

If addition of acid to DMSO solutions of ABA produced only ABA-2HCl (a highly improbable occurrence), the rate constant k_2 for decomposition of ABA-2HCl in these experiments would range from 2.5×10^{-4} sec.$^{-1}$ to 3.7×10^{-4} sec.$^{-1}$ compared to a measured value of 1.7×10^{-4} (Table I). Again it must be pointed out that the assumption of stoichiometric ammonia evolution will cause the first two values of k_2 given above to be minimum values.

It has been shown that the addition of water to DMSO solutions of ABA has a negligible effect on the rate of gas evolution. Addition of a 20 fold molar excess of water to a solution of ABA in DMSO caused only a 25% increase in the rate of gas evolution. The water present in the concentrated hydrochloric acid added during these runs is thus shown to have a negligible effect on the rate of decomposition of ABA.

It may be concluded that these results indicate the presence of an azo-compound in these systems which decomposes at a rate very nearly equal to that of the diprotonated azo-amidines. All evidence

indicates that this is the monoprotonated azo-amidine ABA-HCl or ADEBA-HNC_3.

It might be noted that the values of k_1 in Table IV, for $K_1/K_2 \rightarrow \infty$ are more consistent than those values calculated assuming $K_1/K_2 = 4$. If no experimental error were present in these determinations and if all assumptions were valid, it would be possible to choose the true value of K_1/K_2 as that value which caused all of the rate constants k_1 for a given system to be identical. It has been observed, however, that the rate constants k_1 are relatively insensitive to changes in the equilibrium constant ratio in these experiments. Thus, even a determination of the order of magnitude of this ratio is not feasible in these studies.

Electrostatic Effects on the Ratio K_1/K_2

Bjerrum (28) and Kirkwood and Westheimer (29) have presented treatments for calculation of the equilibrium constant ratio K_1/K_2 for various carboxylic acids. These treatments are basically calculations of the electrostatic interaction between the two negatively charged ends of a dicarboxylate dianion. The basic equation derived by Bjerrum is given in equation 14. N is Avogadro's number, e is the

$$\log (K_1/\sigma K_2) = Ne^2/2.3\,RTDr \qquad (14)$$

charge on an electron, D is the dielectric constant of the medium between the two ends of the molecule, and r is the distance between

point negative charges placed in the carboxylate groups. The quantity σ is the theoretically predicted value of the ratio K_1/K_2 in the absence of all interactions between the two carboxylate groups. This may be calculated from a consideration of symmetry numbers (32, 33), but is more easily understood from an examination of Figure 10. In

$$\text{A-A} + \text{H}^+ \xrightarrow{k_1} \text{HA-A or A-AH}$$

$$\text{HA-A} + \text{H}^+ \xrightarrow{k_2} \text{HA-AH}$$

$$\text{HA-A} \xrightarrow{k_{-1}} \text{A-A} + \text{H}^+$$

$$\text{HA-AH} \xrightarrow{k_{-2}} \text{HA-A or A-AH} + \text{H}^+$$

Fig. 10

terms of simple statistics, $k_1 = 2k_2$, and $k_{-2} = 2k_{-1}$. Since $K_1 = k_1/k_{-1}$, and $K_2 = k_2/k_{-2}$, it is easily shown that $K_1/K_2 = 4$. If the structures for the azo-amidines corresponding to ABA or ADEBA are drawn out in detail, an analysis analogous to that in Figure 10 will lead to the factor 4.

The distance between two point charges on the amidinium groups of ABA-$2H^+$ or ADEBA-$2H^+$ has been estimated to be ~8.4 A from a model of these systems assuming normal bond angles, bond lengths, and a trans configuration about the azo-linkage. The spatial geometry giving the greatest distance between the positive centers was chosen. The ratio $K_1/K_2 = 17.4$ under these conditions.

The Kirkwood-Westheimer treatment is analogous to that of

Bjerrum, except that an effective dielectric constant is used rather than the bulk solvent dielectric constant. The two treatments give essentially the same results for dicarboxylic acids with 3 or more carbon atoms between the carboxyl groups.

A repulsive interaction of approximately 1 kcal. $mole^{-1}$ has been calculated from the equation $\Delta F = 2.3RT\log(K_1/4K_2)$ from the ratio K_1/K_2 given above.

Efficiencies of the Thermal Decomposition Reactions

The origin of the non-stoichiometric production of readily scavengeable free radicals has been previously discussed in terms of the "cage effect." Several methods are available for determining the efficiency of radical production in azo decomposition reactions. Of these methods, the inhibition of oxidation technique (1, 2, 22) and studies of vinyl polymerization have been used to study the azo-amidine systems. The spectrophotometric iodine method (2) is not feasible since iodine reacts with the amidine group (17).

Inhibition of Oxidation Method. This technique has been described previously (2, 22) and has been used to study efficiencies of radical production from ABN (1) and ACC (2).

The solvents utilized in this study were 2:1 (by volume) mixtures of DMSO-cumene or DMSO-tetralin. The added inhibitor was 2,6-di-t-butyl-p-cresol (DBPC). Oxidation was initiated by the thermal

decomposition of the various azo-amidinium salts and azo-amidines. The rates of oxygen uptake were monitored with the aid of a gas apparatus. Typical curves for oxygen uptake with time in systems analogous to the ones in this study have been previously given for ABN (22). The rate of oxygen uptake is slow and zero order in inhibitor until almost all inhibitor has been consumed. It then increases rapidly, reaching the uninhibited rate of oxygen uptake when all inhibitor has been destroyed. The time corresponding to intersection of the uninhibited oxygen uptake curve and the inhibited oxidation curve is defined as the inhibition period. The stoichiometry of inhibition by DBPC has been determined from other oxidation studies with azo compounds (22). The efficiency factor $\underline{a}$ for the thermal decomposition reaction can be calculated using equation 15 (2). The quantities $(DBPC)_0$ and $(RN_2R)_0$

$$\underline{a} = (DBPC)_0/(RN_2R)_0\,(1 - e^{-kt_i}) \qquad (15)$$

are the initial concentrations of inhibitor and azo initiator, respectively. The rate constant k is the specific rate constant for thermal decomposition of the azo initiator and has been obtained from the data in Table I. The quantity t_i is the length of the inhibition period as defined above. The data for oxidation initiated by ABN, ADEBA-$2HNO_3$, and ABA-$2HNO_3$ are presented in Table VI.

Analogous inhibited oxidation studies were performed with the initiators ABA and ADEBA. However, the oxygen uptake curves did not exhibit the marked break distinguishing inhibited and uninhibited

TABLE VI

Efficiency Factors from Inhibited Oxidation Studies of ABN, ADEBA·2HNO$_3$ and ABA·2HNO$_3$

Run[a]	RN_2R	T (°C)	Sol-vent[b]	$DBPC_0^{(c)}$ (moles x 10^4)	$RN_2R_0^{(c)}$ (moles x 10^3)	t_g (min.)	$k^{(d)}$ ($sec.^{-1}$ x 10^5)	a
186	ABN	70	D-C	1.7836	4.0234	27.4	4.90	0.573
193	"	"	"	2.0877	3.0483	42.9	"	0.578
194	"	"	"	"	"	43.1	"	0.576[f]
45	ABA·2HNO$_3$	"	"	1.0121	0.24977	119.3	15.3	0.609
65a	"	"	"	0.5437	0.2607	45.4	"	0.612
65b	"	"	"	"	"	47.6	"	0.589
65c	"	"	"	"	"	46.4	"	0.601[f]
71a	"	"	"	0.52192	0.26096	44.5	"	0.596
71b	"	"	"	"	"	44.2	"	0.600
148	ADEBA·2HNO$_3$	60	D-T	0.58183	0.20973	44.7	20.4[e]	0.66[f]

(a) Run number refers to notebook experiment number.

(b) See footnote (b), Table I.

(c) Amounts of RN_2R and DBPC dissolved together in 25 ml. of solvent.

(d) Taken from Table I.

(e) Average of values in D-T and D-C, Table I.

(f) The volume vs. time data are given in Table VI-A, Appendix.

oxygen uptake which was observed for the azo-amidinium salts, and ABN. Further, the rate of oxidation indicated by these curves was quite low. The rates of uninhibited oxidation of tetralin (in DMSO) at 60° were measured using ADEBA and ADEBA-2HNO$_3$ as initiators. The data are presented in Table VII.

Each azo compound was dissolved in 5 ml. of a 2:1 DMSO-tetralin solution. The rate of oxygen uptake was monitored and corrected for nitrogen evolution from the initiator. The rates $-dO_2/dt$ were determined from the slope of the volume versus time curves at the times t given in Table VII. The rate expression for oxidation of hydrocarbon is given in equation 16 (34). The quantities $\underline{a}$ and k are

$$-dO_2/dt = 2ak\,(RN_2R) + (ak)^{\frac{1}{2}}\, k_3(RH)\,(RN_2R)^{\frac{1}{2}}/k_t^{\frac{1}{2}} \qquad (16)$$

the efficiency factor and rate constant for decomposition of the initiator RN_2R. The rate constant k_3 is that corresponding to reaction of $RO_2\cdot$ with the hydrocarbon substrate RH, and k_t is the rate constant for chain termination by bimolecular reaction of two $RO_2\cdot$. Referring to Table VII, it can be seen that a comparison of $(-dO_2/dt)_t$-$2k\,RN_2R)_t$ for each initiator with the quantity $k^{\frac{1}{2}}\,RN_2R)_t^{\frac{1}{2}}$ indicates that the initiator ADEBA-2HNO$_3$ is apparently much more efficient in initiating oxidation than ADEBA. It is assumed that k_t and k_3 are independent of the initiator, and that RH, being in large excess, is constant. These results imply that the efficiency factor for ADEBA-2HNO$_3$ is much greater than that for ADEBA.

TABLE VII

Uninhibited Oxidation of 2:1 DMSO-Tetralin

ADEBA and ADEBA·$2HNO_3$ as Initiators. 60°

RN_2R	$(-do_2/dt)_t$ moles $sec.^{-1} \times 10^8$	t (min.)	$RN_2R)_o$ (moles $\times 10^5$)	$RN_2R)_t$ (moles $\times 10^5$)	$k \times 10^5$ ($sec.^{-1}$)	$k^{\frac{1}{2}} RN_2R)_t^{\frac{1}{2}}$ (moles$^{\frac{1}{2}}$ $sec.^{-\frac{1}{2}} \times 10^5$)	$2k\,RN_2R)_t$ (moles $sec.^{-1} \times 10^8$)
ADEBA	0.682	40	11.85	11.54	1.09	3.55	0.25
ADEBA·$2HNO_3$	14.81	24	2.0991	1.546	20.0	5.56	0.62

Further experiments disproved this conclusion. The rate of oxidation of 2:1 DMSO-tetralin, initiated by ABN, was studied with and without added ADEBA. The results are given in Table VIII.

TABLE VIII

Rate of Oxidation of 2:1 DMSO-Tetralin Initiated by ABN and ABN-ADEBA. 60°

$(ABN)_o$ $(M \times 10^3)$	$(ADEBA)_o$ $(M \times 10^3)$	ΔV_t (a) (cc)	t (min.)
5.42	0	2.00	25
5.42	8.34	0.35	25

(a) Volume change in gas buret after time t.

The rate constants for thermal decomposition of ADEBA and ABN at 60° are 1×10^{-5} sec.$^{-1}$ and $\sim 1.5 \times 10^{-5}$ sec.$^{-1}$, respectively. Thus nitrogen evolution cannot be used to explain this apparent difference in oxygen uptake. In fact, no correction for oxygen uptake by ADEBA has been made. This will make the ratio of the values ΔV greater than the value of 5.7 calculated from Table VIII. These results lead to the conclusion that ADEBA is acting as an oxidation inhibitor, and prior oxidation experiments (Table VII) do not require the conclusion that it has a low efficiency factor. A search of the literature

revealed that variously substituted amidine free bases can be used as oxidation inhibitors in food and drug preparation (35). It thus appears that the amidine groups in ABA and ADEBA are acting as oxidation inhibitors.

Vinyl Polymerization. It has been found that compounds which inhibit free radical induced oxidation do not necessarily inhibit radical induced vinyl polymerization. In order to obtain an estimate of the efficiency factor for ADEBA, the polymerization of methyl methacrylate (MMA) initiated by ADEBA was studied. Previous studies by Arnett (36) show that polymerization of MMA initiated by ABN follows the normal kinetic rate law for vinyl polymerization (37) reproduced in equation 17.

$$R_p = k_p (M) (ak)^{\frac{1}{2}} (RN_2R)^{\frac{1}{2}} / k_t^{\frac{1}{2}} \qquad (17)$$

If a series of polymerizations are carried out under identical conditions with the same monomer, the quantity $k_p/k_t^{\frac{1}{2}}$ is normally constant and independent of initiator (37). Thus, for two different initiators $(RN_2R)_1$ and $(RN_2R)_2$, the ratio a_1/a_2 may be determined from a knowledge of the rate constants k for decomposition of the initiators, the concentrations of initiator and monomer, in each run, and the rates of polymerization. The rates of polymerization of MMA at 69.8° were determined from the weight of polymer formed after a known reaction time (Table XV). The polymerization reactions were carried out to

less than 6% conversion of monomer. Arnett has shown that the extent of polymerization is proportional to time up to 12-15% total conversion. Thus, the initial rate of polymerization can be calculated from one determination on each polymerization mixture. The rate constants for thermal decomposition of the various initiators have been taken from data in Table I for 2:1 DMSO-cumene solutions at 70°. An attempt was made to determine the rate constants for decomposition of these initiators in 9:1 MMA-DMSO saturated with chloranil (a polymerization inhibitor); however, polymerization was too rapid and initial solvent equilibration was slow, preventing accurate results from gas evolution experiments.

The detailed experimental method for these polymerization studies is given in the Experimental section. The data obtained are reported in Tables IX and XV.

The ratios of the efficiency factors for the initiators have been calculated from the average values in the last column of Table IX. A comparison of the data for ADEBA and ABN gives $a_{ADEBA}/a_{ABN} = 0.67$. If it is assumed that the efficiency factor for ABN is ~0.6 (Table VI), a value of 0.4 is calculated for the efficiency factor of ADEBA. An examination of the data for ADEBA-$2HNO_3$ in an analogous manner leads to an efficiency factor of ~0.2 for this compound. This is much lower than the value (0.66) obtained from oxidation studies (Table VI). An explanation for this discrepancy can

TABLE IX

Polymerization of Methyl Methacrylate Initiated by ABN, ADEBA and ADEBA-$2HNO_3$. 69.8°

Run	Initiator	$(In)_o$ (moles $\ell.^{-1} \times 10^4$)	$(MMA)_o$ moles $\ell.^{-1}$	$R_{p_o} \times 10^3$ (a, b)	$k_p a^{\frac{1}{2}}/k_t^{\frac{1}{2}}$ (c)
1-2	ABN	3.25	8.49	8.39	1.010
1-3	"	"	"	8.31	1.001
2-1	"	"	8.48	8.68	1.046
2-2	"	"	"	8.66	1.044
				(Avg.)	1.025
1-4	ADEBA	2.96	8.49	5.68	0.825
1-5	"	"	"	7.14	1.037
1-6	"	"	"	5.45	0.792
2-5	"	1.49	"	4.37	0.893
2-11	"	"	"	4.10	0.837
				(Avg.)	0.837
2-8	ADEBA·	1.41	8.49	12.33	0.610
2-9	$2HNO_3$	"	"	12.08	0.597
				(Avg.)	0.604

(a) Calculated from data in Table XV and an integrated form of the rate law for vinyl polymerization (eq. 17).

(b) Rate constants used in this calculation were ABN = 4.9×10^{-5} sec.$^{-1}$; ADEBA = 3.7×10^{-5} sec.$^{-1}$ (interpolated from an activation energy plot); and ADEBA-$2HNO_3$ = 6.7×10^{-4} sec.$^{-1}$

(c) Calculated from the equation

$$R_{p_o} = [k^{\frac{1}{2}}(RN_2R)_o^{\frac{1}{2}}(M)_o]\, k_p a^{\frac{1}{2}}/k_t^{\frac{1}{2}} .$$

be found in an examination of ADEBA-$2HNO_3$. Cohen and Wang (23) have found that polymerization of styrene initiated by azobisdiphenylmethane is characterized by a low rate of polymerization and a low polymer molecular weight. This is explained by a stable initiator radical which causes the rate of the initiation process to be low. The rate of chain termination also increases due to coupling of the growing chain with these stable initiator radicals. The rate constant for decomposition of azobisdiphenylmethane (23) at 64° is 3.4×10^{-4} sec.$^{-1}$, and reported activation parameters (23) are E_a = 26.6 kcal. mole^{-1} and $\Delta S^{\ddagger}$ = + 2 cal. mole^{-1}deg.$^{-1}$ The close resemblance of both rate and activation parameters of this azo compound to those of ADEBA-$2HNO_3$ (vide supra) leads to the conclusion that an analogous argument may explain the low value for $k_p a^{\frac{1}{2}}/k_t^{\frac{1}{2}}$ given by ADEBA-$2HNO_3$ (Table IX).

The initiation and termination processes for polymerization and oxidation reactions are quite different. An oxygen molecule is a much better scavenger than a vinyl compound (38). It may be concluded that the efficiency factor for ADEBA-$2HNO_3$ is probably that determined in the oxidation studies (Table VI).

The oxygen uptake curves for ADEBA and ABA in 2:1 DMSO-cumene with added DBPC have been re-examined. Comparing these curves with those obtained from oxygen uptake studies with no added DBPC shows that there is a noticeable inhibition period. Although the azo-compounds are also acting as inhibitors, DBPC is apparently

more efficient. From these curves it is possible to estimate inhibition times t_1. Efficiency factors have been calculated and are given in Table X. These inhibition times will be too long because of the inhibitory action of the amidines. Hence the efficiency factors reported in Table X are approximate lower limits.

Examination of the efficiency factors for the various azo-amidines shows that those for the diprotonated salts are consistently higher (0.6-0.7) than those for the unprotonated compounds (~0.4). This agrees with the predicted effects of repulsion between positively charged geminate amidinium-isopropyl radicals. It is more significant that the diprotonated azo-compounds give 30-40% "cage" reaction; almost as much as ABN (43%) in 2:1 DMSO-cumene. The positive charge of the amidinium groups is dispersed over three atoms. This will tend to reduce repulsions between these neighboring radicals. Also, it may be expected that solvation of the amidinium groups by DMSO is quite extensive. This solvation may shield the groups in such a way as to decrease repulsive interactions, and may also decrease the rate of diffusion of these fragments by increasing their effective bulk. Another explanation may be that interaction of the nitrate ions with the amidinium groups in ion pairs reduces the net positive charge on these groups. In any case, these results indicate that under suitable conditions, two repulsively interacting species, initially formed as a geminate pair, may exist in such a situation long

TABLE X

Efficiency Factors from Inhibited Oxidation Studies of ABA and ADEBA

Run[a]	RN_2R	T °C	Solvent[b]	DBPC[c] (moles$\times 10^5$)	RN_2R[c] (moles$\times 10^3$)	$t_{\frac{1}{2}}$ (min.)	$k \times 10^3$[d] ($sec.^{-1}$)	a[f]
73a	ABA	70	D-C	0.6844	1.030	63.5	0.18[e]	0.4
73b	"	"	"	0.6844	1.041	52	"	0.5
120	ADEBA	80	D-C	4.7563	0.29125	24	13.9	0.4

(a) Run number refers to notebook experiment number.

(b) See footnote (b), Table I.

(c) Amounts of RN_2R and DBPC in 25.0 ml. of solvent.

(d) Taken from Table I.

(e) See page 110.

(f) Volume vs. time data are given in Table X-A, Appendix.

enough to chemically react with each other, and that this effective encounter time is comparable to encounter times for geminate pairs which do not repulsively interact.

Synthesis of 1,1'-azocyano-(N-methyl)-4-azacyclohexane (AACC)

1,1'-azocyano-(N-methyl)-4-azacyclohexane (Fig. 11) has been

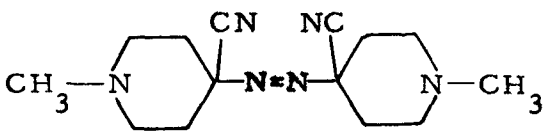

Fig. 11

synthesized from the known ketone, 1-methyl-4-piperidone hydrochloride (39) by modifications of the procedures of Overberger (24) and Hammond (1) for syntheses of aliphatic hydrazo and azo compounds. A complete description of the syntheses is given in the Experimental section. The rate of decomposition of this azo-compound at 90° in chlorobenzene is given in Table I.

Experimental

Melting points were determined with samples of the compounds in thin-walled capillary tubes using a variable temperature circulating oil bath. Melting points are uncorrected. Microanalyses were done by the Elek Micro Analytical Laboratories, Los Angeles, California, and Spang Microanalytical Laboratory, Ann Arbor, Michigan.

Dimethylsulfoxide (DMSO)

This solvent was purified by the procedure previously given (40).

Cumene

Cumene, Matheson, Coleman & Bell, was shaken with portions of concentrated sulfuric acid in a separatory funnel until the acid layer was not decolorized. The material was then washed with several portions of water and dried over anhydrous magnesium sulfate. The solvent was then distilled at reduced pressure (20 mm) and the center fraction distilling over the range 49-50° was collected and stored in a sealed brown bottle in the refrigerator.

Tetralin

Tetralin was purified in the same manner as cumene. The tetralin used in these studies was obtained from Dr. L. Mahoney.

Methyl Methacrylate (MMA)

Methyl methacrylate was purified according to the method of Arnett (36). The purified monomer was stored in a tightly sealed brown bottle in the refrigerator.

"Unstabilized" Chloroform

A 250 ml. sample of reagent chloroform was shaken with three 20 ml. portions of concentrated sulfuric acid in a separatory funnel. The chloroform was then washed with several portions of distilled water, dried over Drierite, and distilled at atmospheric pressure. The center cut, 60°/745 mm , was collected and stored in a tightly stoppered brown bottle in the refrigerator. The head space of the bottle was flushed with nitrogen each time that the bottle was opened and resealed. The above procedure removes ethyl alcohol from chloroform. The resultant "unstabilized" chloroform forms phosgene readily, and precautions must be taken to protect it from heat, light, and oxygen.

Azobisisobutyramidinium Chloride (ABA-2HCl)

ABA-2HCl was obtained from the Yerkes Research Laboratory, E. I. du Pont de Nemours Co., Buffalo, New York. The chloride was recrystallized from water before use in kinetic experiments.

Azobisisobutyramidinium Nitrate (ABA-2HNO_3)

The preparation of this compound has been previously described (41).

Azobisisobutyramidine (ABA)

In a typical experiment, 9.2 g. (0.4 moles) of sodium was added to 300 ml. of dry methyl alcohol (previously distilled from magnesium). After all sodium had dissolved, a 54.2 g. (0.2 moles)

sample of ABA-2HCl was added to the alcohol solution. During addition of the chloride, and for one hour thereafter, the solution was stirred with a magnetic stirrer. The solution was then filtered through a sintered glass funnel, and the clear yellow filtrate was evaporatively distilled under aspirator vacuum at 35°. The resulting solid material was added to 400 ml. of chloroform and the solution was filtered. The yellow chloroform filtrate was evaporatively distilled at 35° under aspirator vacuum, and the resulting solid was dried in vacuo over phosphorous pentoxide and recrystallized from methanol. M.p. 139° dec. Anal. Calculated for ABA, $C_8H_{18}N_6$: C, 48.46; H, 9.15; N, 42.39. Found: C, 48.20; H, 9.30; N, 42.55. A sample of recrystallized material was added to 1N hydrochloric acid. Upon addition of acetone to this solution, a solid was isolated which gave an infrared spectrum (nujol mull) identical to authentic ABA-2HCl. An ultraviolet spectrum of a solution (2.78×10^{-2} M) of ABA in DMSO exhibited the characteristic azo absorption; $\lambda_{max} = 3700$ Å, $\epsilon = 30$ liter mole^{-1} cm.$^{-1}$

Azobis-N,N'-dimethylene-isobutyramidine (ADEBA)

This compound was prepared in the manner previously given(41).

Azobis-N,N'-dimethylene-isobutyramidinium nitrate (ADEBA-2HNO$_3$)

This compound was prepared by the procedure previously given (41).

Tetramethylsuccinodinitrile (TMSN)

A 165 g. sample of ABN was dissolved in 1300 ml. of carbon tetrachloride in a 3 *l*., 3-neck, roundbottom flask fitted with a reflux

condenser and a nitrogen inlet tube. The condenser outlet was attached to a mineral oil bubbler. Dry nitrogen was bubbled through the solution with stirring for 15 minutes. The inlet tube was sealed off and the flask and contents were heated at reflux with continuous stirring for 48 hours. The solvent was evaporatively distilled at room temperature under reduced pressure until a crystalline mush remained in the flask. The residue was filtered on a coarse sintered glass funnel and the resulting white solid was dried at room temperature to give 113.4 g. (84% yield) of product; m.p. 114-125°. The solid was sublimed at 80° under aspirator vacuum and white crystals were obtained; m.p. 153-158°. Recrystallization of this material from Skelly A gave crystals; m.p. 166-167°. Anal. Calculated for TMSN, $C_8H_{12}N_2$: C, 70.50; H, 8.88; N, 20.55. Found: C, 70.86; H, 8.72; N, 20.52.

Tetramethylsuccinic Anhydride (TMSAN)

A 25 g. sample of TMSN was hydrolyzed in 100 ml. of 80% sulfuric acid according to the method of Thiele and Heuser (42). During hydrolysis, white crystals sublimed into the reflux condenser. These were taken up in ether and the reaction mixture was also extracted with several portions of ether. The combined ether layers were dried and evaporated to give 24.8 g. (87% yield) of solid crystals. This material was twice sublimed at 80° under aspirator vacuum to give crystals; m.p. 140-145°. An infrared spectrum of this material

in chloroform showed two strong carbonyl absorptions at 1780 and 1855 cm.$^{-1}$. Anal. Calculated for TMSAN, $C_8H_{12}O_3$: C, 61.62; H, 7.75; O, 30.73. Found: C, 61.56; H, 7.66. (Lit. (42), m.p. 147°)

Tetramethylsuccinimide (TMSI)

Tetramethylsuccinimide was prepared according to the method of Auwers and Gardner (43). Yield, 83%. The imide twice sublimed at 90°/2 mm , gave white crystals; m.p. 186.8-187.8 (Lit. m.p. 187°). An infrared spectrum of TMSI showed two carbonyl absorptions at 1730 cm.$^{-1}$ (S), and 1785 cm.$^{-1}$ (M).

Diethyl β,β'-(N-methylimino)-dipropionate

A modification of the method of McElvain and Rorig (39) was used. A 216 ml. (200 g., 2 moles) sample of ethyl acrylate, Rohm and Haas (stabilized with 0.1% hydroquinone), was placed in a 3-neck, 500 ml., roundbottom flask fitted with a Trubore stirrer, Dry Ice reflux condenser (fitted with a $CaCl_2$ drying tube), and a gas inlet tube. Anhydrous methylamine, Matheson, was then passed into the acrylate with stirring. Almost immediately the temperature of the reaction mixture increased. After methylamine had been passed into the solution for one hour the reaction mixture was cooled to room temperature. The temperature of the solution increased only slightly after this cooling. The solution became noticeably yellow after the reaction had proceeded for about two hours. Methylamine was bubbled into the acrylate for about 8 hours. At the end of this period the solution

volume began to noticeably increase. This indicated the condensation of unreacted methylamine. Flow of methylamine was stopped and the reaction mixture was stirred at room temperature for 8 hours. The solution was dark orange at the end of the reaction. The orange reaction mixture was distilled using a Vigreux column and conventional vacuum distillation head. Unreacted methylamine was removed by simply subjecting the system to vacuum without the application of heat. The distillation of the less volatile materials was accomplished by stirring the solution with a magnetic stirrer while increasing the temperature of the oil bath from 85° to 150° at 0.7 mm. The distillate temperature ranged from 35° to 110°. The main portion of the reaction mixture distilled in the range 105-110°. McElvain reports that the product distills between 118-119° at 0.5 mm. An n.m.r. spectrum was taken of a sample of one fraction distilling at 110°. The spectrum consists of a quartet centered at 240 cps (J = 7 cps), an AB methylene grouping at 147.5 cps (splitting 5 cps), a sharp singlet at 128 cps, and a triplet at 68 cps (J = 7 cps); referenced to external tetramethylsilane (60 Mcps). Integrated ratios are 4:8; 3:6, respectively. These resonances are assigned to the ethyl (CH_2), the -CH_2CH_2- groups, the N-CH_3, and the ethyl (CH_3); theoretical ratios 4:8:3:6, respectively. No protons were observed in the vinyl proton region. Weight of material collected distilling between 105-110° is 138.2 g. Yield 60%.

1-Methyl-3-carbethoxy-4-piperidone Hydrochloride

The procedure of McElvain and Rorig (39) was used without modification. Quantities of reactants and solvents were adjusted to correspond to 70 g. (0.3 moles) of diethyl β,β'-(N-methylimino)-dipropionate. A 51.5 g. (77.5% yield) sample of 1-methyl-3-carbethoxy-4-piperidone hydrochloride was obtained; m.p. 124-129° (Lit. (39) 125-128°). An infrared spectrum of this salt (nujol mull) showed two strong bands at 1625 and 1670 $cm.^{-1}$

1-Methyl-4-piperidone Hydrochloride

The procedure of McElvain and Rorig (39) was used to prepare this compound. A 40 g. (0.18 moles) sample of 1-methyl-3-carbethoxy-4-piperidone hydrochloride was refluxed for two hours in 160 ml. of 20% hydrochloric acid. Evolution of gas was noted in a bubbler. The escaping gas decolorized Ascarite indicating that the decarboxylation was proceeding as anticipated. At the end of the two hour period, the now yellow solution was evaporated under aspirator vacuum at 100°. When most of the water had been removed, the solid was dried in vacuo (1 mm , 100°). The dry solid material was quite yellow. McElvain reports that recrystallization of this hydrochloride can be accomplished from acetone; however, it involved such large quantities of acetone that is was decided to attempt recrystallization from another solvent. The crude product was dissolved in a minimum amount of absolute ethyl alcohol, and this solution was then concentrated on a

hot plate. The solution began to turn dark orange almost immediately and was removed from the heat and cooled in an attempt to facilitate crystallization. No crystallization was observed after several hours at refrigerator temperature. Acetone was then added to the alcohol solution and a bright orange solid was isolated. The acetone-ethyl alcohol solution was concentrated under aspirator vacuum at 40° until solid precipitated from solution. The solution was filtered and a slightly yellowish-white solid was isolated. The filtrate was further concentrated and a second batch of solid was isolated. Further concentration gave very sticky orange material. The combined white solid material was dried under vacuum over P_2O_5. Weight 11.1 g. The IR spectrum in a nujol mull showed no carbonyl absorption and the spectrum in chloroform showed a very weak carbonyl peak at 1725 cm^{-1}. Strong absorption at 1050 $cm.^{-1}$ characteristic of C-O-C stretch, and at 1125-1130 $cm.^{-1}$ characteristic of the ketal linkage, was present in both spectra. A 9.6 g. sample of this solid was refluxed in 100 ml. of 0.1 N hydrochloric acid for one-half hour. The water was evaporated under aspirator vacuum at 80° and the solid material dried at 100° (1 mm) and then over P_2O_5 at 1 mm pressure. The resulting yellowish material weighed 4.37 g. M.p. range 90-130°, corresponding to that reported by McElvain for 1-methyl-4-piperidone-HCl (80-120°). An IR spectrum (nujol mull) of this hydrolysis product, showed a strong carbonyl absorption at 1725 $cm.^{-1}$. The

strong absorptions at 1050 cm.$^{-1}$ and 1125-1130 cm.$^{-1}$ were not present. This product is assumed to be 1-methyl-4-piperidone-HCl. The solid material showing no carbonyl absorption is assumed to be the diethyl ketal of this ketone. Yield of purified ketal was 28%. Yield from ketal hydrolysis was 68%.

A second preparation was attempted using 73.8 g. of 1-methyl-3-carbethoxy-4-piperidone hydrochloride. The yellow solid isolated at the end of the decarboxylation reaction weighed 48.1 g., corresponding to a yield of 97%. This solid was used in subsequent reactions without further purification.

1,1'-Hydrazocyano-(N-methyl)-4-azacyclohexane

The procedure used was derived from that of Overberger (24). A 48 g. (0.3 moles) sample of 1-methyl-4-piperidone hydrochloride, a 25.8 g. sample of hydrazine sulfate, Eastman White Label, recrystallized, and a 17.65 g. sample of sodium cyanide, Baker & Adamson Reagent Grade, were placed in a 300 ml. Erlenmeyer flask. This material was then dissolved in 180 ml. of distilled water, the flask immediately stoppered, and stirred with a magnetic stirrer at room temperature for 24 hours. Sufficient concentrated sodium hydroxide solution was then added to the reaction mixture to give a solution of pH > 10. Upon making the solution basic, a solid white material precipitated from solution. This solid was filtered and found to be slightly soluble in ether, insoluble in water, but soluble in chloroform.

This material was dried in vacuo over P_2O_5. An IR spectrum in chloroform showed no carbonyl absorption, but strong cyano absorption at 2230 cm.$^{-1}$; m.p. 129.5°-132°C. Total weight isolated is 37.1 g. Yield 84%. Anal. Calculated for 1,1'-hydrazocyano-(N-methyl)-4-azacyclohexane, $C_{14}H_{24}N_6$: C, 60.84; H, 8.76; N, 30.41. Found: C, 60.73; H, 8.60; N, 30.45.

1,1'-Azocyano-(N-methyl)-4-azacyclohexane (AACC)

The procedure used in the first attempt to oxidize 1,1'-hydrazocyano-(N-methyl)-4-azacyclohexane to the corresponding azo-compound was based on that of Bickel and Waters (19). A 2.00 g. (7.2×10^{-3} moles) sample of the hydrazo compound was dissolved in 150 ml. of tetrahydrofuran, Matheson, Coleman, and Bell, and to this solution was added 1.6 g. (7.2×10^{-3} moles) of mercuric oxide. The mixture was stirred at 35°C. for 12 hours. At the end of this period, no evidence of reaction could be observed. No mercury was present and the solution retained its original red color. The heterogeneous mixture was filtered and the clear filtrate evaporated giving 2.0 g. of a yellowish-white solid which is assumed to be unreacted hydrazo-compound.

The procedure for the second oxidation attempt is based on that of Wu, Hammond and Wright (2) for oxidation of aliphatic hydrazo-compounds. A 37.1 g. (0.134 moles) sample of 1,1'-hydrazocyano-(N-methyl)-4-azacyclohexane was dissolved in 270 ml. of 2N hydrochloric

acid. Approximately 8 ml. (23 g., 0.14 moles) of bromine was slowly added to the solution with stirring. On addition of the bromine, the solution became warm and a reddish material began to precipitate. The reaction mixture was cooled in an ice bath while being continuously stirred. After stirring for several minutes, a light yellow solid was observed to precipitate from solution. Stirring was continued for 15-20 minutes after all the bromine had been added to the reaction mixture. The solution was then filtered, giving solid material which has not been characterized. Sufficient concentrated sodium hydroxide solution was added to the yellow filtrate to give a solution of pH > 10. The solution became colorless upon addition of the base, and flocculent white solid precipitated. This solid was filtered out of the solution and found to be soluble in ether, chloroform, and chlorobenzene, and insoluble in water. This material was dried in vacuo over phosphorous pentoxide. The weight of this material is 22.5 g., giving a yield of 61% based on the azo-compound. An ultraviolet spectrum of this solid in chlorobenzene gave a characteristic azo absorption; λ_{max} = 3480 Å, $\epsilon \simeq 26$ liter mole^{-1} cm.$^{-1}$ An infrared spectrum (chloroform) showed strong nitrile absorption at 2250 cm.$^{-1}$ M.p. 150-151° dec.

Thermal Decomposition of ABN in DMSO

A 5.0 g. sample of ABN was dissolved in 100 ml. of DMSO in a 300 ml., 3-neck, roundbottom flask fitted with a reflux condenser and a bubbler tube. The condenser outlet was connected to a mineral

oil bubbler. Dry nitrogen was passed through the solution with stirring for 3 minutes. The nitrogen inlet tube was clamped shut and the flask was heated at approximately 70° for 39.5 hours with continuous stirring. The resulting yellow DMSO reaction mixture was continuously extracted with pentane for 20 hours. At the end of this period two layers were observed in the receiver flask. The pentane layer was evaporated and yielded 0.1 g. of solid material which was sublimed at 90°/745 mm , giving pure white crystals. The second layer in the receiver flask (20 ml.) was yellow and was identified as part of the reaction mixture which was being extracted. On addition of 20 ml. of water to this DMSO layer, a solid material precipitated from solution and was filtered off; weight 1.8 g. This DMSO-water solution was further extracted with several portions of pentane in a separatory funnel. Evaporation of the pentane (500 ml.) gave 0.5 g. of a solid.

The remaining 80 ml. of the original reaction mixture was removed from the extraction apparatus and 100 ml. of water was added to it. The solution became cloudy, but no detectable amount of precipitate was obtained. This aqueous DMSO solution was continuously extracted with pentane for 44 hours. The pentane layer was evaporated and 1.1 g. of solid material was isolated. The aqueous-DMSO layer was then shaken with several portions of pentane in a separatory funnel. Evaporation of the pentane (1000 ml.) yielded 0.3 g. of white crystals.

The total weight of solid material isolated was 3.7 g. (89% yield). This was shown to be tetramethylsuccinodinitrile by comparison of its infrared spectrum with that of authentic material. This solid was sublimed twice at 90°/745 mm. No significant amount of residue remained after sublimation. The sublimed material gave a m.p. 150-155°. Authentic TMSN which had been sublimed gave a m.p. of 153-158° (vide supra).

Thermal Decomposition of ABA-$2HNO_3$ in DMSO

A 1.5 g. sample of ABA-$2HNO_3$ was dissolved in approximately 25 ml. of anhydrous DMSO in a 50 ml., single neck, roundbottom flask. This flask had been modified by the addition of a 10/30 outer joint. The flask was fitted with a Liebig condenser which was attached to a mineral oil bubbler. A nitrogen inlet tube was inserted in the 10/30 joint. Dry nitrogen was bubbled through the solution for approximately 30 minutes. The nitrogen inlet tube was then sealed off and the flask was immersed for 30 minutes in an oil bath pre-heated to approximately 100°. Nitrogen evolution was observed only during the first 15 minutes of reaction. The reaction mixture was evaporatively distilled at reduced pressure leaving a light yellow solid. The resultant DMSO distillate had an ammoniacal odor. The solid was washed with anhydrous ether and the washings were discarded. The solid material was then dissolved in anhydrous methyl alcohol and the methanolic solution was heated and filtered to remove trace insoluble impurities.

This solution was then concentrated with stirring under a vacuum bell jar at reduced pressure (~135 mm) until solid material began to precipitate. The flask containing this solution was stoppered and placed in the refrigerator for 24 hours. The solid material was filtered from solution on a sintered glass funnel and dried in vacuo; weight of this material is 0.35 g. M.p. 293-297°. Anal. Calculated for tetramethylsuccinimidinium nitrate, $C_8H_{16}N_4O_3$: C, 44.43; H, 7.46; N, 25.91; O, 22.20. Found: C, 44.52; H, 7.58; N, 24.84. Yield based on the empirical formula is 35%.

A 0.2 g. sample of this salt and 20 ml. of a 16% sodium hydroxide solution were placed in a 50 ml., single neck, roundbottom flask fitted with a reflux condenser. The solution was heated at reflux with continuous stirring for 48 hours. The reaction mixture was acidified with 6 N hydrochloric acid and a solid precipitated from solution. The solid and water layer were extracted with two 200 ml. portions of ether, and the combined ether extracts were evaporated. A yellow oily residue remained which crystallized upon further evaporation in vacuo. An infrared spectrum of the crude solid product was identical to that of an authentic sample of tetramethylsuccinimide.

Thermal Decomposition of ADEBA-$2HNO_3$ in DMSO

A 2.0 g. sample of ADEBA-$2HNO_3$ was dissolved in 25 ml. of DMSO in a special reaction vessel previously described (2). The reaction vessel containing the solution was immersed in an ice-water bath

and degassed. The solution was then allowed to thaw to room temperature in vacuo. The outlet of the vessel was connected to a mineral oil bubbler. Dry nitrogen was bubbled through the solution for several minutes after the degassing procedure. The vessel was then heated at 70° for 3 hours. The reaction mixture was transferred to a 100 ml. single neck, roundbottom flask, which was then placed on a rotary evaporator. The solvent was evaporated at 45°/1 mm , leaving a smooth, caramel-colored mush weighing 2.21 g. A 10 ml. portion of absolute alcohol was added to the residue, giving a white solid and a yellow solution. The solution and solid were carefully transferred to a preweighed, fine sintered glass funnel, and filtered with the aid of aspirator vacuum. The filtrate was used to wash the flask and this washing was again passed through the funnel. A final washing of the flask was done with a small amount of absolute ethyl alcohol and this washing was passed through the filter funnel. The solid was dried in the funnel with the aid of an aspirator vacuum for several minutes. This funnel containing the solid was dried in vacuo over phosphorous pentoxide, and the funnel and solid were weighed. By difference the weight of the solid was 0.54 g. This material chars at 217°, and melts at ~225° with decomposition. Anal. Calculated for N,N'-dimethylene-tetramethylsuccinamidinium nitrate, $C_{12}H_{24}N_6O_6$: C, 41.37; H, 6.94; N, 24.13; O, 27.56. Found: C, 41.36; H, 6.80; N, 24.05. Yield based on the empirical formula is 29.2%. An n.m.r.

spectrum of this material in deuterium oxide shows two sharp singlet resonances at 85 and 240 cps (60 Mcps.; reference, tetramethylsilane, external) in the ratio 12:8. A proton signal for water is visible at 282 cps. An n.m.r. spectrum of ADEBA-2HNO$_3$ in deuterium oxide shows two sharp singlets at 94 cps and 245 cps in the ratio 12:8. These are identified as CH_3-C- and N-CH_2-C protons, respectively. The water resonance signal is found at 283 cps. The infrared spectra (nujol mull) of ADEBA-2HNO$_3$ and the solid product are almost identical. Each possesses the following characteristic bands: C-N stretch, 1750 cm.$^{-1}$ (w), 1600 cm.$^{-1}$ (s) and 1460 cm.$^{-1}$ (s); a broad nitrate ion band 1400-1250 cm.$^{-1}$ The fingerprint regions are superimposable with only minor variations.

The ethyl alcohol filtrate was placed in a 50 ml., single neck, roundbottom flask which was then placed on the rotary evaporator. This sample was lost when the water aspirator backed up.

In a second reaction, a 2.0 g. sample of ADEBA-2HNO$_3$ was dissolved in 20 ml. of DMSO and decomposed in the same manner as described above. The resultant reaction mixture was evaporated until only 2-3 ml. of solvent remained. To this solution was added 10 ml. of 20% sulfuric acid. The resultant solution was divided into two parts, each of which was placed in a tube with a constricted neck. The tubes were sealed and immersed in an oil bath at 78° for 5 days. At the end of this period, the tubes were opened and the combined contents extracted

with several portions of ether totalling 100 ml. The ether layer was dried over magnesium sulfate and evaporated to a total volume of 1-2 ml. The resultant ether solution was orange and smelled very much like isobutyric acid. A piece of blue litmus paper turned red when held over the top of the flask containing this solution. Similarly, blue litmus paper turns red when it is held over an open bottle of isobutyric acid. A preliminary analysis of this ether solution was done by vapor phase chromatography, using a 7 ft. Carbowax 20M column at 160° in a Wilkens Corp., Aerograph Vapor Phase Chromatography instrument. The majority of the peaks were broad and exhibited marked tailing. Retention times for the components are referenced to the ether peak. The chromatograph indicated components having retention times of 1.7, 3.2, 9.9, 19, 23.5, and 34.3 min. A sample of authentic isobutyric acid and tetramethylsuccinic anhydride in ether gave three peaks. Retention times based on the ether peak are 17.3, and 36.5 min. for the acid and anhydride, respectively. A sample of isobutyric acid and the reaction mixture were mixed. The peak giving the retention time of 19 min. in the reaction mixture increased in size in comparison to the other peaks. These peaks are sufficiently broad so that two components which differ in retention time by 1 min. would not be resolved.

Thermal Decomposition of ADEBA in DMSO

A 6.8 g. sample of ADEBA and 200 ml. of DMSO were placed

in a 1-liter, 3-neck, roundbottom flask fitted with a reflux condenser, an immersion thermometer, and a sintered glass gas dispersion tube. The condenser was connected to a mineral oil bubbler. Dry nitrogen was bubbled through the heterogeneous solution for 10 minutes. The gas dispersion tube was then quickly replaced with a dropping funnel containing about 200 ml. of DMSO. The flask was immersed in an oil bath preheated to 85° and sufficient DMSO was added from the dropping funnel to give complete solution of the azo-compound at 85°. The solution was heated at 90° for 3 hours with stirring. The reaction mixture was evaporatively distilled at 65° under reduced pressure to give approximately 100 ml. of solution containing a solid. The solution was filtered and the filtrate placed in a 300 ml. roundbottom flask. The resulting solid was washed with ether and dried in vacuo over phosphorous pentoxide; weight 1.50 g. This solid was dissolved in excess chloroform and filtered to remove trace insoluble impurities. The chloroform solution was concentrated until solid began to precipitate from solution and was then placed in the refrigerator. The solid was filtered from solution and dried over phosphorous pentoxide in vacuo; softens at 171°, m.p. 174-176°.

An n.m.r. spectrum was taken of a solution of this solid in "unstabilized" chloroform (vide supra). This spectrum is complex and has not been analyzed. The spectrum showed the following resonances. Sharp singlets at 72 and 75 cps, a weak singlet at 82 cps,

and a broad singlet at 92.5 cps. The region 165-275 cps consists of a series of complex multiplets. Proceeding downfield, the first multiplet appears at first glance to be a triplet; however, the three signals have maxima at 172.5, 177.5, and 184 cps. The central signal has a shoulder at about 178-179 cps, indicating that the multiplet might be composed of two superimposed doublets centered at 175.5 and 180.5 cps ($J \simeq 6$ cps). A similar multiplet is visible further downfield with maxima at 209, 215, and 220 cps. Again, a shoulder on the central signal at approximately 213 cps is visible. This could correspond to two superimposed doublets with $J \simeq 6$ cps. The next multiplet consists of 8 resolvable components at 226 and 231.5 cps (minor); 238.5, 245, 250, and 256.5 cps (major); and 268.5 and 273.5 cps (minor). The components designated as minor are considered to arise from a different compound than that corresponding to the major components. The major components exhibit fine structure which may be second order splitting, or due to overlap of more complicated multiplet patterns. Integration gives the following results: the ratio of the protons giving signals between 0-100 cps to those giving the complicated multiplet patterns from 150 to 275 cps is 31.1 to 17.7, or approximately 14 to 8. The broad singlet at 92.5 cps accounts for 2.2 of the 14 protons in the region 0-100 cps. The complex multiplet consisting of 8 components accounts for 3.7 protons in the region 150-275 cps. and the two "triplet" patterns at $\sim$ 215 and $\sim$ 177 cps account for 2.2 and 2.0 protons, respectively.

The n.m.r. spectrum of ADEBA in "unstabilised" chloroform gives a very simple spectrum consisting of a sharp singlet at 88 cps and a broad singlet at 221 cps, which are in the ratio 14 to 8.1 by electronic integration. The higher field singlet has a small shoulder on the low field side. It is assumed that the higher field signal corresponds to the $C-CH_3$ and N-H protons, while the lower field signal is due to the $C-CH_2-N$ protons.

The n.m.r. spectrum of the unknown solid material in 15% sulfuric acid is extremely simple. Besides the solvent signal which obscures the region immediately below 300 cps, only two other sharp singlets are observed at 94 and 248 cps in the ratio of 12 to 7.2, respectively. The n.m.r. spectrum of ADEBA in 15% sulfuric acid gives two sharp singlets at 98 and 249 cps in the ratio of 12 to 8.0, respectively. The signals for ADEBA are identified as the $C-CH_3$ protons and the $C-CH_2-N$ protons, respectively.

N.m.r. spectra of ethylenediamine in 15% sulfuric acid containing ADEBA or the unknown product, gave a single resonance signal at 215 cps distinct from the other signals.

The infrared spectra of both the unknown solid product and ADEBA in chloroform have been recorded. The spectra differ considerably. A sharp band present at 3430 $cm.^{-1}$ for ADEBA is absent in the unknown. The unknown shows strong bands at 1700 and 1650 $cm.^{-1}$, while ADEBA shows a single strong band at 1625 $cm.^{-1}$ The

band at 1625 cm.$^{-1}$ for ADEBA exhibits a weak shoulder at about 1560 cm.$^{-1}$, while the band at 1650 cm.$^{-1}$ for the unknown has a slightly more pronounced shoulder at 1575 cm.$^{-1}$ A broad band from 1410-1425 cm.$^{-1}$ is present in both spectra, but is more intense for ADEBA. The unknown shows moderately strong bands at 1375 cm.$^{-1}$ and 1300 cm.$^{-1}$, while ADEBA possesses a weaker doublet (1375 and 1360 cm.$^{-1}$) and an intense broad band at 1275 cm.$^{-1}$ The remainder of the fingerprint regions in each spectrum are practically superimposable.

Further concentration of the DMSO filtrate (45°/1 mm) using a rotary evaporator gave 0.5 g. of solid material, which gave an n.m.r. spectrum in chloroform identical to that of the first isolated solid. The total yield of solid material based only on loss of nitrogen from ADEBA is 33.6%.

The residual reaction mixture consisted of a viscous dark orange liquid. An n.m.r. spectrum was taken of this crude material in chloroform. The region 50-100 cps is quite complicated, consisting of a series of closely spaced signals at 70, 73.5, 77, 80, 81.5, 86, 88, and 93 cps. The DMSO solvent signal appears at ~ 162 cps, and two strong singlets at 220 and 223 cps are present. A broad singlet is also present at 345 cps. The signals given above are almost as intense as the solvent signal, indicating that the viscous orange liquid still contains a large concentration of products. An infrared spectrum of a chloroform solution of this orange liquid appears to be a superposition of the spectra for the unknown solid and ADEBA.

Gas Apparatus and Procedure for Gas Evolution or Uptake Runs

The apparatus used for measuring rates of gas evolution or gas uptake was designed by Drs. C. H. Wu and B. Seidel. It is based on a closed system consisting of a gas buret, filled with mercury, connected to a reaction vessel, and a mercury leveling bulb.

Burets. The apparatus has three precision gas burets of 10, 30 and 100 cc. capacity. Each of these burets has an outer jacket through which thermostated water (29.5°) is passed. Each buret is filled with mercury and has its own mercury leveling bulb attached to the bottom opening with flexible tygon tubing. At the top of each buret is a high-vacuum stopcock which allows the buret to be independently opened or closed to the rest of the system. The burets are connected in parallel to a thick-walled capillary manifold.

Reaction Vessel. The gas apparatus reaction vessel consists of a small chamber with two openings. The top opening is sealed directly to a short water-jacketed condenser which has a ground-glass outer joint at the top. The side opening is sealed to a ground-glass outer joint. The chamber is surrounded by a jacket through which water of the desired reaction temperature is passed. The top opening of the condenser is directly attached to one extreme end of the thick-walled capillary manifold by a ground-glass joint. During a run, the side opening is sealed with a ground-glass plug.

Water of the desired reaction temperature is rapidly circulated

around the reaction vessel by means of a thermostated, high speed circulating water bath made by the Haake Co., West Germany. Short lengths (~ 2 ft.) of thick-walled butyl rubber tubing are used to make the connection between the vessel and the bath. A bypass has been installed on the water outlets of this bath so that it may be running constantly prior to the experiment. Closure of the bypass with simultaneous opening of the tubes to the reaction vessel diverts the water through the reaction vessel outer jacket. The rate of attainment of the reaction temperature in the vessel has been qualitatively measured. The reaction vessel was filled with a solvent and a thermometer was inserted into the top of the vessel so that the bulb was immersed under the liquid. The solution in the vessel was stirred continuously by a magnetic stirrer during this determination in a manner analogous to a normal run. The side arm of the vessel was partially sealed with a one-hole rubber stopper to prevent a pressure increase in the vessel. The water was diverted from the bypass into the vessel at t = 0. The data for temperature increase with time are given in Table XI.

The reaction bath was regulated at 69.8°, but the therometer used for these measurements was a simple -10 to 110° (uncalibrated) thermometer, and no stem correction was made. Thus, the low reading of 68.7° is not significant. It may be seen that the temperature reaches its maximum value in less than 2.5 min.

TABLE XI

Rate of Attainment of Reaction
Temperature in Gas Reaction Vessel

t(min.)	T(°C)	t(min.)	T(°C)
0.0	31.5	2.5	68.7
0.5	62	3.5	68.7
1.0	67.0	4.5	68.7
1.5	68.5	7.5	68.7

Pressure Regulator. A pressure regulator is attached to the thick-walled capillary manifold between the reaction vessel and the first gas buret. This consists basically of a large bore glass tube in the shape of a "J." The long part of this "J" tube has an outer jacket through which thermostated water (29.5°) is passed. A vacuum stopcock is attached to the top of the "J" tube. Above this stopcock is a thick-walled capillary tube which runs to the manifold. A second piece of capillary tubing has been connected at right angles to the tube above the stopcock, and this is then connected to the foot of the "J" tube. The bottom of the "J" tube is filled with mercury. When the stopcock is open, both mercury surfaces are subjected to the pressure in the capillary manifold. When the stopcock is closed, the long water-jacketed side of the tube is isolated from the system at a

pressure equal to that in the system at the time of closure; the "reference pressure." The pressure exerted on the other mercury surface is equal to the pressure in the system during a run.

Mercury Leveling Bulb Rack. A mercury leveling bulb from one of the burets, rests on a ring which is attached to a long vertical threaded steel rod. This rod may be turned by a reversible motor, Bodine Electric Co., Chicago, and causes the leveling bulb to be raised or lowered, depending on the motor direction. The speed of the motor is variable and determined by a rheostat, Minarik Electric Co., Los Angeles. The motor and corresponding rheostat are so constructed that the motor stops instantly when the power is shut off.

Auxiliary Equipment. A large glass bulb with three attached joints is connected at the other extreme end of the capillary manifold. A high vacuum pump is connected to one joint, and the other two joints are connected to nitrogen and oxygen cylinders. The bulb may be closed to the manifold by a vacuum stopcock. The nitrogen and oxygen cylinders, as well as the pump, may be separately opened to the bulb by vacuum stopcocks. Nitrogen gas is Matheson Prep. grade. Oxygen is passed through a drying tower before it enters the apparatus.

Procedure. Before rates of nitrogen evolution are to be measured, the total system is evacuated and re-filled with nitrogen three times. A fine capillary tube attached to the manifold by a stopcock allows a purposely induced positive pressure in the apparatus to be

reduced to atmospheric pressure before the run is begun. The capillary tube is sufficiently small to prevent back diffusion of air into the system.

The same procedure is used for preparing the system for oxygen uptake measurements, except that the nitrogen flushing procedure is replaced by oxygen flushing. During evacuation, the reaction vessel containing the solution to be studied is carefully opened to the system to allow degassing of the solution.

After the flushing procedure has been completed, the mercury leveling bulb corresponding to the buret to be used is placed on the rack. The burets which will not be used are closed to the manifold, and the reaction vessel is opened to the manifold. At this point both sides of the pressure regulator are open to the system. The bulb rack is positioned so that the mercury level is at the top or bottom of the buret, depending on whether gas evolution or uptake is to be measured. The induced positive pressure in the system is reduced to atmospheric pressure and the stopcock of the pressure regulator is closed, establishing the "reference pressure." Water of the desired reaction temperature is pumped around the reaction vessel chamber. If gas evolution (uptake) is being studied, a positive (negative) pressure will develop in the system in relation to the reference pressure. This will cause the two mercury surfaces to be at unequal levels in the pressure regulator. A Thermo-Cap relay, Niagara Electron Laboratories,

Andover, N. Y., detects this mercury level change and activates the screw motor lowering (raising) the mercury leveling bulb until the pressure in the system is equal to the "reference pressure." When the pressure is re-equilibrated, the relay automatically turns off the motor. A volume reading and time reading are then taken. A finite pressure difference is required to activate the relay. Thus, the pressure in the system is equilibrated intermittently, depending on the relay adjustments.

The apparatus is sensitive to small pressure changes and excellent results have been obtained on samples which evolve as little as 5 cc. of gas over the entire course of the reaction. The temperature of the water in the Haake bath is regulated to $\pm 0.05°$.

Attempts to Remove Ammonia from Evolved Gas. ABA in DMSO

a) A gas apparatus reaction vessel was modified in the following manner. An additional length of glass tubing was added above the reflux condenser. This section was thermostated by the condenser water jacket. A glass wool plug was inserted into this tube so that it rested at the point where the top of the condenser was attached to the bottom of this tube. Fine boiling chips which had been soaked in sulfuric acid were then poured onto the glass wool plug in sufficient amount to fill the tube. A 0.200 g. sample of ABA was placed in the gas reaction vessel and 5 ml. of DMSO was added. The rate of gas

evolution was monitored giving a rate constant $k = 5.0 \times 10^{-6}$ sec.$^{-1}$

b) The modified gas apparatus reaction vessel described in a) was used. Instead of filling the tube with boiling chips, fine crystals of p-toluene sulfonic acid monohydrate were used. A layer of Drierite and a plug of glass wool were placed on top of the acid crystals. A 0.2017 g. sample of ABA, and 5 ml. of DMSO were added to the reaction vessel. The rate of gas evolution at 70° was monitored, giving a rate constant $k = 2.6 \times 10^{-6}$ sec.$^{-1}$

c) A second gas reaction vessel, containing concentrated sulfuric acid, was connected to the thick-walled capillary manifold of the gas apparatus between the normal reaction vessel and the first gas buret. A 0.2153 g. sample of ABA and 5 ml. of DMSO were placed in the normal vessel. The rate of gas evolution at 70° was monitored, giving a rate constant of 3.2×10^{-6} sec.$^{-1}$

Ammonia Evolution from ABA in DMSO

A 2.0035 g. (0.0101 moles) sample of ABA was dissolved in 50 ml. of DMSO in a reaction vessel previously described (2). This vessel is designed so that nitrogen gas can be passed through the solution and out of the vessel during a decomposition run. A piece of tygon tubing connected the outlet of the reaction vessel to a second vessel which was used to determine the rate of ammonia evolution from the decomposition reaction. This second vessel consisted of a 600 ml. beaker fitted with a large rubber stopper containing five holes.

Two of the holes were fitted with Beckman Glass and Calomel electrodes. The third hole was fitted with the tip of a micro-buret; the fourth with a sintered glass dispersion tube; and the fifth was used as a gas outlet. The beaker was filled with sufficient water to cover the electrodes and the gas dispersion tube. The electrodes were connected to a Beckman Model G pH meter which had been calibrated with pH 7 buffer under experimental conditions. The reaction vessel was immersed in a thermostated oil bath, regulated at 70°. Dry nitrogen gas was passed simultaneously through and above the DMSO reaction mixture. This gas stream was then bubbled into the water solution contained in the beaker. A known volume of standardized 0.0968 N hydrochloric acid was added to the water solution from the micro-buret. The pH of the solution was recorded as a function of time. The ammonia evolved from the reaction mixture neutralized the added acid in the water solution. When the pH of the solution reached approximately 7, another aliquot of acid was added to the solution. No detectable amount of ammonia escaped from the water solution. Plots of pH versus time were made, and the time interval between two identical pH readings (normally pH = 6.2-6.6) gave the amount of time that was required for the evolving ammonia to neutralize the known amount of added acid. The average rate of ammonia over this given time interval was then calculated. The data are presented in Table XII.

TABLE XII

Ammonia Evolution from ABA in DMSO. 70°

Reaction Time (hrs)	Δt (min.)	Equivalent of Added Acid $\times 10^5$	$dNH_3/dt \times 10^5$ (R x 10^5) (eq./hr.)	log R + 6
103.56	28.5	1.94	4.08	1.6107
104.13	38.3	2.90	4.55	1.6580
104.66	26.7	1.94	4.35	1.6385
122.50	30.1	1.94	3.86	1.5866
123.03	29.7	1.94	3.91	1.5922
123.57	30.6	1.94	3.80	1.5798
125.58	31.7	1.94	3.66	1.5635
126.21	47.1	2.90	3.70	1.5682
126.88	31.0	1.94	3.75	1.5740
147.00	35.2	1.94	3.30	1.5185
147.58	35.0	1.94	3.32	1.5211
148.18	36.1	1.94	3.22	1.5079
148.82	35.7	1.94	3.25	1.5119
195.18	47.8	1.94	2.43	1.3856
196.37	94.8	3.87	2.45	1.3892

The Reaction Time refers to the total time of reaction corresponding to the rate of ammonia evolution listed in the fourth column. It is an average value of the reaction times at the beginning and end of a given neutralization. Data prior to the 103 hour reaction

time have been obtained but there is extremely large scatter present due to poor experimental technique.

Initial Rates of Gas Evolution. ABA in DMSO with Added Acid

Thin-walled capillary tubes (15 cm. long) were broken into sections ~ 4 cm. long. Each of these sections was weighed and then partially filled with concentrated hydrochloric acid, Baker Reagent Grade (sp. gr. 1.19). Each tube was sealed at both ends in a small flame and reweighed. The number of equivalents of acid in each tube was determined from the weight difference and the specific gravity of the acid. In a typical decomposition run, a weighed amount of ABA was added to the gas reaction vessel, along with 5 ml. of DMSO. One of the capillary tubes containing acid was then added to the solution and broken under the liquid. The initial rate of gas evolution was then measured at 70°. The data are given in Table XIII.

Rates of Gas Evolution. Mixed Solutions of ADEBA and ADEBA-$2HNO_3$ in DMSO at 60°

In a typical experiment, known weights of ADEBA and ADEBA-$2HNO_3$ were placed together in a gas reaction vessel and 5 ml. of DMSO was added. The initial rate of gas evolution was measured. The data are given in Table XIV.

Polymerization of Methyl Methacrylate

The general procedure used with each of the initiators (ABN, ADEBA, and ADEBA-$2HNO_3$) is given below. A weighed sample of

TABLE XIII

Initial Rates of Gas Evolution. ABA in DMSO with Added Acid. 70°

Run	P mm Hg.	ABA_o (moles x 10^4)	HCl_o (eq. x 10^5)	$(dGas/dt)_o$ (a) (moles $sec.^{-1}$ x 10^9)	k (b) ($sec.^{-1}$ x 10^6)
5	743.2	2.526	2.12	3.946	15.62 (b)
1	743.4	2.506	4.33	5.482	21.88 (b)
2	743.1	2.521	6.25	7.594	30.12 (b)

(a) Calculated from graphical plots of time versus volume measurements given in Table XIII-A , Appendix.

(b) $k = [dG/dt]_o / ABA_o$

TABLE XIV

Initial Rates of Gas Evolution. ADEBA and ADEBA·$2HNO_3$ in DMSO. 60°

Run	t (b) (sec.)	$ADEBA_o$ (a) (moles x 10^4)	$ADEBA \cdot 2HNO_{3_o}$ (a) (moles x 10^4)	$(dN_2/dt)_t$ (b) (moles $sec.^{-1}$ x 10^8)
1	600	0.471	1.355	3.214
2	600	0.256	1.331	2.944
4	600	0.824	1.051	3.366
5	600	0.745	0.810	2.569
6	1200	0.809	0.399	1.331
7	900	-	1.198	2.041
8	~3000	0.655	-	0.066

(a) The amounts placed in the reaction vessel.

(b) Graphically determined from a tangent at time t to a plot of time versus volume measurements. See data Table XIV-A, Appendix.

the initiator was placed in a 25 ml. volumetric flask and dissolved in sufficient DMSO to bring the solution to volume. After the solution was thoroughly mixed, a 5.0 ml. aliquot of each DMSO solution was pipetted into a 50 ml. volumetric flask. The flask was stoppered and weighed. Sufficient purified methyl methacrylate was then added to each flask to bring the solution to volume. The flasks were again stoppered and weighed. The concentration of monomer was determined from the weight difference. Aliquots of 10.0 ml. volume were taken from each 50 ml. flask and pipetted into individual 18 x 150 mm culture tubes (Kimble) which had been constricted near the top. These tubes had been cleaned in a manner analogous to that previously described for n.m.r. sample tubes (44). The tubes were immediately attached to a multi-outlet vacuum line and immersed in a Dry Ice-isopropyl alcohol slurry. The design of the vacuum line outlet system is such that each tube may be opened to the system by a separate stopcock. Thus, several tubes may be simultaneously degassed. When the samples had been frozen, the head space in each tube was evacuated by opening the stopcocks to the vacuum system. The stopcocks were then closed and the tubes were allowed to thaw at room temperature. When the solution in each tube had completely melted, the contents of the tubes were again frozen in the Dry Ice slurry. On completion of the freezing process, the tubes were again opened to the vacuum line. This cycle was repeated four times. At the end of

the fourth cycle, the degassed tubes were individually immersed in liquid nitrogen and sealed off at the constriction with an oxygen torch. They were then allowed to thaw to room temperature, and shaken for several minutes to assure a homogeneous solution. All of the tubes were then simultaneously placed in a constant temperature bath regulated at 69.8°. An initial drop in temperature of 0.4° was noted. The bath re-equilibrated in less than seven minutes. After a predetermined length of time, the tubes were removed from the bath and immediately quenched in ice water, and then immersed in a Dry Ice-isopropyl alcohol slurry. The total length of time (to the nearest minute) from initial immersion of the tubes in the constant temperature bath, to quenching in ice-water, was taken to be the reaction time. The tubes were stored in Dry Ice in the dark until analysis was performed. Analyses were carried out within two days of the kinetic run.

A typical analysis for polymer content will be described. The tube was warmed to room temperature and carefully broken open. Previously, a Waring blendor had been filled with approximately 500 ml. of absolute methyl alcohol. The blendor was attached to the electrical line through a Variac transformer so that the rotation speed of the blades could be controlled. The alcohol solution was stirred at a moderate speed (Variac setting 30-40) and the contents of the tube were rapidly, but carefully, poured into the blendor. The tube was washed

with several small portions of benzene and the washings were transferred to the blendor. When all of the reaction mixture had been transferred, the blendor speed was increased (Variac setting ~90-100) and the heterogeneous mixture was stirred for 4-5 minutes. The supernatant liquid and solid flocculent polymer were rapidly transferred to a 1 liter Erlenmeyer flask with the aid of a large powder funnel, taking care to avoid loss of polymer due to seepage of liquid down the side of the blendor container. The sides of the blendor container were scraped with a spatula while a stream of methyl alcohol was directed on them to remove a small amount of residual polymer. These washings were transferred to the 1 liter Erlenmeyer flask. The funnel was also carefully washed. The heterogeneous mixture in the flask was then filtered through two dry and pre-weighed sintered glass crucibles with the aid of an aspirator vacuum. The flask was rinsed with several washings of methyl alcohol and these were passed equally through the two crucibles. The tops of the crucibles were covered with filter paper and allowed to stand at room temperature for several hours. The crucibles were then dried in an oven at 70° for 45 minutes. These were reweighed and the total weight of polymer in the two crucibles determined. The data are summarized in Table XV.

The first number in the sample code refers to the run. For example, all samples labelled 1 were prepared, placed in the bath, and analyzed concurrently. The second number refers to the sample

TABLE XV

Polymerization of Methyl Methacrylate. 69.8°

Sample	Initiator	$(In)_o$ (moles liter^{-1} x10^4)	$(MMA)_o$ moles liter^{-1}	Reaction Time (min.)	Wt. of Polymer (grams)
1-2	ABN	3.25	8.49	30	0.24785
1-3	"	"	"	"	0.24585
2-1	ABN	3.25	8.48	55	0.44717
2-2	"	"	"	"	0.44639
1-4	ADEBA	2.96	8.49	30	0.16552
1-5	"	"	"	"	0.20826
1-6	"	"	"	"	0.15914
2-5	ADEBA	1.49	8.49	55	0.22955
2-11	"	"	"	"	0.21580
2-8	ADEBA·2HNO$_3$	1.41	8.49	20	0.20094
2-9	"	"	"	"	0.19718

tube number in a run. Duplicate samples of one initiator within a given run were obtained from the same stock solution. Table XV contains the results of all samples that were analyzed.

Potentiometric Titration of Aqueous ABA-2HCl with 0.1N Sodium Hydroxide

A 0.0468 g. (0.0017 moles) sample of ABA-2HCl was dissolved in 100 ml. of distilled water and titrated with 0.1 N sodium hydroxide

solution. A Beckman Model G pH meter and Beckman Glass and Calomel electrodes were utilized in this titration. The pH meter was standardized under experimental conditions with pH 7 buffer. The ABA-2HCl solution was stirred with a magnetic stirrer during titration. The data are presented in Table XVI.

TABLE XVI

Titration of Aqueous ABA-2HCl

with 0.1 N Sodium Hydroxide

ml. NaOH Solution	pH	ml. NaOH Solution	pH
0.00	5.50	12.00	10.24
1.00	8.92	16.00	10.49
2.00	9.28	19.00	10.62
3.00	9.49	20.00	10.69
4.00	9.61	21.00	10.72
5.00	9.74	22.00	10.79
6.00	9.84	25.00	10.90
7.00	9.91	30.00	11.13
8.00	10.00	35.00	11.34
9.00	10.09	40.00	11.50
10.00	10.14	50.00	11.70
11.00	10.20		

The resultant titration curve was shown to be immediately reversible by back titration with 0.1 N hydrochloric acid. At high

pH, the odor of ammonia was detected during the titration. This is assumed to be base catalyzed hydrolysis of the amidinium group. The immediately reversible nature of the titration curves indicates that the rate of this hydrolysis reaction is sufficiently slow so as not to invalidate the titration data in Table XVI.

Potentiometric Titration of ABA in Methyl Alcohol with Methanolic Hydrogen Chloride

The methanolic hydrogen chloride solution was prepared in the following manner. A 100 ml. portion of absolute methyl alcohol was placed in a 250 ml. filter flask fitted with a bubbler tube and a $CaCl_2$ drying tube attached to the side arm of the flask. The apparatus was weighed. Anhydrous hydrogen chloride was bubbled into the solution until a weight increase of 3.5 g. was obtained. This gives a solution approximately 1 N in acid. A 10 ml. aliquot of this 1 N solution was pipetted into a 100 ml. volumetric flask and brought to volume with methyl alcohol, giving a solution ~ 0.1 N in hydrogen chloride.

A 0.1565 g. (7.9×10^{-4} moles) sample of ABA was dissolved in 50 ml. of anhydrous methanol in a 250 ml. beaker. The solution was stirred with a magnetic stirrer and titrated with the 0.1 N methanolic hydrogen chloride solution. The course of the titration was followed with a Beckman Model G pH meter in conjunction with Beckman Glass and Calomel electrodes. The millivolt scale was used. Data are presented in Table XVII.

TABLE XVII

Potentiometric Titration of ABA in Methyl Alcohol with 0.1 N Methanolic-HCl

ml. MeOH-HCl Solution	m.v.	ml. MeOH-HCl Solution	m.v.
0.00	-2.45	15.00	-0.10
1.00	-2.31	16.00	+4.70
2.00	-2.22	17.00	+5.05
3.00	-2.10	18.00	+5.20
4.00	-2.00	19.00	+5.30
5.00	-1.87	20.00	+5.34
6.00	-1.78	21.00	+5.39
7.00	-1.69	23.00	+5.45
8.00	-1.50	25.00	+5.50
9.00	-1.40	27.00	+5.52
10.00	-1.27	29.00	+5.55
11.00	-1.15	30.00	+5.60
12.00	-1.00	31.00	+5.60
13.00	-0.80	32.00	+5.61
14.00	-0.55	33.00	+5.61

A single inflection point occurs at ~15.5 ml. corresponding to 1.55×10^{-3} equivalents of acid.

REFERENCES

1. G. S. Hammond, C. S. Wu, O. D. Trapp, J. Warkentin, and R. T. Keys, J. Am. Chem. Soc., 82, 5394 (1960).
2. C. S. Wu, G. S. Hammond, and J. M. Wright, ibid., 82, 5386 (1960).
3. C. Walling, "Free Radicals in Solution," John Wiley and Sons, Inc., New York, 1957, p. 511.
4. H. Zollinger, "Azo and Diazo Chemistry," Interscience Publishers, Inc., New York, 1961, p. 266.
5. J. Franck and E. Rabinowitch, Trans. Faraday Soc., 30, 120 (1934).
6. R. M. Noyes, J. Am. Chem. Soc., 77, 2042 (1955).
7. S. W. Benson, "The Foundations of Chemical Kinetics," McGraw-Hill Co., New York, 1960, p. 494.
8. R. W. Upson, U. S. Patent No. 2,599,299, June 3, 1952; Chem. Abstrs., 47, 4359f (1953).
9. R. W. Upson, U. S. Patent No. 2,599,300, June 3, 1952; Chem. Abstrs., 47, 4359i (1953).
10. A. Pinner, Ber., 16, 1654 (1883); 17, 178 (1884).
11. E. I. du Pont de Nemours and Co. to G. S. Hammond, personal communication.
12. See Table I, p. 108 of this Dissertation.

13. G. S. Hammond, personal communication.

14. This Dissertation, p. 142.

15. P. Nylen, Z. anorg. allgem. Chem., 246, 227 (1941).

16. E. J. Corey and M. Chaykovsky, J. Am. Chem. Soc., 84, 866 (1962).

17. T. J. Dougherty, ibid., 83, 4849 (1961).

18. L. Eberson, Acta Chem. Scan., 14, 641 (1960).

19. A. F. Bickel and W. A. Waters, Rec. trav. chim., 69, 312 (1950).

20. A. F. Bickel and W. A. Waters, ibid., 69, 1490 (1950).

21. M. Talat-Erben and S. Bywater, J. Am. Chem. Soc., 77, 3710, 3712 (1955).

22. C. E. Boozer, G. S. Hammond, C. E. Hamilton, and J. N. Sen, ibid., 77, 3233 (1955).

23. C. H. Wang and S. G. Cohen, ibid., 77, 2457 (1955).

24. C. G. Overberger, M. T. O'Shaughnessy, and H. Shalit, ibid., 71, 2661 (1949).

25. S. G. Cohen, S. J. Grossos, and D. B. Sparrow, ibid., 72, 3947 (1950).

26. See for example S. W. Benson, op. cit., p. 33.

27. See for example H. F. Walton, "Principles and Methods of Chemical Analysis," Prentice-Hall, Inc., New York, 1952, p. 243.

28. N. Bjerrum, Zeits. f. physik. Chemie, 106, 219 (1923).

29. J. G. Kirkwood and F. H. Westheimer, J. Chem. Phys., 6, 506 513 (1938).

30. H. C. Ramsperger, J. Am. Chem. Soc., 49, 912, 1495 (1927); 50, 714 (1928); 51, 2134 (1929).

31. S. G. Cohen and C. H. Wang, ibid., 75, 5504 (1953).

32. N. Davidson, "Statistical Mechanics," McGraw-Hill Co., New York, 1962, p. 173.

33. S. W. Benson, J. Am. Chem. Soc., 80, 5151 (1958).

34. G. S. Hammond, C. E. Boozer, C. E. Hamilton, and J. N. Sen, ibid., 77, 3238 (1955).

35. A/S Niro Atomizer, Danish Patent No. 64773, Sept. 9, 1946; Chem. Abstrs., 41, 988a (1947).

36. L. M. Arnett, J. Am. Chem. Soc., 74, 2027 (1952).

37. C. Walling, op. cit., p. 54.

38. C. Walling, op. cit., p. 169.

39. S. M. McElvain and K. Rorig, J. Am. Chem. Soc., 70, 1820 (1948).

40. This Dissertation, p. 65.

41. This Dissertation, p. 67.

42. J. Thiele and K. Heuser, Ann., 290, 40 (1896).

43. K. Auwers and J. A. Gardner, Ber., 23, 3622 (1890).

44. This Dissertation, p. 69.

APPENDIX

TABLE VI-A

Run	t (min.)	Vol. (cc)	Run	t (min.)	Vol. (cc)
193	0.00 (t=0)	--	193	61.71	3.860
	1.80	9.144		63.42	3.480
	6.11	9.051		65.07	3.100
	8.61	9.000		66.42	2.804
	10.29	8.933			
	12.75	8.884	65c	0.00 (t=0)	--
	13.96	8.830		2.42	17.62
	15.40	8.775		5.50	17.55
	17.08	8.718		7.02	17.57
	19.30	8.641		9.00	17.55
	21.26	8.582		10.95	17.51
	22.84	8.513		12.97	17.49
	24.63	8.448		14.87	17.45
	26.95	8.294		16.23	17.41
	29.91	8.210		18.87	17.36
	32.17	8.092		21.47	17.30
	34.70	7.980		23.35	17.24
	37.42	7.820		24.82	17.27
	39.42	7.710		27.48	17.15
	41.28	7.581		29.58	17.12
	42.80	7.480		31.17	17.10
	44.43	7.304		33.48	17.05
	45.52	7.220		35.05	17.02
	47.38	6.989		36.98	16.96
	49.00	6.712		37.62	16.91
	49.98	6.530		39.77	16.90
	51.01	6.300		40.88	16.85
	52.16	6.055		43.65	16.74
	53.38	5.761		46.10	16.69
	54.39	5.539		47.92	16.58
	55.37	5.308		49.72	16.45
	56.58	5.030		53.25	16.22
	57.70	4.750		55.85	16.02
	59.24	4.400		57.25	15.92
	60.43	4.138		59.33	15.72

TABLE VI-A (continued)

Run	t (min.)	Vol. (cc)	Run	t (min.)	Vol. (cc)
65c	61.22	15.56	148	33.06	5.739
	64.57	15.27		33.47	5.701
	67.10	15.05		34.51	5.606
	69.00	14.87		35.96	5.481
				36.84	5.383
				37.37	5.345
148	0.00 (t=0)	--		38.97	5.179
	2.33	7.990		39.95	5.074
	3.20	7.932		41.06	4.946
	3.88	7.891		41.93	4.872
	4.44	7.851		42.60	4.807
	6.28	7.730		43.07	4.742
	8.22	7.611		43.82	4.635
	8.99	7.560		44.96	4.518
	10.80	7.453		45.51	4.440
	11.59	7.400		45.91	4.383
	12.18	7.360		46.56	4.320
	13.08	7.291		47.40	4.217
	14.01	7.212		47.86	4.173
	15.66	7.110		48.42	4.080
	16.27	7.071		48.76	4.034
	17.11	7.027		49.13	3.990
	18.63	6.931		49.67	3.920
	19.48	6.841		50.05	3.870
	20.70	6.770		50.37	3.830
	22.30	6.639		50.73	3.769
	23.09	6.563		51.01	3.723
	24.51	6.470		51.60	3.662
	25.45	6.382		51.89	3.620
	26.99	6.270		52.57	3.513
	28.31	6.155		52.92	3.461
	29.78	6.030		53.79	3.340
	30.69	5.946		54.23	3.270
	32.18	5.820		54.62	3.213

TABLE VI-A (continued)

Run	t (min.)	Vol. (cc)
148	55.46	3.076
	55.97	2.999
	56.93	2.850
	57.25	2.810
	57.68	2.731
	58.08	2.660
	58.73	2.568
	59.06	2.503
	59.39	2.453
	60.21	2.322
	60.55	2.258
	61.15	2.139
	62.70	1.880
	63.28	1.775
	64.63	1.525
	65.30	1.410
	66.34	1.223
	67.37	1.032
	68.07	0.900

TABLE X-A

Run	t (min.)	Vol. (cc)	Run	t (min.)	Vol. (cc)
73a	0.00 (t=0)	--	73b	106.43	4.220
	3.63	15.24		112.30	4.190
	5.95	15.25		118.83	4.140
	12.85	15.24			
	24.40	15.22	120	0.00 (t=0)	--
	28.77	15.22		2.90	17.78
	33.98	15.21		3.97	17.80
	51.17	15.19		5.73	17.79
	56.90	15.20		7.73	17.78
	61.53	15.18		10.53	17.77
	65.80	15.17		13.85	17.71
	70.23	15.15		15.88	17.70
	99.72	15.05		18.21	17.72
	104.03	15.01		20.15	17.68
	166.58	14.78		23.09	17.65
				26.75	17.65
73b	0.00 (t=0)	--		30.18	17.60
	6.93	4.525		34.15	17.54
	17.90	4.525		38.85	17.49
	23.02	4.520		43.76	17.40
	30.65	4.530		52.02	17.35
	38.73	4.500		55.50	17.30
	45.98	4.480		58.42	17.26
	50.78	4.460		67.35	17.12
	61.27	4.420		73.45	17.06
	67.25	4.400		80.20	16.98
	73.55	4.360		88.39	16.87
	77.77	4.345		96.97	16.81
	83.35	4.325		107.02	16.75
	89.85	4.295		113.54	16.67
	96.73	4.250		117.21	16.60
	101.17	4.245		121.30	16.64
				122.38	16.65
				124.64	16.61
				127.26	16.61
				129.94	16.65
				134.15	16.48
				137.00	16.54

TABLE XIII-A

Run	t (min.)	Vol. (cc)
1	0.00 (t=0)	--
	5.20	1.940
	22.57	2.055
	31.22	2.135
	82.35	2.555
	105.75	2.740
	120.73	2.870
	137.38	2.995
2	0.00 (t=0)	--
	3.48	2.090
	15.60	2.165
	30.18	2.335
	75.42	2.860
	90.78	3.020
	105.10	3.175
	125.40	3.380
5	0.00 (t=0)	--
	6.60	1.800
	15.25	1.830
	30.78	1.930
	45.20	2.000
	60.72	2.100
	74.95	2.180
	90.50	2.275
	106.68	2.390

TABLE XIV-A

Run	t (min.)	Vol. (cc)	Run	t (min.)	Vol. (cc)
1	306.25 (t=0)	--	2	44.75	4.780
	306.77	5.511		45.35	4.819
	308.10	5.560		46.33	4.871
	308.68	5.608		47.84	4.938
	309.40	5.650		49.33	4.980
	310.03	5.690		50.60	5.040
	310.65	5.730		51.88	5.120
	311.17	5.761		53.60	5.171
	311.51	5.778		55.51	5.260
	312.20	5.841		56.90	5.309
	313.74	5.925		59.86	5.380
	314.70	5.974		60.42	5.430
	315.47	6.002		61.38	5.456
	317.12	6.089		62.22	5.496
	317.85	6.120		62.71	5.512
	318.37	6.153		64.79	5.598
	320.64	6.210		66.99	5.687
	321.51	6.260		68.61	5.733
	322.27	6.310		867.	8.370
	323.09	6.350			
	325.90	6.470	4	0.00 (t=0)	--
	328.38	6.582		2.19	4.765
	329.77	6.631		3.55	4.830
	330.30	6.650		4.44	4.871
	331.12	6.690		5.34	4.935
				6.27	4.972
2	37.80 (t=0)	--		6.79	5.014
	40.89	4.594		7.52	5.060
	41.88	4.645		8.56	5.127
	42.65	4.672		10.06	5.182
	43.29	4.712		10.92	5.240
	43.99	4.742		12.38	5.290

TABLE XIV-A (continued)

Run	t (min.)	Vol. (cc)	Run	t (min.)	Vol. (cc)
4	13.76	5.360	5	21.48	5.430
	15.00	5.419		23.46	5.487
	16.13	5.470		25.77	5.562
	17.16	5.515		27.45	5.632
	18.11	5.552		29.66	5.689
	19.35	5.619		31.37	5.710
	20.49	5.654			
	21.60	5.691	6	0.00 (t=0)	--
	22.65	5.740		2.08	5.072
	23.80	5.772		6.75	5.145
	25.48	5.881		8.79	5.220
	27.49	5.953		13.05	5.281
	29.38	6.092		14.45	5.314
	32.88	6.160		16.26	5.352
	34.25	6.222		18.62	5.392
	35.77	6.264		19.85	5.421
	36.67	6.290		22.42	5.470
				24.63	5.498
5	0.00 (t=0)	--		26.00	5.540
	2.30	4.630		27.90	5.580
	3.21	4.692		31.48	5.630
	4.61	4.752		35.02	5.680
	5.73	4.790			
	6.58	4.839	7	165.70 (t=0)	--
	7.42	4.881		166.69	4.680
	8.74	4.942		169.70	4.755
	9.90	4.973		171.52	4.803
	11.48	5.064		172.57	4.852
	13.04	5.102		173.53	4.920
	13.81	5.151		175.57	4.960
	15.55	5.192		176.12	4.985
	16.67	5.240		177.43	5.015
	18.14	5.305		178.06	5.051
	19.92	5.370		179.50	5.088

TABLE XIV-A (continued)

Run	t (min.)	Vol. (cc)
7	180.90	5.127
	181.87	5.171
	183.28	5.200
	184.31	5.225
	185.24	5.275
	186.77	5.333
	189.16	5.392
8	497.0 (t=0)	--
	497.49	4.500
	500.33	4.460
	502.93	4.443
	580.07	4.520
	657.54	4.560
	701.36	4.590
	833.54	4.708
	906.38	4.743
	957.87	4.790

PROPOSITIONS

PROPOSITION I

Investigations of the homolytic thermal decomposition of phenyl-azo-triphenylmethane have shown that the enthalpy and entropy of activation for this reaction increase with increasing solvent polarity (1, 2). Eleven solvents have been studied varying in polarity from cyclohexane ($\Delta H^{\ddagger}$ = 24.5 kcal. mole^{-1}, $\Delta S^{\ddagger}$ = -1.2 cal. mole^{-1} deg.$^{-1}$) to n-propyl alcohol ($\Delta H^{\ddagger}$ = 31 kcal. mole^{-1}, $\Delta S^{\ddagger}$ = +19 cal. mole^{-1} deg.$^{-1}$). These results have been interpreted to indicate a decrease in the ionic character of this azo-compound as it proceeds from the ground state to transition state. As solvent polarity increases, the ground state solvation of the azo-compound becomes greater, causing an increase in the enthalpy of activation for the decomposition reaction. Concurrently, a decrease in polar character in the transition state will be accompanied by desolvation which will give rise to more positive values of $\Delta S^{\ddagger}$ as solvation of the ground state becomes more pronounced.

A determination of the partial molar volume change of activation (3-5), $\tilde{\Delta}V^{\ddagger}$, for this decomposition reaction, as a function of solvent, may allow an independent determination of the importance of solvation.

Partial molar volume changes of activation are considered to

be composed of two terms, $\tilde{\Delta}_1 V^{\ddagger}$ and $\tilde{\Delta}_2 V^{\ddagger}$ (4, 5). The former is the molecular volume change component and reflects the partial molar volume change of the reactant or reactants going from the ground state to transition state. The second term is commonly referred to as the electrostriction component, and reflects the partial molar volume change of the system due to changes in solvation of the reactants from the ground state to transition state. These terms are related by the simple expression shown in equation 1 (4, 5).

$$\tilde{\Delta} V^{\ddagger} = \tilde{\Delta}_1 V^{\ddagger} + \tilde{\Delta}_2 V^{\ddagger} \qquad (1)$$

In practice, the partial molar volume change of activation is obtained from the relationship given in equation 2 (3-5).

$$(d \log k/dP)_T = - \tilde{\Delta} V^{\ddagger} / 2.3 RT \qquad (2)$$

The quantity $\tilde{\Delta} V^{\ddagger}$ is pressure dependent, and hence care must be taken to evaluate this term at P = 1 atm., either graphically or by appropriate theoretical methods (6).

Volumes of activation have been studied for two major types of systems. These are non-ionic, unimolecular processes (7-9) for which the electrostriction term is approximately zero ($\tilde{\Delta} V^{\ddagger} \simeq \tilde{\Delta}_1 V^{\ddagger}$); and ionic reactions which normally can be rationalized by $\tilde{\Delta} V^{\ddagger} \simeq \tilde{\Delta}_2 V^{\ddagger}$, since the electrostriction term apparently swamps the molecular volume change term (5). No systems have yet been studied which allow a simultaneous estimation of each of the terms in equation 1.

In cyclohexane, electrostriction effects may be considered unimportant, and the partial molar volume change of activation for decomposition of phenyl-azo-triphenylmethane in this solvent may be set equal to $\tilde{\Delta}_1 V^{\ddagger}$. As the solvating power of the solvent increases, the electrostriction term will become a significant contributor to $\tilde{\Delta} V^{\ddagger}$. If it is assumed that the quantity $\tilde{\Delta}_1 V^{\ddagger}$ is independent of solvent, the electrostriction term $\tilde{\Delta}_2 V^{\ddagger}$ may be evaluated for any solvent system from the measured partial molar volume change of activation, equation 1, and the value of $\tilde{\Delta}_1 V^{\ddagger}$ obtained in cyclohexane. If the ionic character of the azo-compound decreases as the transition state for thermal decomposition is approached, it is expected that the partial molar volume of the system will increase due to desolvation in polar solvents (5). The magnitude of $\tilde{\Delta}_2 V^{\ddagger}$ in a solvent will give an indication of the solvation power of that solvent.

Experimental methods for these variable pressure studies have been reviewed (5, 7).

References

1. M. G. Alder and J. E. Leffler, J. Am. Chem. Soc., 76, 1425 (1954).
2. G. L. Davies, D. H. Hey, and G. H. Williams, J. Chem. Soc., 4397 (1956).
3. E. A. Moelwyn-Hughes, "The Kinetics of Reactions in Solution," 2nd Ed., The Clarendon Press, Oxford, 1947, p. 338.
4. M. G. Evans and M. Polanyi, Trans. Faraday Soc., 31, 875 (1935).
5. S. D. Hamann, "Physico-Chemical Effects of Pressure," Butterworths Scientific Publications, London, 1957, p. 160.
6. S. W. Benson and J. A. Berson, J. Am. Chem. Soc., 84, 152 (1962).
7. C. Walling et al., ibid., 79, 4776, 4782, 4786 (1957); 81, 5365 (1959).
8. A. H. Ewald, Disc. Faraday Soc., 22, 138 (1956).
9. A. E. Nicholson and R. G. W. Norrish, ibid., 22, 97 (1956).

PROPOSITION II

Benzenediazonium-2-carboxylate (I) was reported by Hantzsch and Davidson in 1896 (1). The compound was formulated as the cyclic diazo structure (II) (2). Recently, Stiles and Miller (3) have reported

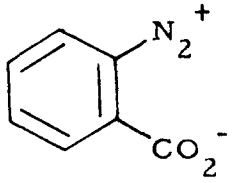

I

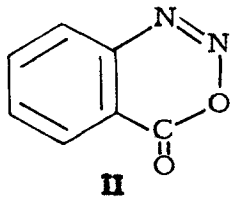

II

preliminary studies of the thermal decomposition of this compound in water and hydrocarbon solvents. From spectral evidence and solubility properties they conclude that the zwitterionic form I is a better representation of this compound in the solid state.

The mode of decomposition of aromatic diazonium salts has been found to be quite dependent on reaction medium (4). Under acidic conditions in aqueous (5, 6) or alcoholic solvents (7-9), decomposition appears to be an S_N1 solvolysis of the aryldiazonium cation to give phenols or arylethers and quantitative nitrogen evolution (10, 11). However, under neutral or basic conditions, diazonium salts appear to decompose by a homolytic mechanism giving rise to products expected from aryl radicals. These homolytic decompositions are postulated to involve neutral diazo forms of these molecules (4). For example, DeTar has studied the decomposition of benzenediazonium fluoroborate in methanol with added acetate buffer (10, 12). Under

these conditions, the nature of the products is quite sensitive to oxygen, and in the absence of oxygen, benzene is the major product. The mechanism is assumed to involve diazonium coupling with acetate ion to give benzenediazoacetate, which then decomposes by a homolytic process.

Benzenediazonium-2-carboxylate offers an extremely interesting system, since under appropriate conditions the diazoacylate II may form intramolecularly, and it is not unreasonable to conclude that the decomposition of this species may proceed by a homolytic mechanism.

The decomposition of benzenediazonium-2-carboxylate in water has been shown to yield salicylic acid (88%) after 36 hours at 45° (3). This result can be explained by a typical benzenediazonium heterolytic cleavage process. Solvolysis undoubtedly proceeds through the zwitterionic form I. The mode of decomposition in non-polar solvents appears to be quite different. Thermal decomposition of a suspension of this diazonium salt in benzene or toluene has been found to give stoichiometric nitrogen evolution, but less than a stoichiometric amount of carbon dioxide (59% in benzene), depending on "conditions" (3). The non-gaseous products have not been resolved and are largely polymeric. Decompositions in furan, or an anthracene-benzene mixture, give 1,4-dihydronaphthalene-1,4-endoxide (55%) and tryptycene (30%), respectively (3). Decomposition in benzene or p-xylene in the presence of a slight excess of benzoic acid gives phenyl benzoate (25 and

22%, respectively) and with excess m-toluic acid, phenyl m-toluate is isolated (3). These results have been rationalized in terms of the benzyne intermediate (3).

Under these non-polar reaction conditions, it is interesting to speculate on the mechanism shown in Figure 1.

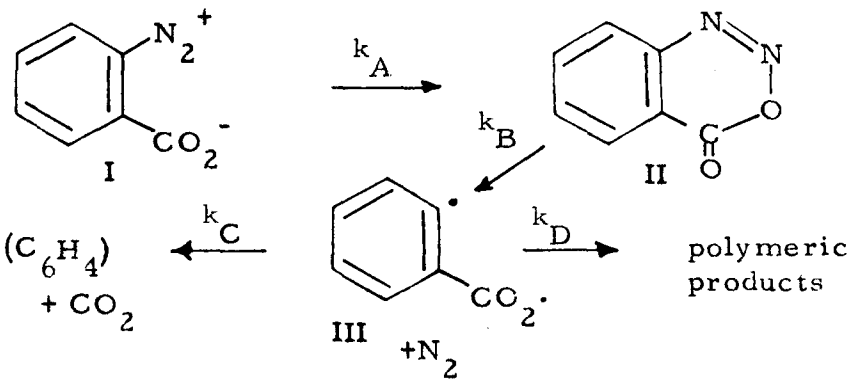

Fig. 1

Initially, the diazonium ion I is in a heterogeneous phase (3). The rate of formation of II (k_A) may be expected to be slow due to the unfavorable cis geometry about the azo linkage; or the formation of II may require prior solution of I. The process represented by k_B may be quite rapid due to the cis configuration of the azo linkage. Thus, the formation of II may be rate-determining in this decomposition reaction. The discrete existence of III in solution is not unreasonable on the basis of prior studies of the somewhat analogous benzoyloxy radicals (13). The fact that III has a finite lifetime will account for the non-stoichiometric evolution of carbon dioxide in these reactions due to competition between decarboxylation (k_C) and other reactions

(k_D). Diradicals produced from decomposition reactions of cyclic azo compounds show an extremely high percentage of geminate intramolecular coupling (14), but this might be expected to be insignificant in the case of III, due to the resultant strain in the product that would be formed.

Mechanistic studies in these non-polar systems will be complicated by their heterogeneous nature. In the light of DeTar's studies on benzenediazonium ions in methyl alcohol with added acetate buffer, the thermal decomposition of I in methyl alcohol may demonstrate the presence of II in solution. Normal heterolytic cleavage of I in methanol will give o-methoxybenzoic acid. Decomposition proceeding through II may give benzene, anisole, benzoic acid, and other minor products, depending on the fate of III.

Nitrogen may be evolved in processes which do not necessarily pass through the diazoacylate II. In order to determine the importance of II in the decomposition process, a series of diazonium compounds may be studied. The decomposition of a 2-diazoniumbenzoic acid (V) may exhibit a considerably slower rate of nitrogen evolution if the rate-determining step in the decomposition of I involves II. In order to estimate the inherent change in decomposition rate due to differences in the inductive and resonance contributions in I and V, the rates of the thermal decomposition of a 4-diazoniumbenzoic acid (VI) and a 4-diazoniumbenzoate salt (VII) may be compared. The effect of added

benzoate, or acetate ion on the rates of nitrogen evolution from the salts I, V, VI, and VII would be useful. If decomposition of the ionic species I proceeded through II as a rate-determining step, it would be expected that added carboxylate ion would have relatively little effect on the rate of nitrogen evolution from solutions of I. On the other hand, addition of these salts to systems containing V, VI, and VII might be expected to cause marked increases in the rate of nitrogen evolution.

References

1. A. Hantzsch and W. B. Davidson, Ber., 29, 1535 (1896).
2. A. Hantzsch and R. Glogauer, ibid., 30, 2548 (1897).
3. M. Stiles and R. G. Miller, J. Am. Chem. Soc., 82, 3802 (1960).
4. H. Zollinger, "Azo and Diazo Chemistry," Interscience Publishers, Inc., New York, 1961, p. 137.
5. E. S. Lewis and W. H. Hinds, J. Am. Chem. Soc., 74, 304 (1952).
6. D. F. DeTar and D. I. Relyea, ibid., 76, 1680 (1954).
7. A. Hantzsch and E. Jochem, Ber., 34, 3337 (1901).
8. J. L. Beeson, Am. Chem. J., 16, 235 (1894).
9. A. W. Hofmann, Ber., 17, 1917 (1884).
10. D. F. DeTar and M. N. Turetsky , J. Am. Chem. Soc., 77, 1745 (1955).
11. D. F. DeTar and A. R. Ballentine, ibid., 78, 3916 (1956).
12. D. F. DeTar and M. N. Turetzky, ibid., 78, 3925, 3916 (1956).
13. C. Walling, "Free Radicals in Solution," John Wiley and Sons, New York, 1957, p. 474.
14. H. Zollinger, op. cit., p. 274.

PROPOSITION III

It has been shown that diboron tetrachloride (Cl_2B-BCl_2) and the corresponding tetrafluoride (1-3) react at low temperatures with olefinic linkages to give simple products of the form X_2B-C-C-BX_2 (4, 5). Diboron tetrachloride also reacts with acetylene and cyclopropane to give analogous 1:1 adducts (5). Similar reactions with vinyl halides and other haloethylenes do not occur (5). Diboron tetrafluoride reacts much more slowly than diboron tetrachloride in these reactions, but provides more stable products. A recent report describes the reaction of benzene and naphthalene with B_2Cl_4 (6). Naphthalene apparently reacts in a manner analogous to olefins giving 1, 2, 3, 4-tetra(dichloroboryl)tetralin, while benzene gives phenyldichloroborane. These reactions proceed much more slowly than reactions with the olefins.

Practically no mechanistic consideration has been given to these reactions. Ceron et al. (5) comment that the low reactivity of haloethylenes toward these reagents is characteristic of their low reactivity in electrophilic addition reactions. Wartik (6) implies that diboron tetrachloride initially forms a complex with both benzene and naphthalene before subsequent reaction occurs. It has been previously shown that BCl_3 forms complexes with olefins (7). Stable ether complexes of diboron tetrahalides have also been reported (2, 3). The

stability of diboron tetrafluoride is greatly enhanced by solution in the unreactive halo-olefins (5). These observations all indicate the presence of B_2X_4-olefin complexes in solution.

Several mechanistic possibilities for these reactions can be considered. These are stepwise ionic, or free radical, processes; or four-center reactions. The stepwise process is distinguished from a four-center process in that the former, a discrete intermediate is formed which requires an intermolecular addition step to complete the reaction.

Free radical stepwise processes are unattractive. The reaction of B_2Cl_4 with cyclopropane to form a 1:1 acyclic adduct is difficult to explain by a free radical process. The observed reactions with acetylene, and naphthalene, are equally difficult to rationalize by such a mechanism.

If a stepwise ionic process were considered to be similar to other electrophilic addition reactions to olefins, the first step would be addition of a B_2X_4 molecule or BX_2^+ to give an electron deficient intermediate. It is unlikely that such an intermediate would react with another similarly electron deficient B_2X_4 molecule to give the product. Further, the product from reaction with naphthalene is certainly not characteristic of an electrophilic reaction with an aromatic system.

It is proposed that four-center models best explain the reactions of compounds of the type B_2X_4 with the organic substrates discussed above. Two types of four-center processes may be considered*: 1) Concerted; and 2) "Stepwise." Process 1) can be envisioned as a direct overlap of the unoccupied boron p-orbitals and the p-π-orbitals of the olefin. Rehybridization at carbon with simultaneous cleavage of the B-B bond will give product. Process 2) can be thought of as involving preliminary bond formation between one boron atom and a carbon of the olefin giving a zwitterionic (or a diradical) species which would then collapse internally to the product. An initial olefin-B_2X_4 complex which may rearrange to the transition state described for process 1) or 2) fits easily into a four-center mechanism.

The stereochemical outcome of these addition reactions will be strongly dependent on mechanism. A concerted four-center process will require cis addition. A four-center mechanism which is not concerted may give product of less than pure cis addition, depending on the rate of rotation about the C-C single bond formed in the intermediate (9). A stepwise mechanism with a discrete intermediate can give a variety of stereochemical results, depending on the nature of the intermediate.

Indirect evidence for cis-addition has been reported. The adduct formed by reaction of B_2Cl_4 and acetylene (5) has been assigned

*Strictly speaking, process 2) is not a four-center mechanism(8).

the structure $Cl_2BHC{=}CHBCl_2$ from a molecular weight and micro-analytical determination, and an infrared absorption at 1609 $cm.^{-1}$ indicative of olefinic linkages (10). The fact that this absorption is visible argues for the presence of at least some cis-1,2-di-(dichloroboryl)-ethylene, since trans olefins do not give absorption in this characteristic double bond region (10).

The reaction of B_2Cl_4 with 2-butene (unknown stereochemistry) has already been reported (5). The products of cis-addition of diboron tetrahalides to the cis and trans olefins will be the meso and dl adducts, respectively. These 1,2-adducts may be converted to the known 1,2-diols (11, 12) by reaction with dimethyl zinc (4, 5) and oxidation (13, 14) of the resultant trialkyl boron compounds; a process which supposedly gives overall retention of configuration. The steric course of this addition reaction may thus be determined.

Dipole moment measurements on the B_2Cl_4-acetylene adduct or derivatives would also be a valuable aid for the determination of the steric course of the reaction.

It has been pointed out that concerted four-center additions to cis-olefins may produce unfavorable steric strain in the transition state (9). A comparison of the rates of addition of the diboron tetrahalides to cis and trans-2-butene should allow a test for this mechanism. It would be expected that a stepwise process would relieve strain in cis-2-butene to a greater degree than in trans-2-butene.

Conversely, a four-center concerted process would cause eclipsed interactions between the methyl groups in cis-2-butene, but not in the trans form.

The rate of reaction may be conveniently followed by alkaline hydrolysis of aliquots of the reaction mixture. Alkaline hydrolysis of compounds containing the B-B covalent linkage yields a stoichiometric amount of hydrogen gas for each B-B bond (1). The rate of disappearance of the diboron tetrahalide may be followed by this technique.

Recently, convenient synthetic techniques for the preparation of various diboron compounds have appeared. These include the chloride (15, 16), as well as tetraamino (17) and tetraalkoxy compounds (18). These latter species are much more stable than the halides. This is attributed to overlap of non-bonding electrons on nitrogen and oxygen with the electron deficient boron atoms (17, 18). Reactions of these latter materials with olefins have not been examined, and although they will undoubtedly be less reactive than the halides, they are capable of withstanding much higher temperatures (15-18) and may prove to be more useful for mechanistic studies.

References

1. T. Wartik, E. H. Moore, and H. I. Schlesinger, J. Am. Chem. Soc., 71, 3265 (1949).
2. G. Urry, T. Wartik, E. H. Moore, and H. I. Schlesinger, ibid., 76, 5293 (1954).
3. A. Finch and H. I. Schlesinger, ibid., 80, 3573 (1958).
4. G. Urry, J. Kerrigan, T. Parsons, and H. I. Schlesinger, ibid., 76, 5299 (1954).
5. P. Ceron, A. Finch, J. Frey, J. Kerrigan, T. Parsons, G. Urry, and H. I. Schlesinger, ibid., 81, 6368 (1959).
6. W. B. Fox and T. Wartik, ibid., 83, 498 (1961).
7. E. L. Muetterties, ibid., 82, 4163 (1960).
8. J. Hine, "Physical Organic Chemistry," McGraw-Hill Co., 1962, New York, p. 79.
9. F. G. Bordwell and W. E. Garbisch, J. Am. Chem. Soc., 82, 3588 (1960).
10. L. J. Bellamy, "The Infra-Red Spectra of Complex Molecules," J. Wiley and Sons, Inc., New York, 1958, p. 38.
11. R. W. Watson, J. A. R. Coope, and J. L. Barnwell, Can. J. Chem., 29, 885 (1951).
12. A. J. Kluyver, M. A. Scheffer, U. S. Patent No. 1,899,156, Feb. 28, 1933; Chem. Abstrs., 27, 3029 (1933).

13. H. C. Brown and G. Zweifel, J. Am. Chem. Soc., 81, 247, 5832 (1959).

14. S. Winstein, E. L. Allred, and J. Sonnenberg, ibid., 81, 5833 (1959).

15. A. L. McCloskey, J. L. Boone, and R. J. Brotherton, ibid., 83, 1766 (1961).

16. A. L. McCloskey, R. J. Brotherton, and J. L. Boone, ibid., 83, 4750 (1961).

17. R. J. Brotherton, A. L. McCloskey, L. L. Petterson, and H. Steinberg, ibid., 82, 6242 (1960).

18. R. J. Brotherton, A. L. McCloskey, J. L. Boone, and A. M. Manasevit, ibid., 82, 6245 (1960).

PROPOSITION IV

The nature of X-irradiated single crystals of malonic acid has been thoroughly investigated (1, 2). A study of the hyperfine splitting obtained in e.p.r. spectra of oriented malonic acid crystals has shown that the effects of irradiation are to produce the relatively stable $CH(COOH)_2$ radical along with one or several other unstable radicals. The carbon, oxygen, and carboxyl hydrogen atoms of the $CH(COOH)_2$ radical have nearly the same position in the unit cell as those of the parent malonic acid molecule. Since the crystal structure of malonic acid had been previously determined, it was possible to show that the cartesian coordinate axes of the parent malonic acid molecule (assumed to be nearly the same for the radical) corresponded to the "canonical orientations" of the single crystal in an external magnetic field. That is, orienting the crystal so that the applied field was parallel to any of the three cartesian axes gave anisotropic hyperfine splittings due to the proton on the α-carbon which were invariant to the magnitude of the applied field. From these splittings, it was possible to calculate an isotropic coupling of 61 ± 3 Mcps., indicating nearly unit unpaired electron spin-density on the α-carbon atom.

The nitrogen analog of malonic acid, malonoamidinium ion (I), offers a potentially interesting system for analogous e.p.r. studies.

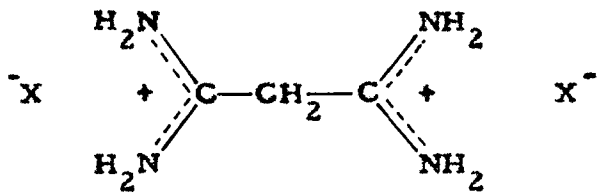

I

The diamidinium ion I is a logical extension to studies of the isoelectronic malonic acid, and the presence of the magnetic nitrogen nuclei offer the possibility of investigating their interaction with an unpaired electron produced in I by X-ray damage.

I has not been reported in the literature, but should be easily synthesized from malononitrile by the method of Pinner (3, 4). This diamidinium salt will certainly be a crystalline compound, which may yield acceptable single crystals on careful recrystallisation. X-irradiation of I should produce the stable radical II. Whereas the analogous radical from malonic acid has an unpaired electron spin-

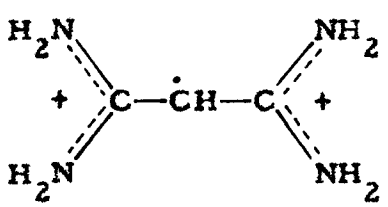

II

density of essentially unity on the α-carbon atom, it might be expected that II would exhibit a somewhat lower spin-density on the α-carbon atom. Studies of thermal decompositions of aliphatic aso-compounds indicate that amidinium groups offer greater stabilization to the

resultant alkyl radicals than do ester groups. The rate of thermal decomposition of azobisisobutyramidinium nitrate (5) (H_2O, 70°) is 1.5×10^{-4} sec.$^{-1}$, (DMSO, 70°) is 1.7×10^{-4} sec.$^{-1}$; while the rate of decomposition of dimethyl azobisisobutyrate (7) (nitrobenzene, 80°) is 1.6×10^{-4} sec.$^{-1}$; activation parameters are $\Delta H^{\ddagger}$ = 29 kcal. mole^{-1}, $\Delta S^{\ddagger}$ = +9 e.u. (6); and $\Delta H^{\ddagger}$ = 31 kcal. mole^{-1}, $\Delta S^{\ddagger}$ = +5 e.u. (7), respectively. Although ester groups and carboxylic groups undoubtedly differ in their ability to stabilize an alkyl radical, it may be expected that they are more similar than are ester and amidinium groups. The stabilization of an alkyl radical by an amidinium group can be thought of as a mixing of the alkyl-carbon p-orbital containing the unpaired electron with orbitals of the atoms in the amidinium group giving a lower energy molecular orbital. The above comparison of amidinium and ester groups implies that unpaired electron spin-density may be greater in the amidinium groups of II than in the carboxylic acid groups of the analogous malonic acid radical. It must be stressed, however, that extrapolation of radical stabilities from solution to the solid phase is at best a crude approximation.

Since no crystal structure determination is available for I, it is impossible to predict the complexity of the e.p.r. spectra that may be obtained for II. It may be that the crystal structure is sufficiently analogous to that of malonic acid that, in the absence of unpaired electron interactions with the amidinium nitrogens, relatively

simple two-line spectra, due to interaction with the proton on the α-carbon atom (1), would be obtained. Even if interactions with the nitrogen nuclei are present, it may be possible to determine the spin-density on the α-carbon if hyperfine splittings due to nitrogen are relatively small and the basic two-line spectrum is resolvable from the multiplet structure.

It would be advantageous to synthesize the malonoamidinium-^{15}N salts. If hyperfine splittings were present due to interaction of the unpaired electron with the nitrogen atoms, the complexity of the spectra would be reduced considerably by substituting ^{15}N ($I = \frac{1}{2}$) for ^{14}N ($I = 1$).

In the case of a more complicated crystal structure, it would be necessary to examine the spectra before ease of analysis could be estimated.

References

1. H. M. McConnell, C. Heller, T. Cole, and R. W. Fessenden, J. Am. Chem. Soc., 82, 766 (1960).
2. H. M. McConnell and C. R. Giuliano, J. Chem. Phys., 35, 1910 (1961).
3. A. W. Dox, Org. Syn., Col. Vol. I, J. Wiley and Sons, Inc., New York, 1941, p. 5.
4. A. Pinner, Ber., 16, 1654 (1883); 17, 178 (1884).
5. This Dissertation, Part II.
6. T. J. Dougherty, J. Am. Chem. Soc., 83, 4849 (1961).
7. K. Ziegler, W. Deparade, and W. Meye, Ann., 567, 141 (1950).

PROPOSITION V

Studies of the thermal decomposition of azobis-N,N'-dimethylene-isobutyramidine and its dinitrate, and azobisisobutyramidine and its dinitrate, have indicated that stabilization of the resultant radical is probably the most important factor in determining the rates of decomposition of the diamidines and their diamidinium salts (1). Protonation of the amidine groups in either amidine system not only introduces electrostatic interactions in the molecule, but increases the ability of the amidine group to stabilize the resultant radicals which are produced. It is of interest to determine the magnitude of pure electrostatic effects on the rates of decomposition of azo-compounds. The compound 1,1'-azocyano-4-azacyclohexane (I) is suggested as a suitable system in which to study pure electrostatic effects on the azo decomposition reaction.

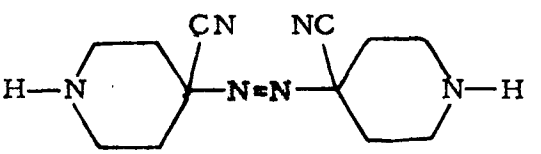

I

The stability of the radicals which are produced in the decomposition reaction will be determined by the nitrile groups (2) and should be independent of changes made at the nitrogen atoms in the cyclohexane rings. Comparison of the rates of decomposition of I and the diprotonated salt of I would demonstrate the effect of repulsive interactions between the charged ends of the diprotonated molecule.

The extent of geminate recombination of pairs of radicals is expected to be influenced by their stabilities (1). Since the stabilities of the radicals from decomposition of I (or its conjugate acids) should be independent of the nature of the ring nitrogen (neglecting solvation), the electrostatic effect on geminate recombinations may be more clearly analyzed.

It was pointed out that the stability of the radicals may not be independent of the nature of the ring nitrogen atoms (3). The radicals produced in the decomposition of I may gain added stabilization through charge-transfer interactions (3) such as represented in Figure 1.

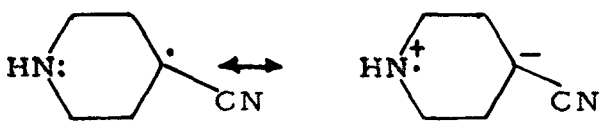

Fig. 1

The azo compound 1, 1'-azocyano-(N-methyl)-4-azacyclohexane (II) has been synthesized (4). This is analogous to I except for the substitution of methyl groups for the nitrogen protons in I. The rates of thermal decomposition of II and 1, 1'-azocyanocyclohexane (III) (5) have been compared in chlorobenzene at 90°. No significant difference in rates was observed (6). Since the radicals from III cannot undergo charge-transfer stabilization of the type shown in Figure 1, it is concluded that such interactions in the transition state for decomposition of II are negligible. It is felt, however, that such

interactions are not unreasonable and may be exhibited by the larger ring analogues of I or II.

The ratio of the acidity constants for the first and second conjugate acids of II (or I) will indicate the magnitude of the repulsive interaction between the positively charged nitrogens in diprotonated I or II (7, 8). Since the positively charged nitrogens can be well approximated by point charges, the repulsive interaction can be calculated by the Bjerrum (7) or Kirkwood-Westheimer (8) treatments as a function of molecular geometry or effective dielectric constant (8) between the charges. A comparison of these calculated repulsive interactions with the differences in measured acidity constants will allow an estimation of either molecular geometry of effective dielectric constant. A comparison of the differences in enthalpies of activation for decomposition of II (or I) and diprotonated II (or I) (it is assumed that entropies of activation will be nearly the same) with the energy of the repulsive interaction (vide supra) will indicate if the Kirkwood-Westheimer (8) and Bjerrum (7) treatments can be extended to predict differences in activation energies for these decomposition reactions.

References

1. This Dissertation, Part II.
2. H. Zollinger, "Azo and Diazo Chemistry," Interscience Publishers, Inc., New York, 1961, p. 269.
3. G. S. Hammond, personal communication.
4. This Dissertation, p. 140, 145-151.
5. C. S. Wu, G. S. Hammond, and J. M. Wright, J. Am. Chem. Soc., 82, 5386 (1960).
6. This Dissertation, p. 108.
7. N. Bjerrum, Zeits. f. physik. Chemie, 106, 219 (1923).
8. J. G. Kirkwood and F. H. Westheimer, J. Chem. Phys., 6, 506, 513 (1938).